Master Thesis

Hydroprocessing and Catalytic Cracking of Fischer-Tropsch Biowaxes to Biokerosene

performed for the purpose of obtaining the academic degree of
Master of Science under the direction of

Dipl.-Ing. Dr.techn. Reinhard Rauch (TU Vienna)

and

Dr. Eleni F. Iliopoulou (CERTH/CPERI Thessaloniki)

Institute of Chemical Engineering

submitted at the Technical University of Vienna
Faculty of Mechanical and Industrial Engineering

of

Ing. Marjana Jovicic BSc

Matr.Nr. 0725745

Affidavit

I declare under penalty of perjury, that I have made this thesis independently and without use of any aids specified. Parts of the experiments in this thesis were done by the research center CERTH/CERPI in Thessaloniki, Greece. The acquired thoughts, directly or indirectly from other sources, are identified as such. The thesis has not been submitted to any other examination board in identical or similar form and not yet published.

In the course of this work a publication was written, which was published on the 3rd International Conference on Processing Technologies for the Forest and Bio-based Products Industries (PTF BPI 2014), Kuchl/Salzburg, Austria, September 24-26, 2014

Vienna, Nov. 2014

Marjana Jovicic

Abstract

This thesis presents the investigation of a new process to produce biokerosene from Fischer-Tropsch biowaxes. Wood chips were converted in the Fischer-Tropsch test-facility Güssing (Austria) to biowaxes and further converted via hydroprocessing and catalytic cracking at CPERI/CERTH research institute (Thessaloniki). Two types of biowaxes were explored that consisted almost entirely of linear paraffin. These two feedstocks differed in their melting points, one was about 95°C and the other about 132°C. The wax with the lower melting point was used as a feedstock for the catalytic cracking process in a lab scale automated fixed bed unit. The catalytic cracking process was performed to investigate the conversion of the Fischer-Tropsch biowaxes with conventional zeolite based catalysts. The heavy melting wax was used in the hydrodesulfurisation pilot plant unit for the hydroprocessing experiments. For the hydroprocessing procedure, nickel molybdenum and a dewaxing catalyst were used. In addition, a parameter variation was conducted to determine the optimal parameters for the biokerosene production. These experiments were one of the first attempts to convert Fischer-Tropsch biowaxes to biokerosene.

Acknowledgement

This idea was centralised in the project Brisk (The European Research Infrastructure for Thermochemical Biomass Conversion), which was a cooperation between the company REPOTEC Umwelttechnik GmbH, Vienna University of Technology and the research center CERTH/CERPI in Thessaloniki, Greece. Mainly the European Commission, additionally the COMET funding competence center program, the Austrian Climate and Energy Fund and the Austrian TAKE OFF funding program, supported this work.

Danksagung

Ich möchte mich an dieser Stelle bei allen bedanken, die mich während meines Studiums und meiner Diplomarbeit begleitet und unterstützt haben. Allen voran Danke ich Reinhard Rauch, meinem Betreuer an der Technischen Universität Wien und meinen Betreuern beim Forschungszentrum Certh in Thessaloniki für die umsichtige und kompetente Betreuung meiner Diplomarbeit. Einen besonderen Dank an meinen Freund, für unzählige fachliche und nicht-fachliche Diskussionen und für seine Unterstützung während des gesamten Studiums. Ein weiterer besonderer Dank, geht an meine Schwester, die mich auf meinem Weg immer wieder in meinen Entscheidungen bestärkt hat. Des Weiteren möchte ich meinen Eltern danken, die mich während meines Studiums finanziell unterstützt haben.

Marjana Jovicic

List of Contents

List of Figures

List of Tables

1 INTRODUCTION

Transportation has a high value in our society. It is essential for the carriage of people and goods and it is also indispensable for the economic development. The world transportation system grows with technologies based on fossil resources, therefore global industrialization depends on fossil material. Especially oil is one of the finite and depleting fossil resources that is most affected. (Miller et al. 2014) So the inevitable fact is that oil supply is a non-renewable resource and limited from a geological point of view. (Andruleit et al. 2011, pp. 9-12) Oil supply depends on the availability from the earth crust and also on the general consumption rate. (Hallock et al. 2004) If the population and urbanisation especially in developing countries grow as forecasted the oil demand will increase about 40 million b/d and reach 120 million b/d by 2030. (Dorian et al. 2006) Even with a large amount of oil reserve the fast consumption cannot satisfy the global oil market. (Bentley 2002) The International Energy Agency (IEA) expects that if the demand for fossil fuels continued to rise rapidly, the main crude oil supplies would be depleted by 2035. (Andruleit et al. 2011, pp. 9-12) However, not only the limitation of crude oil also the immense expenses of fossil resources, the massive pollution and the impacts of climate change are essential reasons to use alternative fuel sources. Climate change is probably the greatest concern in connection with fossil resources. The pollution that originated with handling fossil material was one of the reasons for global warming. These pollutants were greenhouse gas emissions that warmed the atmosphere and the ocean and have been the reason for rising sea levels and recent nature catastrophes. The central contributing greenhouse gases to the global warming are carbon dioxide (CO_2), methane (CH_4) and nitrogen compounds (NO_x). (Stocker 2013)

Figure 1 shows the correlation between greenhouse gas concentration and global temperature, as well as the possible outcome scenario at different stages. The concentration and the temperature are directly dependent, so when the greenhouse gas emissions are increasing, the global temperature is too. Hence, with rising temperature the scenario could bring irreversible consequences. The current trends are forecasting an average global temperature up to 6°C for a long-term scenario. (Birol 2008, pp. 37, *407- 434*)

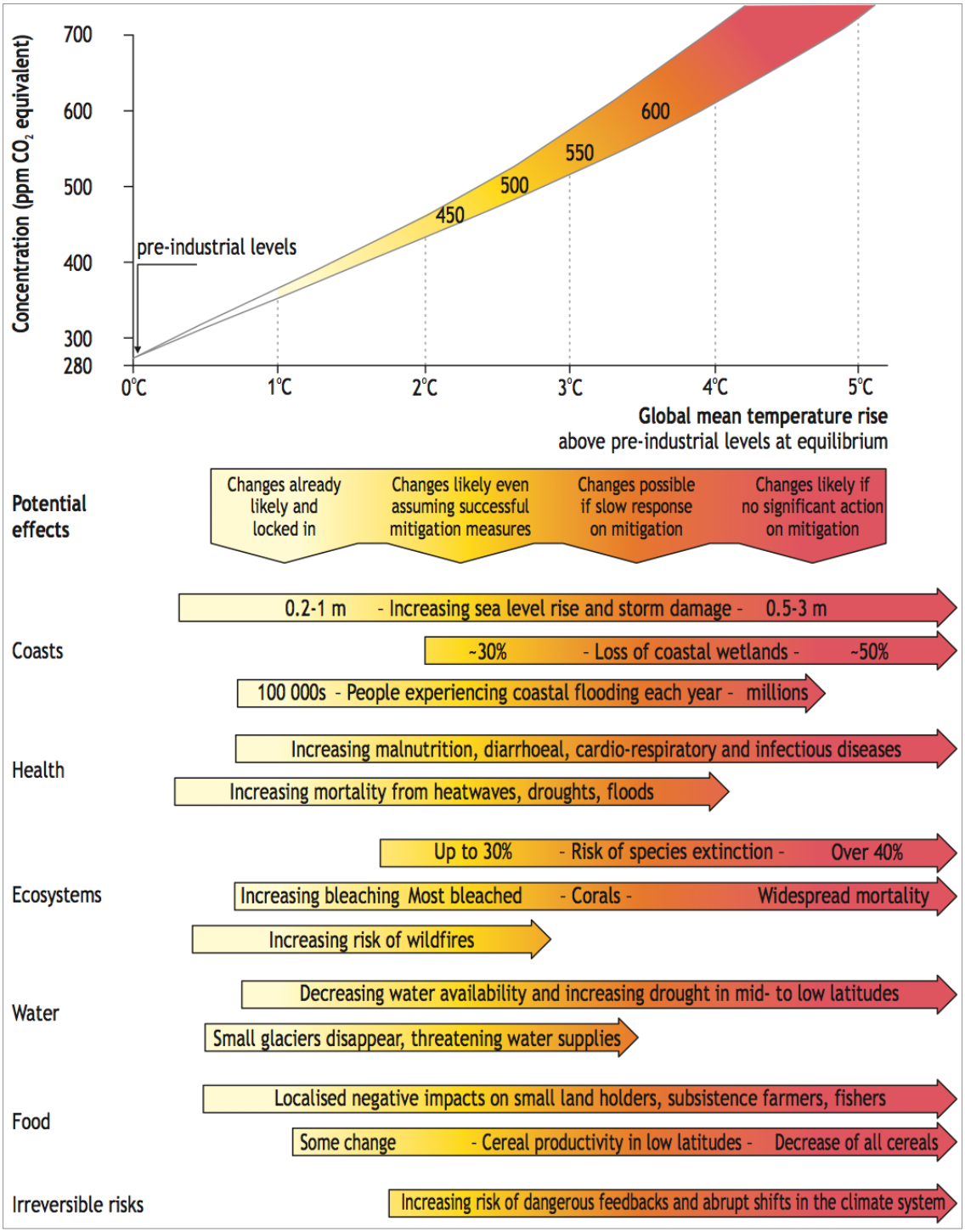

Figure 1: Forecasting an average global temperature (Birol 2008,pp. 412)

Apparently the urgent need for innovation and new technologies to encourage the climate mitigation and reduce the greenhouse gas emissions is high. The implementation of one alternative fuel source is the production of transportation fuels from biomass.

The United Nation Framework Convention of Climate Change defines biomass as:

“Non-fossilized and biodegradable organic material originating from plants, animals and micro-organisms. This shall also include products, by-products, residues and waste from agriculture, forestry and related industries as well as the non-fossilized and biodegradable organic fractions of industrial and municipal wastes. Biomass also includes gases and liquids recovered from the decomposition of non-fossilized and biodegradable organic material.” (UNFCCC 2005)

The biomass used for the experiments in this work is composed of wood chips. Woody biomass is considered a renewable resource that is carbon dioxide (CO_2) neutral. The CO_2 circuit of biomass is declared closed because the absorbed CO_2 from the living plant is going to be released at the follow-up procedures. Therefore biomass composed of plants does not add CO_2 to the total CO_2 balance. (Basu 2010, pp. 28-29) (Naik et al. 2010)

Biomass is economically considerable and has less environmental impact than the production of conventional fuels. For biomass fuel production out of “1.generation biomass” the fruits of plants such as corn, sugarcane, soybean, rapeseed and palm oils has been used. This generation of biofuel sparked heated discussions. The main topics of those arguments were the growing food prices and reduced biodiversity in some landscapes. The acceptable solution for this problem was the “2.generation biomass”. These biofuels are an appropriate replacement that can be produced from all kinds of biogenic residues and waste materials such as plant remains, organic waste and wood residues. (Damartzis et al. 2011) (Antizar-Ladislao et al. 2008)

The European Union wants to establish a sustainable biofuel for the global market. The second generation biofuels are not yet available in large scale quantities because there are several difficulties to overcome before using them in an commercial capacity. (Havlík et al. 2011) (Agarwal 2007) State of the Art is to add biofuels in a defined percentage to the conventional fuels until mass production is possible. The EU - Renewable Energy Directive 2009/28/EC regulates the use of biofuels in Europe. It controls the sustainability of biofuels and ensures that within the EU a minimum of 5% biofuel is used for now. By 2020 the growth rate of biofuels should be at least 10% and in some European countries up to 20% of the European fuel market. The aim of the European Union is fossil fuel independency. (Beurskens et al. 2011, pp.17-27) (Schnepf 2006)

1.2 Biofuel Kerosene

In this work the focus lies particularly on the aviation fuel based on biokerosene. To use biokerosene as sustainable jet fuel it must approach the properties and technical requirements of fossil kerosene as close as possible and need to have a similar composition. Fossil kerosene distilled from crude oil is a middle distillate with a boiling point at 150-300°C and mostly contains of compounds with a carbon number of C_8-C_{16}. (Thompson et al. 2009, pp. 137,172) The composition of fossil kerosene has a range of variation. It has usually a composition of alkanes (50-65% vol.), mono- and poly- aromatics (10-20% vol.) and cycloalkanes (mono- and polycyclic, 20-30% vol.) mixed with corresponding additives. (Gaïl et al. 2007)

Fossil kerosene as jet fuel also has fitting properties like smoke point, freezing point (pour point, cloud point), flash point, density, viscosity, oxidative stability and specific heating value. Following, an explanation about the most important properties is given. Specification values of each property are represented in table 1. (De Klerk 2012, pp. 270)

Freezing Point

The freezing point signifies the lowest temperature where the fuel is still a liquid. Below the freezing point the fuel becomes solid. Linear compounds have a high freezing point therefore they must be isomerized to meet the specification. (De Klerk 2012, pp. 276) To modify the freezing point to even lower temperatures anti-freezing additives can be used. (Wauquier 200, pp. 128)

Cloud Point

At the temperature of the cloud point the crystallisation starts but the fuel is still liquid. (Speight 2011, pp. 378) Linear compounds have a high cloud point they must be isomerized to meet the specification.(Jones et al. 2006, pp. 311)

Pour Point

The temperature of the pour point is below the temperature of the cloud point. The pour point is the point where the fuel can no longer flow or be poured. (Speight 2011, pp. 378) Linear compounds have a high pour point to meet the specification they must be isomerized. (Jones et al. 2006, pp. 311)

Smoke Point

The smoke point represents the particle (black smoke) formation during combustion. Particles cause erosion in the engine and tend to block the air supply. The particle formation depends on the chemical structure of the fuel. Linear paraffines have a high smoke point and burn relatively clean, branched paraffines have a low smoke point and aromatics have an even lower point. (Wauquier 2001, pp. 127) Usually fuels from Fischer-Tropsch syncrude have very low aromatic compounds. (De Klerk 2012, pp. 276)

Flash Point

The flash point is the lowest temperature where an ignitable air-vapour mixture can ignite, which is formed above a fuel. This contains the risk of explosion if the volume of the mixture is large enough. (Dukek et al. 1979, pp. 22) The flash point depends on the boiling point whereby the boiling point increases with increasing carbon number. (McElroy 2009, pp. 126) Increasing the initial boiling point temperature can control the flash point. (De Klerk 2012, pp. 290)

Viscosity

The viscosity of jet fuels is an important specification and increases with the molecule chain length. Technical design of the engines are highly influenced by viscosity of the fuel, e.g. to create an optimal droplet size distribution the geometry of the engine needs to be fitted for the viscosity of the fuel. (De Klerk 2012, pp. 275)

Density

The density of jet fuels is determined by the compounds of the fuel. It is difficult for biokerosene to meet the required density therefore aromatics have to be added. (De Klerk 2012, pp. 275, 492)

Additives

Additives influence the chemical composition and the chemical reactivity of the aviation fuel, however the addition is regulated in the jet fuel standards. The typical additives are chemical compounds such as antioxidants, metal deactivators, anti-freezing additives, lubricant additives and corrosion inhibitors. (National Research Council, US 1997)

The properties differ from jet fuel to jet fuel. Nowadays the most common fuels are Jet A, Jet A1, JP5 and JP8. Thereby Jet A and Jet A1 are commercial aviation fuels JP5 and JP8 are used for military purposes and have more specific properties for military operations. The standard specifications in which all properties are specified for Jet A and Jet A1 are DEF STAN 91-91 (Jet A-1), ASTM specification D1655 (Jet A-1), and IATA Guidance Material (Kerosene Type), NATO Code F-35, ASTM specification D1655 (Jet A).

The standard specification data for Jet A and Jet A1:

	Jet A	Jet A1
Freezing Point max.	-40°C	-47°C
Smoke Point min.	25 mm	25 mm
Flash Point min.	38°C	38°C
Density at 15°C	775 – 840 kg/m^3	775 – 840 kg/m^3
Viscosity at -20°C	8 mm^2/s	8 mm^2/s
Aromatic content	25 Vol%	25 Vol%

Table 1: Specification data for Jet A and Jet A1 (De Klerk 2012, pp. 270)

2 THEORETICAL FOUNDATION

2.1 Biomass

Biomass is considered a significant infinite resource in future energy supply for green transportation fuels, especially aviation fuels. This work is about the production of alternative aviation fuel biokerosene, which is converted through many process steps of biomass. (Hamelinck et al. 2006) One systematic approach is the general characterizing of biomass for sustainable transportation fuel in lignocellulose biomass such as sugar, starch crops and oil plants. (Kaltschmitt et al. 2011, pp. 2)

Types of each particular plant group

Lignocellulose biomass: Straw or cereal plants, husk, wood, scrap, slash, etc.

Oil Plants: Rape seed, soybean, palm sunflower seed, coconut, jatropha, etc.

Sugar and starch crops: Corn, sugar cane, sugar beet, wheat, etc.

(Basu 2010, p. 29-32)

Lignocellulose biomass will be elaborated in detail because it is used as a biomass resource for the experiments in this work. Lignocellulose biomass is the most suitable renewable material for fuel production. This has several reasons like high fuel yield, general low energy consumption and it grows under difficult conditions. (Hamelinck et al. 2006)

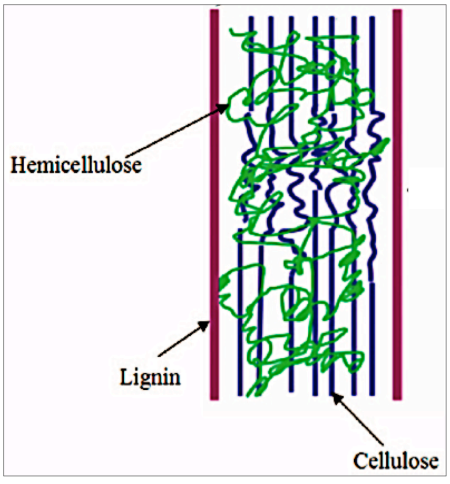

Figure 2: Structure of lignocellulose biomass (Kumar et al. 2009)

Lignocellulose biomass is composed of plant material consisting primarily of cellulose, hemi-cellulose and lignin. Lignocellulose has also a few quantities of other compounds like pectin, protein, nonstructural materials, nitrogenous material, chlorophyll, waxes and ash. Figure 2 shows the structure of lignocellulose biomass. Cellulose is the main structural component, which consists of linear polysaccharides that can be in a crystalline and amorphous shape. It is responsible for the stability of the plant.

Hemicellulose is composed of different branched polysaccharides and acts as a linkage between lignin and cellulose. Lignin has a complex molecule structure. It holds the polysaccharides together and forms the plant wall. The chemical structure of each compound of lignocellulose is presented below. (Kumar et al. 2009) (Reddy et al. 2005) (Stöcker et al. 2008)

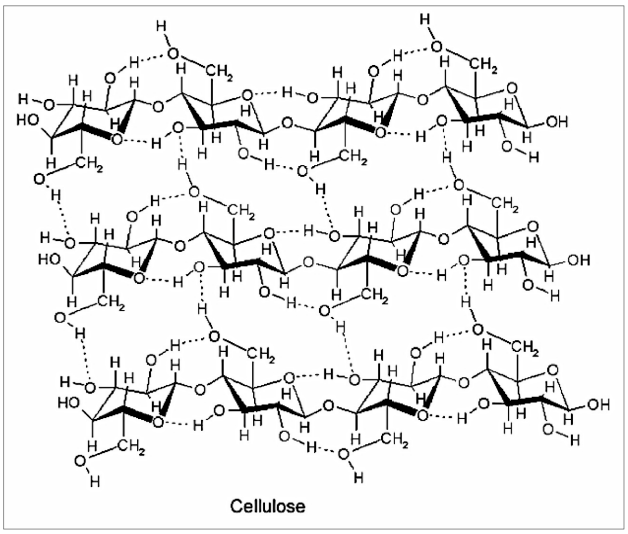

Figure 3: Chemical structure of cellulose (Stöcker et al. 2008)

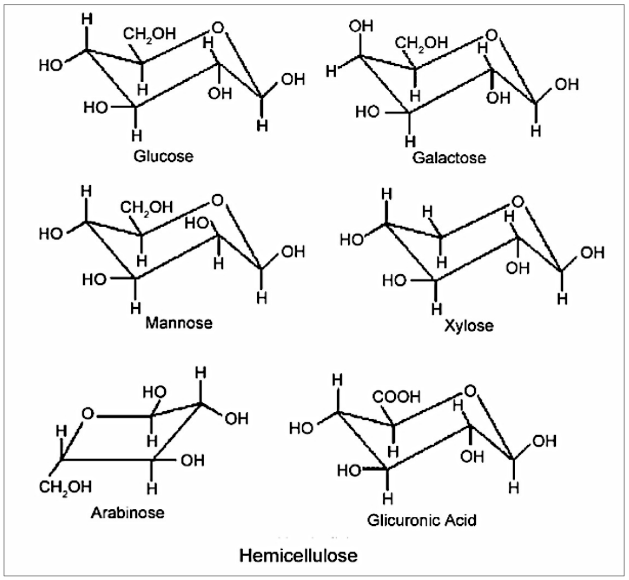

Figure 4: Chemical structure of hemicellulose (Stöcker et al. 2008)

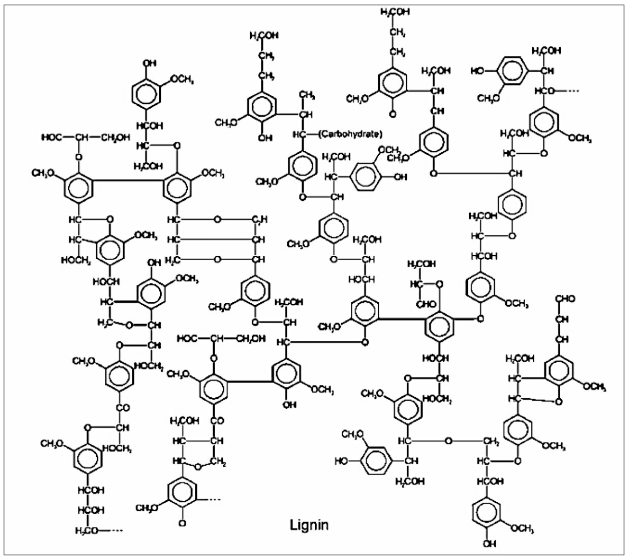

Figure 5: Chemical structure of lignin (Stöcker et al. 2008)

Generally, there are diverse procedures to convert lignocellulose biomass into biofuels. The biomass materials can be transformed into a solid, liquid or gaseous secondary energy carrier by different process routes. (Demirbas et al. 2007) These routes can be thermochemical, physicochemical or biochemical refining procedures. The *thermochemical procedure* is a process where biomass is converted into solid, liquid and gaseous materials under heat influence. The characteristic thermochemical conversions are gasification, pyrolysis and combustion. The gasification process is explained in detail in chapter 2.2.1. The *physicochemical procedure* is a conversion of oleaginous biomass. Therefore, it is necessary to separate the oil phase of the oil plants, which can be realised through compression and extraction from the oleaginous biomass. After the extraction of the oil, it needs several refining process steps to achieve a certain quality so it can be used as fuel. The *biochemical conversion* is a biological process for the production of biofuel. The organic materials are microorganisms that were used for fermentation to produce the end product. (Kaltschmitt et al. 2011, p.5-6) These three main conversion routes each consist out of many process steps. Since it is not possible to cover all in this work, the focus lies on the thermochemical route of the experimental production of biokerosene.

Boichenko et al. (2013) presents an overview of alternatives and traditional production of kerosene. Accordingly there are different approaches to synthesize kerosene from different raw material. Kerosene can be produced by derivation from conventional oil, unconventional oil (oil sands and oil shale), from natural gas and coal via the Fischer-Tropsch process, from biomass via the Fischer-Tropsch process, renewable oils (vegetable oil) or derived from alcohols (ethanol and buthanol). The focus in this work lies on the alternative production of kerosene basically over the conversion of biomass via Fischer-Tropsch process but the rivalry methods like the derivation from renewable oils are also briefly explained.

Llamas et al. (2012), Chiaramonti et al. (2014), Chuck et al. (2014), Jansen (2013) and Demirbas (2008) are few examples of literature where the production of biokerosene from renewable oils is described. Different sorts of usually oleaginous biomass like croton, sunflower, soybean, coconut and some other plants have been extracted. Generally, the physicochemical route was used for the production of biokerosene with additionally refining steps. The difficulties to meet the technical requirements of aviation kerosene have caused the approach of different techniques. One technique is called “Biomass to liquid” process and is usually a conversion route with many process steps. In You et al. (2011), Lappas et al. (2004), Baliban et al. (2013) are presented some examples of biokerosene production through “Biomass to liquid”-process.

2.2 Biomass to liquid (BTL)

From biomass to biokerosene

“Biomass to liquid” is the entire manufacturing process from the biomass to the sustainable biofuel. The procedure of lignocellulose biomass to biokerosene includes processes starting from the thermochemical step gasification, to the “Fischer-Tropsch synthesis” and ends with two forms of cracking procedures for product recovery. Figure 6 shows a simplified schematic illustration of the conversion from woody biomass to biokerosene using the BTL-process.

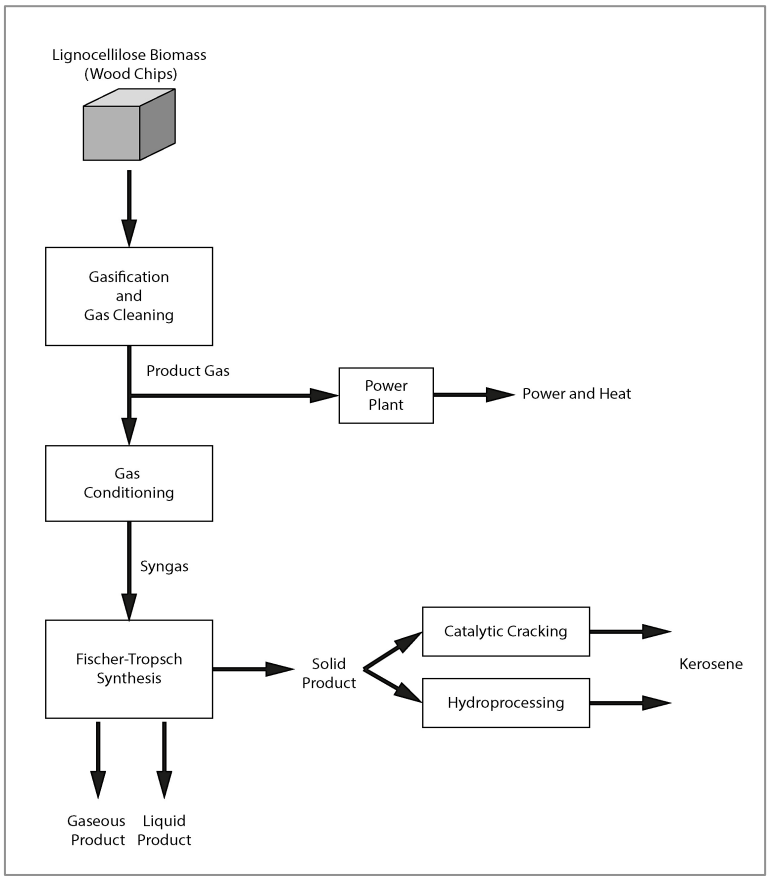

Figure 6: Simplified schematic illustration of the conversion from woody biomass to biokerosene.

In this work, lignocellulose biomass was used as wood chips for the experiments. The wood chips were residues from forestry that were scrabbled and naturally dried before further processed. The first step was the biomass gasification in a unique gasifier where wood chips were transformed into product gas. The product gas has two purposes, one as gas fuel in a power plant for the heat and power production, second as raw material in form of synthesis gas for the Fischer-Tropsch syncrude. For the product gas to meet the requirements of the synthesis gas additional cleaning and further treatment is required.

At the Fischer-Tropsch synthesis, gaseous products as well as liquid products like diesel and gasoline and also a high amount of solid biowaxes were produced in presence of a catalyst. The biowaxes, which are usually by-products at the Fischer-Tropsch synthesis, were used for a new approach of biokerosene. The waxes were converted via catalytic cracking and hydroprocessing into biokerosene. The used technologies are discussed in detail in the following chapters. (Rauch et al. 2004/1)

2.2.1 Biomass Gasification

Gasification technology has managed to become essential for the biofuel market during the last century. With the biomass gasification technology almost any kind of plants can be gasified. (Prins et al. 2007) (Rezaiyan et al. 2005, pp.1-2) This technology was initially used for coal gasification. The similarity of biomass chemistry in comparison to coal allows biomass to be used in the gasification technology. This similarity is based on the thermal decomposition and thereby arising product gases of coal and biomass. (Klass 1998, pp.289-290)

The biomass gasification is a thermochemical conversion of solid biomass. It is a thermal decomposition followed by secondary reactions of the extant volatile matter to produce gaseous products. (Küçük et al. 1997) The gaseous products can be used for many applications like power and heat production, fuel production and as a fuel for co-firing in combustions. The gasification is carried out in a gasifier with a gasification agent. It is a chemical reaction under the influence of temperature and pressure. The end products of the gasification are gaseous products such as hydrogen (H_2), carbon monoxide (CO), carbon dioxide (CO_2), water (H_2O) and methane (CH_4), as well as small yields of other gases like nitrogen and sulphur compounds. Also solid particles residues such as dust, char and tar are produced. (Pfeifer et al. 2011)

2.2.2 Mechanism Gasification

The chemical decomposition mechanism behind the gasification technology of biomass is very complex. The knowledge of the decomposition of each wood component of lignocellulose biomass is not yet fully consistent. (Kaltschmitt et al. 2011, p. 385) The process of chemical decomposition follows a series of steps that are proceeding simultaneously and cannot be strictly separated from each other. They are divided in preheating and drying, pyrolysis, gasification and oxidation (combustion) (Figure 7). (Basu 2010, p. 119)

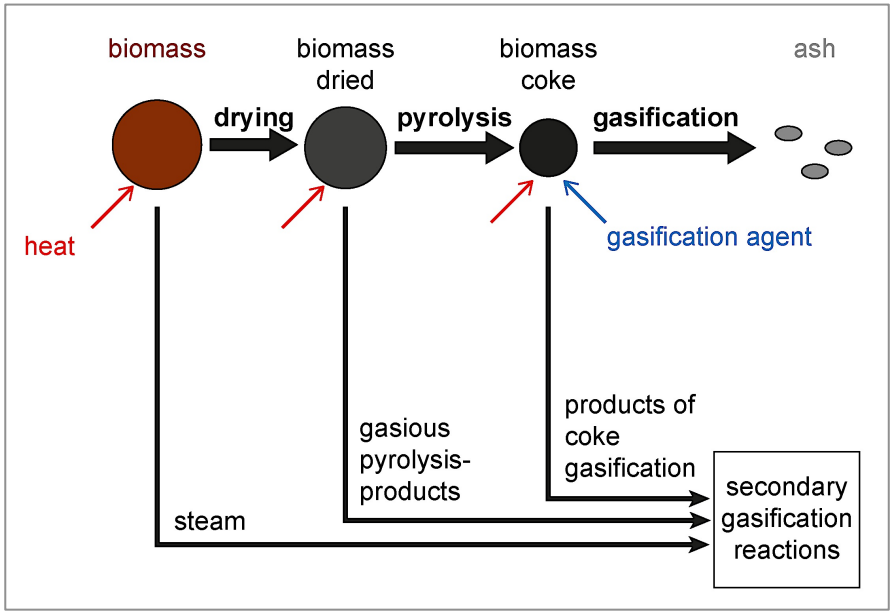

Figure 7: Simplified biomass gasification steps (Kaltschmitt et al. 2011, pp.394)

Preheating and Drying

During the heating and drying process at temperatures of 100-200°C the water and low-molecular-weight gases start to vaporize. (Kaltschmitt et al. 2011, p. 378) At this stage hemicellulose is the first wood compound that starts to decompose because it contains more moisture than lignin and cellulose. (Basu 2010, p.77-81)

Pyrolysis

The pyrolysis of lignocellulose biomass is the conversion of hemicellulose, cellulose and lignin into pyrolysis products at approximately 200-600°C. The pyrolysis products can be solid (char, carbon), liquid (tars, heavier hydrocarbons) and gaseous (CO, CO_2, H_2O, C_nH_m, ect.).

The compositions of the pyrolysis products depend on process conditions that vary with the pyrolysis temperature, heating rate and the duration in the reaction zone. Each compound of lignocellulose biomass decomposes at a different temperature range, hemicellulose at 150–350 °C, cellulose at 275–350 °C and lignin at 250–500 °C. (Basu 2010, p. 69-74)

Gasification

The gasification is a further conversion step of produced solid, liquid and gas products in the previous pyrolytic decomposition. Essential is the conversion of residual carbon material like pyrolysis coke into gases. The gasifying decomposition is initiated through further exposure to heat in a temperature range of about 500-1500°C and in the presence of a gasifying agent. (Kalkschmitt et al. 2011, p. 389-390)

The gasifying agent defines the product gas composition and the heating value of the biomass gasification. It is important that the agent contains oxygen for the decomposition of carbon material. The typical gasifying agents are oxygen (O_2), water vapour (H_2O), carbon dioxide (CO_2) and air (21% O_2, 79% N_2). Air is usually a low-priced agent but reduces the heating value of the product gas because of the high nitrogen amount, which dilutes the product gas. (Devi et al. 2003)

The amount of gasifying agent needed for a process is given by the air/fuel equivalent ratio λ. For the gasification process an air/fuel equivalent ratio λ between $0 < \lambda < 1$ is required. λ is generally defined as the ratio of the air amount that is used for the conversion of carbon compared to the stoichiometric amount of air required. For other gasification agents, like water vapour, a similar gasification agent/fuel equivalent ratio can be calculated. (Kaltschmitt et al. 2011, p. 376-389)

$$\lambda = \frac{m_{air,tot}}{m_{air,sto}} \qquad (1)$$

λ	air/fuel equivalent ratio	[1]
$m_{air,tot}$	total mass of air used for the reaction	[kg]
$m_{air,sto}$	mass of air of a stoichiometrical reaction	[kg]

Table 2 lists gasifying agents and their corresponding product gases

Raw material	Gasifying agent	Product gas
Carbon (C)	Oxygen (O_2)	CO, CO_2
Carbon (C)	Water vapour (H_2O)	CO + H_2 (syngas)
Carbon (C)	Carbon dioxide (CO_2)	2CO
Carbon (C)	Air (21% O_2, 79% N_2)	CO + N_2

Table 2: Different gasifying agents and their product gases (Kaltschmitt et al. 2011, p. 600)

The gas-solid gasification reactions are shown in detail in the following paragraphs. (Kaltschmitt et al. 2011, p. 390-391)

$$C + O_2 \rightarrow CO_2 \quad \Delta H = -393,5 \frac{kJ}{mol} \tag{2}$$

$$C + \frac{1}{2} O_2 \rightleftharpoons CO \quad \Delta H = -110,5 \frac{kJ}{mol} \tag{3}$$

$$C + H_2O \rightleftharpoons CO + H_2 \quad \Delta H = +118,5 \frac{kJ}{mol} \tag{4}$$

$$C + CO_2 \rightleftharpoons 2CO \quad \Delta H = +159,9 \frac{kJ}{mol} \tag{5}$$

$$C + 2H_2 \rightleftharpoons CH_4 \quad \Delta H = -87,5 \frac{kJ}{mol} \tag{6}$$

Considering all processes involved in the gasification reactions, the overall process is endothermic. The equilibrium of the reactions depends on the temperature and pressure. Equation (2) is complete carbon oxidation reaction, equation (3) is partially carbon oxidation reaction, equation (4) is heterogeneous water-gas reaction, equation (5) is the Boudouard-Reaction and equation (6) is methane reaction.

The ensuing reactions of the gasification process are gas-gas reactions and presented below.

$$CO+H_2O \rightleftharpoons CO_2+H_2 \quad \Delta H = -40,9\frac{kJ}{mol} \tag{7}$$

$$CO+3H_2 \rightleftharpoons CH_4+H_2O \quad \Delta H = -203\frac{kJ}{mol} \tag{8}$$

$$C_mH_n + mH_2O \rightleftharpoons mCO + (m+\frac{n}{2})H_2 \tag{9}$$

Equation (7) is the water-gas shift reaction, equation (8) is the methanation reaction and equation (9) is a reformation of hydrocarbons.

2.2.3 Gasification Plants

Gasification reactors (a.k.a. gasifiers) can be differentiated by their properties like the type of heat supply, the reactor type, the gasification agent and the pressure conditions in the gasification reactor. The used gasifying agent depends mainly on the required end product. The pressure conditions differ usually between atmospheric and elevated pressure up to 300 bar. The heat supply of the biomass gasification can be allothermic or autothermal. Allothermal gasification is based on external heat supply, that means the heat supply is transferred via heat exchanger or circulating bed material indirectly to the gasification chamber. Autothermal gasification is an internal heat supply, which means that part of the biomass is burned in the gasification chamber and allows a direct heat supply. (Kaltschmitt et al. 2011, p.601) For the biomass gasification, three main gasification reactor types are used. These are the fixed bed gasifier (for low temperatures 425-650°C), the fluid bed gasifier (for middle temperatures about 900-1050°C) and the entrained flow gasifier (for high temperatures about 1250-1600°C). (De Klerk et al. 2011, p.6)

These types of gasifiers are explained in detail in the literature. (Basu 2010, p. 167-192), (Kaltschmitt et al. 2011, p.601- 619) and (Quaak et al.1999, p. 26-33) The gasifier used for the production of syngas in this work is a special gasifier that will be described in detail in the following section.

2.2.4 Biomass gasification at the CHP Plant Güssing

The biomass gasifier power plant in Güssing is used as a heat and power producer and also for the production of nitrogen-free product gas (syngas). The gasification process at the power plant uses a “Dual Fluidised Bed” (DFB) reactor. The process is parted in two zones, the first zone is the gasification and the other is a combustion zone. (Bolhàr-Nordenkampf et al. 2003)

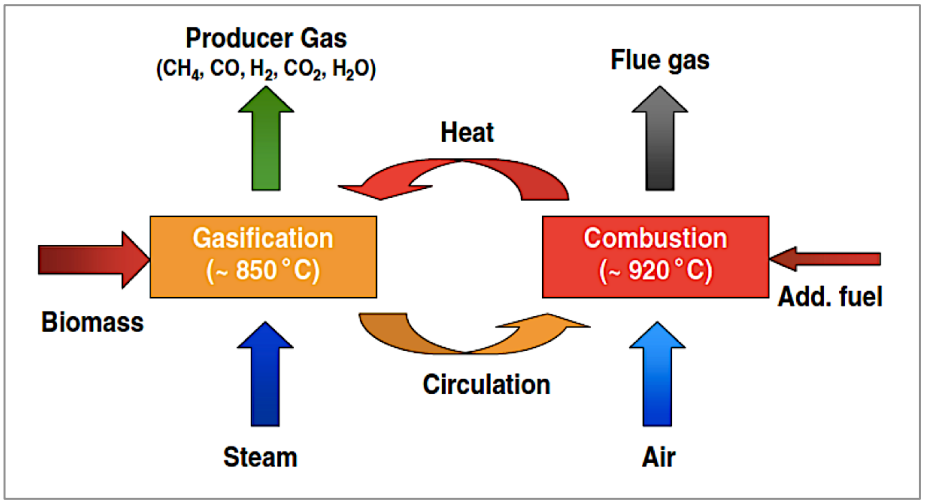

Figure 8: Two spatially separated zones in the reactor. (Pfeifer et al. 2011)

In both zones different agents and operating parameters are used. The temperature in the gasification zone is about 850°C, the gasification area is fluidised with steam for an appropriate syngas product and a high caloric value. The temperature in the combustion zone is about 920°C, the zone is fluidised with air and the fluidised bed material is olivine.

Olivine is an iron and magnesium orthosilicate $(Mg, Fe)_2 SiO_4$, which is a catalytic active material and it is also attrition resistant. The heat supply is allothermal whereby the bed material circulates between the two zones. This is beneficial for the efficient heat use in the power plant. (Rauch et al. 2004/2) Through interaction with biomass ash, calcium rich layers are created on the olvine particles and increase their catalytic activity even further. (Kirnbauer et al. 2011)

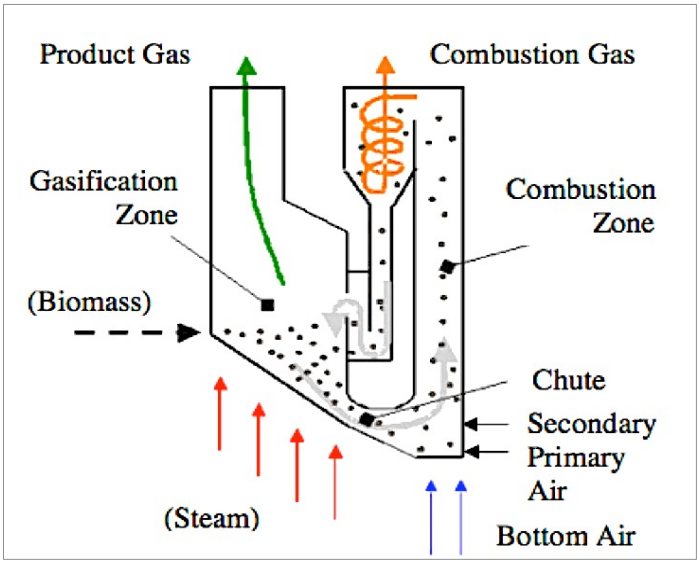

Figure 9: Circulating fluidised bed reactor (Bolhàr-Nordenkampf et al. 2002/1)

Figure 9 illustrates the way of the biomass through the circulating fluidised bed reactor. At first, wood chips with a water content of 20-30% are transported from a metering bin into the fluidised bed reactor with a rotary valve system. The wood chips are gasified in the gasification zone. The product gas is escaping at the top of the zone and further transported to the gas cleaning. The bed material and a part of not gasified biomass (carbon) are transported to the combustion zone through the chute. The remaining biomass residues (carbon) and new wood chips were regular burned to deliver the required temperature of the bed material. Afterwards, the bed material passes a cyclone, where the combustion gas (flue gas) is separated from the bed material and the bed material is circulated back to the gasifier zone. The combustion gas is released at the stack after a gas cleaning procedure. (Bolhàr-Nordenkampf et al. 2002/1) (Bolhàr-Nordenkampf et al. 2002/2)

To meet the requirements of the synthesis gas (syngas) the product gas from the gasification zone needs to be cleaned before further processing. The contaminations of the product gas are solid particles, dust, char and tar but also sulfuric components such as hydrogen sulfide (H_2S), carbonyl sulfide (COS) and nitrogen components like ammonia (NH_3) and hydrogen cyanide (HCN). (Pfeifer et al. 2011)

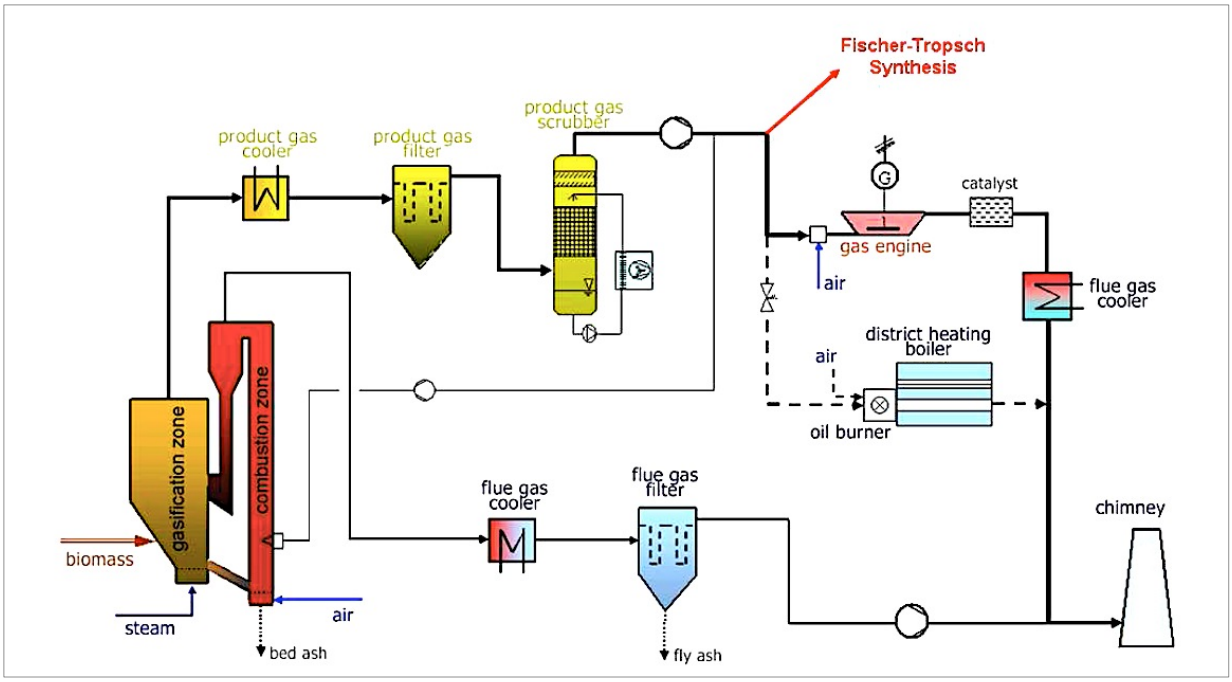

Figure 10: Flow sheet of the CHP power plant Güssing (Sauciuc et al. 2012)

Figure 10 shows the CHP power plant Güssing with the gasifier and the cleaning steps of the product gas. The cleaning is parted into a few steps, which start with cooling of the gas stream from 850°C to 160 - 180°C. A particle filter for separation of particles from the product gas follows this step. These particles are led back in the combustion zone and burned in the circulating fluidised bed reactor. The remaining tars and partly nitrogen and sulphuric components (table 3) were removed from the product gas (table 4) by the scrubber.

The cleaned gas is transported to the Fischer-Tropsch plant, which is described in the next chapter. Additional information is available in the literature Bolhàr-Nordenkampf et al. (2004) and Sauciuc et al. (2012).

Example table for the main components of the product gas from the gasification plant Güssing

Component	Range	Dimension
Hydrogen (H_2)	35-45	Vol%
Carbon monoxide (CO)	20-30	Vol%
Carbon dioxide (CO_2)	15-25	Vol%
Methane	8-12	Vol%
Nitrogen	3-5	Vol%

Table 3: Components of the product gas from the gasification plant Güssing (Bolhàr-Nordenkampf et al. 2004)

Example table for the contaminants in the product gas from the gasification plant Güssing

Component	Raw gas	Clean gas	Dimension
Particles	5000-10000	<5	mg/Nm^3
Tar (larger naphthalene)	1500-4500	10-40	mg/Nm^3
Ammonia	1000-2000	< 400	ppm
Hydrogen sulfide	Not measured	20-40	ppm

Table 4: Contaminants in the product gas from the gasification plant Güssing (Bolhàr-Nordenkampf et al. 2004)

2.3 Fischer-Tropsch Synthesis

Today Fischer-Tropsch Synthesis is one of the most important syncrude for the production of alternative transportation fuels. (Schulz 1999) The synthesis has gained more attention since the need for sustainable fuels is growing. It is a promising way to produce biofuels in a commercialised scale for the fuel market. (Sauciuc et al. 2012) The biofuel production with the Fischer-Tropsch synthesis can be established through the synthesis gas that has been produced at the previous explained biomass gasification process. Thereby syngas can be converted under certain process condition in presence of a catalyst into light (C_2-C_5), middle (C_5-C_{35}) and heavy (C_{35}-C_{120}) hydrocarbons and byproducts like oxygenates, alcohol, ether, ester, aldehyde, ketone, carboxylic acids and water. (De Klerk et al. 2010, p.1) (Boerrigter et al. 2003)

The main reactions of the Fischer-Tropsch Synthesis:

$$nCO + 2nH_2 \rightarrow (CH_2)_n + nH_2O \quad (10)$$

$$nCO + (2n+1)H_2 \rightarrow H(CH_2)_nH + nH_2O \quad (11)$$

$$nCO + 2nH_2 \rightarrow H(CH_2)_nOH + (n-1)H_2O \quad (12)$$

$$nCO + (2n-1)H_2 \rightarrow (CH_2)_nO + (n-1)H_2O \quad (13)$$

$$nCO + (2n-2)H_2 \rightarrow (CH_2)_nO_2 + (n-2)H_2O, n > 1 \quad (14)$$

$$CO + H_2O \rightleftharpoons CO_2 + H_2 \quad (15)$$

The chemical reaction behind the Fischer-Tropsch synthesis is very complex and does not refer to one end product. The reactions of the Fischer-Tropsch syncrude are displayed above and represent the basic products. Equation (10) shows the alkenes reaction that is responsible for the alkene production, equation (11) the alkanes reaction, equation (12) the alcohol reaction, equation (13) the carbonyl reaction, equation (14) the carboxyl acid reaction and (15) the water-gas shift reaction. (De Klerk et al. 2012, p.73)

The reaction mechanisms of the syncrude underlays several chain growth reactions that also interact with each other, however the controlling mechanism is still controversial. The start of the Fischer-Tropsch reaction is initiated by the chemisorption of carbon monoxide (CO) on the catalyst surface to form metal carbides. After that chain growth takes place in form of different mechanisms. (Ciobîcă et al. 2002) (De Klerk et al. 2012, pp. 74-76)

In Ciobîcă et al. (2002) and De Klerk et al. (2012, pp. 74-76) the most probable mechanisms in respect to chain growth in the Fischer-Tropsch process are explained. These mechanisms are the carbene mechanism, the oxygenate mechanism and the CO-insertion mechanism. In the *carbene mechanism,* the carbon monoxide (CO) from the syngas adsorbs and dissociates on the catalyst surface to metal-carbon and then hydrogenates to form CH_x monomers. The CH_x monomers react with each other and form mainly alkanes and alkenes. The chemical reactions of the *carbene mechanism* are shown in equation (16) to (19).

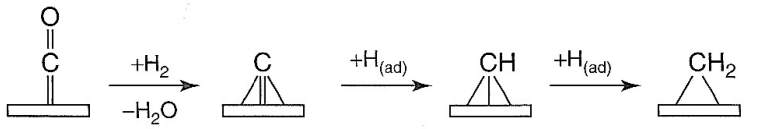

(16)

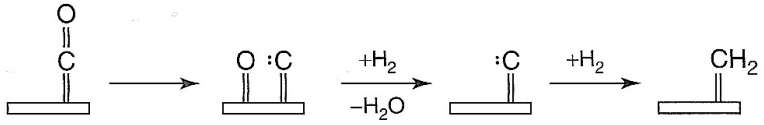

(17)

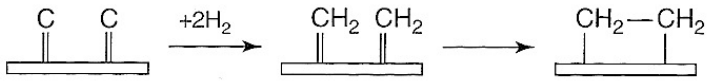

(18)

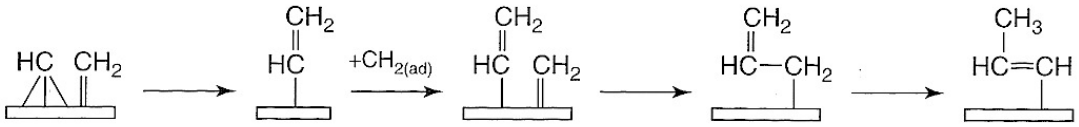

(19)

In the *oxygenate mechanism,* carbon monoxide (CO) adsorbs without dissociation and afterwards hydrogenates in various routes. After further reactions hydrogenated monomers form different end products such as alkanes, alkenes, alcohols and carboxylic acids. The chemical reactions of the *oxygenate mechanism* are shown in equation (20) to (24).

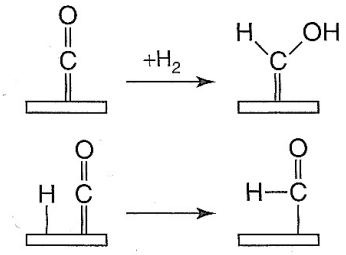

(20)

(21)

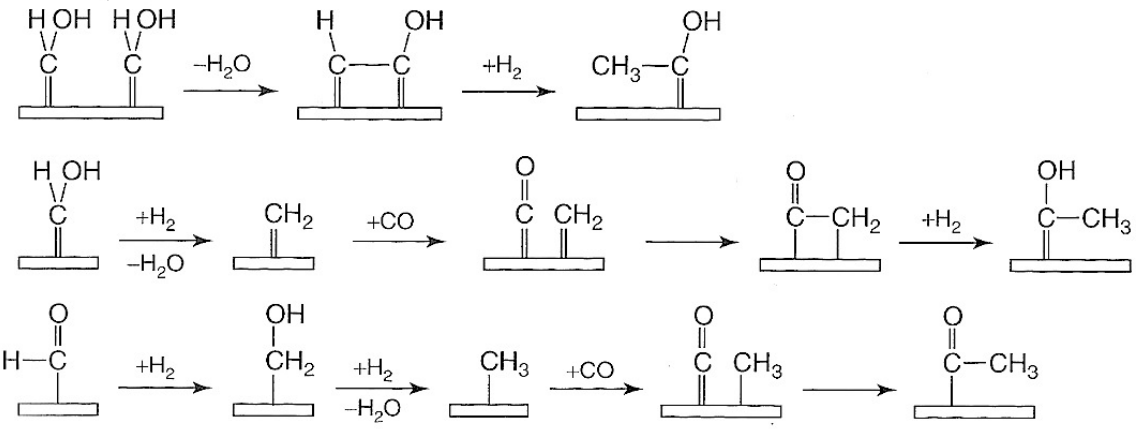

(22)

(23)

(24)

In the *CO-insertion mechanism,* carbon monoxides are inserted into the catalyst surface. The hydrocarbon monomers are built from the oxygen by products oxygenates. The chain growth termination reaction of the mechanism is not a controlled process.

It is possible to expect an estimation of the chain length with certain parameters variations and the corresponding catalysts. The chain length is important because it determines the properties of the end products. (Patzlaff et al. 1999) The estimation of the chain length distribution can be defined by the mathematical model of Anderson-Schulz-Flory (ASF). This model assumes that the chain growth probability is independent of the chain length and the growth of the chains is performed by addition or insertion of monomers as described before. The Anderson-Schulz-Flory (ASF) model implies that the chain length depends on the speed ratio of the termination to chain growth reaction. (Tavakoli et al. 2008)

Equation (25) describes the interaction of the carbon number distribution of the products and the chain growth over the catalyst.

$$x_n = (1-\alpha)\cdot\alpha^{(n-1)} \tag{25}$$

x_n molecular fraction of each carbon number in the product
α probability of chain growth
n carbon number

The chain length and the branching factor of the Fischer-Tropsch products depend on the process conditions like temperature, pressure, catalyst, the syngas H_2/CO ratio and the used reactor. (Boerrigter et al. 2003) The process conditions will be discussed in this section.

Catalyst

The typical catalysts for the Fischer-Tropsch syncrude are cobalt (Co), nickel (Ni), iron (Fe), and ruthenium (Ru). Cobalt (Co) and iron (Fe) indicate to be economically practical so they are usually used as catalysts for the synthesis. The important properties of these catalysts are a high activity and a certain selectivity for linear hydrocarbons. (Sauciuc et al. 2012)

H_2/CO ratio

The ideal syngas H_2/CO ratio for the Fischer-Tropsch synthesis is 2:1. The ratio can be adjusted by the water-gas-shift-reaction (Eq.7) in the same reactor as the Fischer-Tropsch synthesis if an iron based FT catalyst is used or by an upstream process. The process temperature is about 200-500°C in presence of an catalyst and above 900°C without a catalyst. (De Klerk et al. 2010, p.7-10)

Fischer-Tropsch operating process conditions

The Fischer-Tropsch synthesis can be realized by two main process routes. Either by the high-temperature synthesis (HTFT) or the low-temperature synthesis (LTFT). The variation in the temperature is justified by its significant influence on the product selectivity. Increasing of the temperature results in a shift of the chain length distribution to lighter products.

Hence, the high-temperature synthesis is generally used for the production of light hydrocarbons like ethylene, propylene, butenes and a gasoline and takes place at temperatures above 320°C. The low-temperature synthesis works at temperatures under 250°C and is used for the middle and heavy hydrocarbon production like diesel and waxes. (De Klerk et al. 2010, p.16-17)

Fischer-Tropsch reactor

For the Fischer-Tropsch synthesis the following three main reactors are in use. The fixed bed reactor, the fluidised bed reactor and slurry bubble column. (De Klerk et al. 2010, p.14) The slurry bubble column was used for the Fischer-Tropsch synthesis in this work and will be explained in the section 2.3.1. The fixed bed and fluidised bed reactor are explained in detail in the literature. (Maitlis et al. 2013, pp. 61-70) (Steynberg et al. 2004, pp. 64-77) (De Klerk 2010, p. 14-15) The Fischer-Tropsch plant used in this work will be described in detail in the following section.

2.3.1 Fischer Tropsch Synthesis at Güssing

The Fischer Tropsch plant is important for further conversion of the synthetic gas that was produced and cleaned at the gasification plant Güssing. For more details about the gasification plant and the pre-cleaning see chapter 2.2.4. The Fischer Tropsch plant consists of gas cleaning units and conversion units to get liquid and heavy fuel products from the syngas. The schematic Fischer-Tropsch plant is represented in figure 11. (Sauciuc et al. 2011)

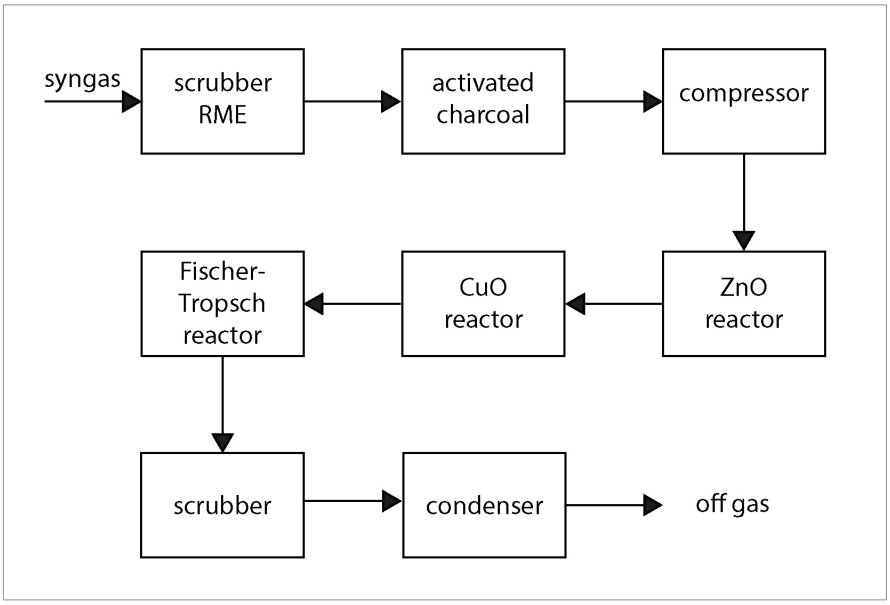

Figure 11: Simplified schematic illustration of the Fischer-Tropsch process (Sauciuc et al. 2011)

The main parts of the Fischer Tropsch plant are:

- Rapeseed Methyl Ester (RME) scrubber
- Activated charcoals
- Compression
- Catalytical cleaning (with various fixed bed reactors like ZnO, CuO).
- Slurry Fischer-Tropsch reactor
- Off-gas scrubber
- Off-gas condenser

Rapeseed Methyl Ester (RME) scrubber

The syngas (table 3) leaves the gasification unit and enters the Rapeseed Methyl Ester (RME) scrubber in counter flow with 70°C. The scrubber is a conventional packed column with structured packings. At the scrubber, water and the last remaining residues of tars and dust were removed from the syngas. As gas cleaning agent solvent rapeseed methyl ester was used because of its capability to remove water and impurities from the syngas. (Hofbauer et al. 2005, pp.57-69)

Activated charcoal adsorber

The charcoal adsorber is essential to remove the sulfur compounds from the syngas because sulphur can deactivate the Fischer-Tropsch catalyst. The charcoal is formed of pellets with an approximate length of 0.7 cm and a diameter of 0.3 cm. The activated charcoal adsorbs the most sulfur compounds and most of the aromatic compounds in the syngas. (Götz 2010, pp. 19-25)

Catalytical cleaning

Before the syngas enters the fixed bed reactor of ZnO and CuO it gets compressed in two steps up to 28 bar. First, with a diaphragm pump and afterwards with a compressor. This is necessary for a better adsorption. The gas cleaning is important to remove the remaining sulfur compounds in the syngas to prevent a deactivation of the Fischer-Tropsch catalyst. The precisely gas cleaning can be done with the chemisorption of hydrogen sulfide on metal oxide. For the chemisorption a fixed bed adsorption reactor with zinc-oxide (ZnO) catalyst and then a cupper-oxide (CuO) catalyst were used. The reaction temperature is 230°C for the zinc-oxide chemisorption and about 70°C for the cupper sorption. In case of deactivation of the catalyst, the metal oxides could be regenerated by oxidation. (Götz 2010, pp. 19-25)

Slurry Fischer-Tropsch reactor

The Fischer Tropsch synthesis is carried out in a slurry bubble column reactor. In the reactor, the cleaned syngas was introduced at the bottom via a gas distributor into the suspension. The suspension consists of liquid product waxes, which bear solid catalyst particles. In the reaction chamber the gas rises in form of bubbles through the suspension, where the reactants diffuse out of the gas phase through the liquid phase to the catalyst surface, and react there. Since the reaction is highly exothermic, the heat can be removed by cooler tubes, which also where used to generate steam via heat exchanger. The gaseous reaction products exit at the top, the liquid products (wax) in the middle of the reactor. Filters are installed at the reactor gate to separate the catalyst particles from the liquid Fischer-Tropsch products. Low-temperature synthesis (LTFT) was used as operating process condition, which is convenient for the production of heavy hydrocarbons such as waxes. The reaction temperature is 240°C, the pressure 20 bar and the used catalyst is cobalt with a mass of 2,5 kg. The reactor has a height of 2,5 m and an inside diameter of 10 cm. The reactor is heated from the outside and is insulated with ceramic bowls. (Götz 2010, pp.19-25)

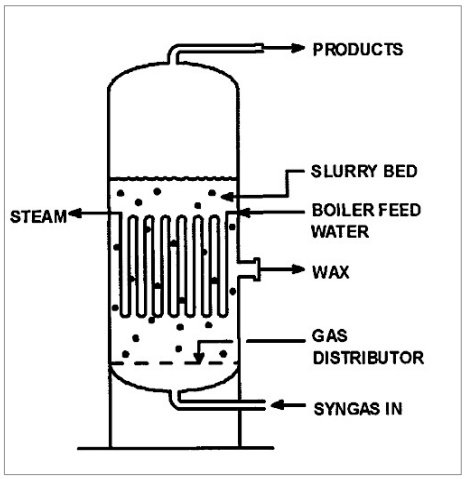

Figure 12: Slurry Fischer-Tropsch reactor (Steynberg et al. 2004, pp. 71)

Off-gas scrubber

At the off-gas scrubber the Fischer-Tropsch gas (off-gas) gets neutralised and separated from remaining waxes residues. The scrubber is similar to the Rapeseed Methyl Ester (RME) scrubber and has also structured packings. The solvent is water with a small amount of potassium hydroxide (KOH), because the product gas is acidic so it can simultaneously get neutralised. The water condenses the residues of the waxes in the gas. The benefit of water as a solvent is that it does not mix with the waxes and keeps part of the waxes in the liquid phase for better transport. (Götz 2010, pp.19-25)

Off-gas cooler

The off-gas condenser cooled the gas down to 0°C thereby all remaining light Fischer-Tropsch products could be collected at the bottom of the condenser. These light products are usually naphtha and part of diesel fraction but can also remain water vapour. (Götz 2010, pp. 19-25)

2.3.2 Fischer-Tropsch Products

The Fischer-Tropsch process has a wide product range. It reaches from light hydrocarbons like gasoline with a carbon number of C_2-C_5, middle hydrocarbons such as kerosene and diesel with a carbon number of C_5-C_{35} and heavy hydrocarbons like biowaxes with a carbon number higher than C_{35}. (Speight 2011, pp. 245) The Fischer-Tropsch fuels contain also very low aromatic, sulfur and nitrogen compounds, which is ideal for further treatment. (Dupain et al. 2005) The Fischer-Tropsch products cannot be used directly as fuels so they need several refining steps. These steps are usually downstream distillation or fractional distillation. (Hofbauer et al. 2005)

Of particular interest is the high amount of biowax fraction, which can be constitute up to 50% of the crude product. The biowaxes consist of linear long chain hydrocarbons, which are basically composite of liner alkanes and few quantities of other compounds that can be formed at the Fischer-Tropsch process. The biowaxes can be refined in various ways of cracking such as thermal cracking and catalytic cracking. The biowaxes were cracked via hydroprocessing and catalytic cracking, which will be explained in detail in the following chapter 2.4.

2.4 Cracking

At the Fischer-Tropsch synthesis a high amount of biowaxes is produced. This begs the question of how to convert the long-chain hydrocarbon waxes into short hydrocarbons to get the required biofuel. This can be realized through the cracking process, where long-chain hydrocarbons are converted into low-boiling products. Thereby primarily C-C but also C-H bonds get broken and form saturated and unsaturated shorted hydrocarbons. Increasing temperature changes the position of the breaking point. Fractures occur at low temperatures such as 400 - 600°C in the middle of the chain, the higher the temperature the more likely the chain splits asymmetrically, in a smaller and larger fragment. (Latscha et al. 2008, pp. 483) Mainly three commercial types of cracking processes are in use. Thermal cracking, catalytic cracking and hydrocracking (hydroprocessing).

Their diversity is primarily based on process conditions such as temperature, pressure and nature of the atomic sphere. The cracking process will be described in detail in the following section. The Fischer-Tropsch biowaxes of the experiments in this work were cracked mainly via catalytic cracking and hydrocracking (hydroprocessing), which will be explained in this chapter in the section 2.4.2 and 2.4.3. (De Klerk. 2010 pp.115)

2.4.1 Thermal Cracking

Thermal cracking is a cracking process mainly influenced by the temperature. Thereby C-C and then C-H bonds of long-chain hydrocarbon start to crack at approximately 400°C. The total reaction of the thermal cracking proceeds by a free radical mechanism. Based on initiated vibration through the temperature a bond cracks and forms two hydrocarbon radicals. These radicals react next to the abstraction of hydrogen, with disproportionation and recombination and form shorter hydrocarbons (Figure 13-17) (Wollrab 2009, pp. 281-282)

Hydrogen-Abstraction mechanism:

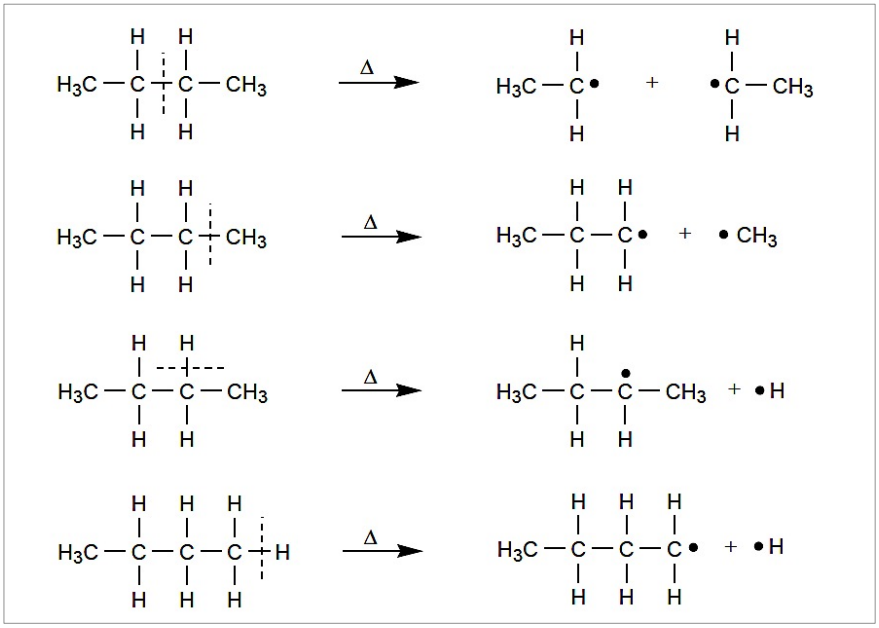

Figure 13: Example reaction of Hydrogen-Abstraction Mechanism (Wollrab 2009, pp. 281)

Termination Reactions:

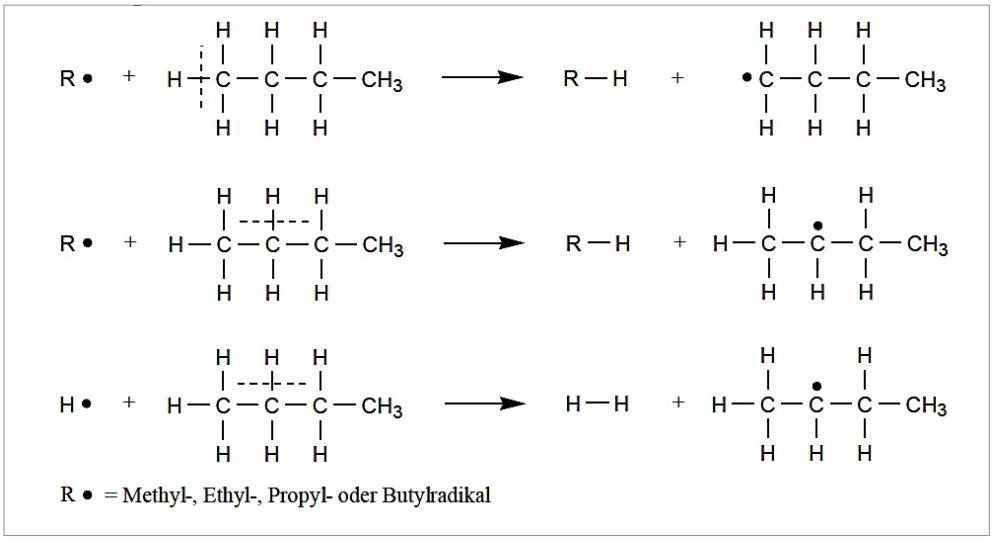

Figure 14: Example reaction of Termination Mechanism (Wollrab 2009, pp. 282)

Recombination Mechanism:

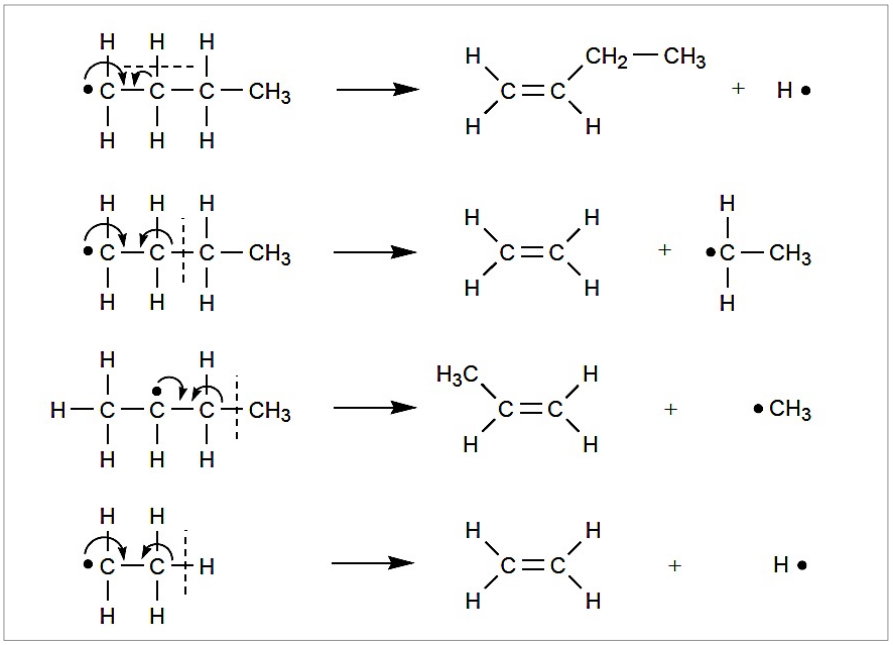

Figure 15: Example reaction of Recombination Mechanism (Wollrab 2009, pp. 282)

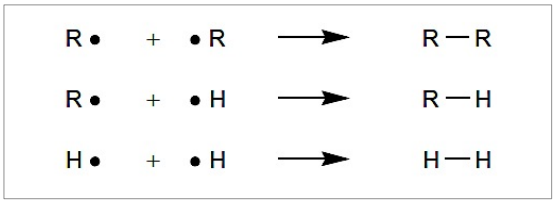

Figure 16: Recombination Mechanism (Wollrab 2009, pp. 282)

Disproportionation Mechanism:

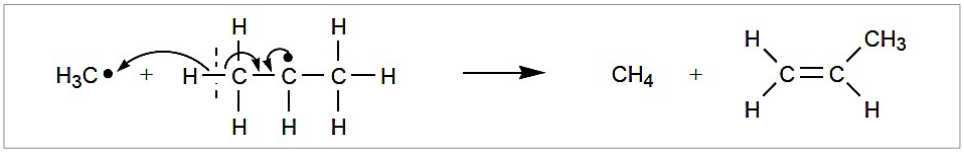

Figure 17: Example reaction of Disproportionation Mechanism (Wollrab 2009, pp. 282)

2.4.2 Catalytic Cracking Process

Catalytic cracking is equated to thermal cracking in the presence of a catalyst. The cracking process takes place mainly in fluidised bed reactors to prevent coke formation that inactivates the catalyst. (Latscha et al. 2008, pp. 483) The advantage of the catalyst gives the possibility to crack the long-chain hydrocarbons at lower temperatures. For the cracking process especially catalysts like synthetic zeolite based aluminosilicate were used, see chapter 2.5. and 3.2.1 for more details. The reaction proceeds via carbenium ion mechanism, which results in a high percentage of branched hydrocarbons, which are ideal for the fuel production. Cracked bonds caused by catalytic cracking form carbenium ions after intermediate steps (Eq.26), which form alkenes and alkanes as end products through alkylation. Equation (27) represents the alkylation, (28) the alkanes reaction and (29) the alkenes reaction. (Wollrab 2009, pp. 285)

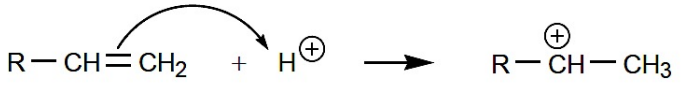

(26)

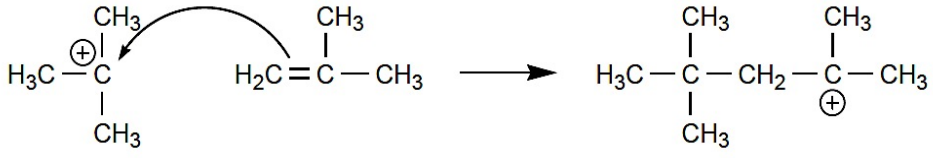

(27)

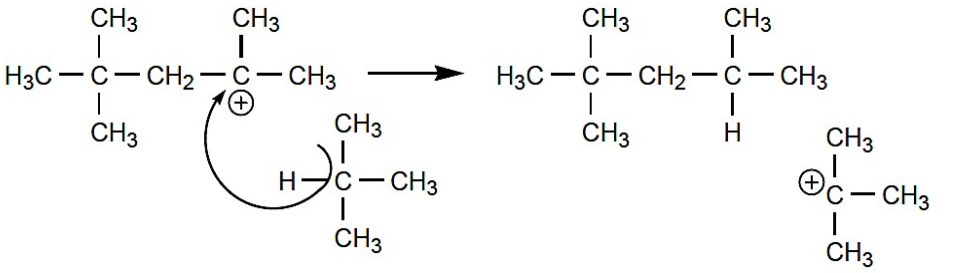

(28)

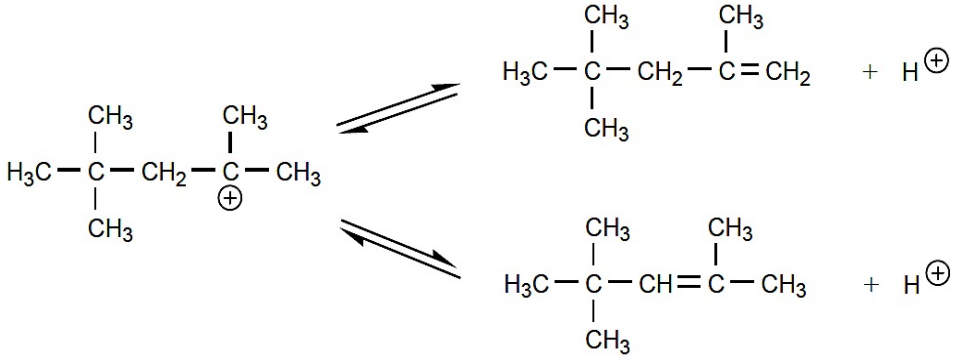

(29)

2.4.3 Hydroprocessing (Hydrocracking)

Hydrocracking accords to the same principle as catalytic cracking but is superimposed with hydrogenation due to it taking place in hydrogen atmosphere. (Scherzer et al.1996, pp. 75) The process operates in a wide temperature (270-450°C) and pressure range (80-200 barg). The hydrocracking mechanism is selective for the crack-ability of long-chain hydrocarbons and was used for wax cracking (>C_{21}) in the experiments in this work. (Weissermel et al. 2008, pp. 60) The cracking mechanism is depending on the used catalyst. Catalysts used at the hydroprocessing will be elaborated in chapter 2.5. The reaction mechanism is initiated by the carbenium-ionic mechanism, which is coupled with isomerisation and hydrogenation. An example for the reaction mechanism is showed below. (Marafi, et al. 2010, pp. 22)

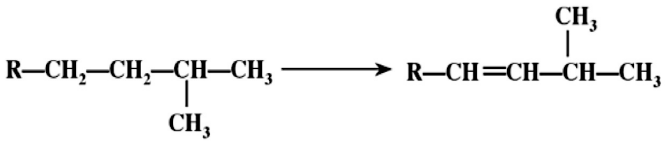

(30)

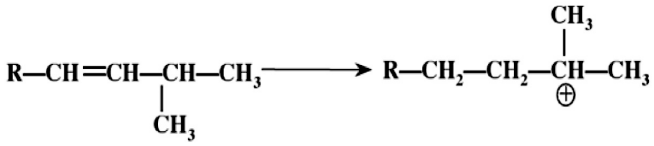

(31)

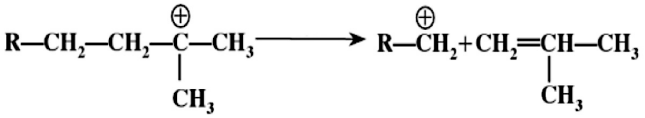

(32)

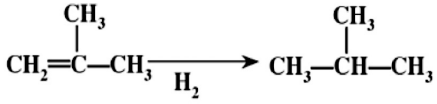

(33)

The equation (30) shows the formation of an alkene. This formation initiates the start of the hydroprocessing mechanism. The next step is the protonation of the alkenes, which form carbenium ions (Eq.31). Then the carbenium ions isomerise and crack to smaller linear hydrocarbons (Eq.32). The last step is the hydrogenation as shown in equation (33). The end product can crack always further and produce smaller products. (Jones et al. 2006, pp. 295-296)

2.5 Catalyst for the Cracking Process

The typical catalysts for a catalytic cracking process are natural or synthetic zeolite based aluminosilicate catalysts. Zeolite is a porous material based on a pore channel system with different shapes like Y, Z or X, which can be one-, two or three-dimensional structured. Zeolites consist entirely of aluminum, silicone and oxygen atoms. The aluminum, which is bound as a metal oxide in the zeolite, provides the strong acidity of the catalyst. The acidity is one of the important properties of zeolites, it defines the acidity of the catalyst and depends on the microstructure of the zeolite. Other main properties are shape selectivity, which is unique for the zeolite and is based on the molecular sieving properties of the zeolite. The shape properties determine based on the pore size, which molecules get cracked. Also the loading properties of the zeolite are significant because they influence the acidity of the catalyst. (Niwa et al. 2010, pp. 1-7)

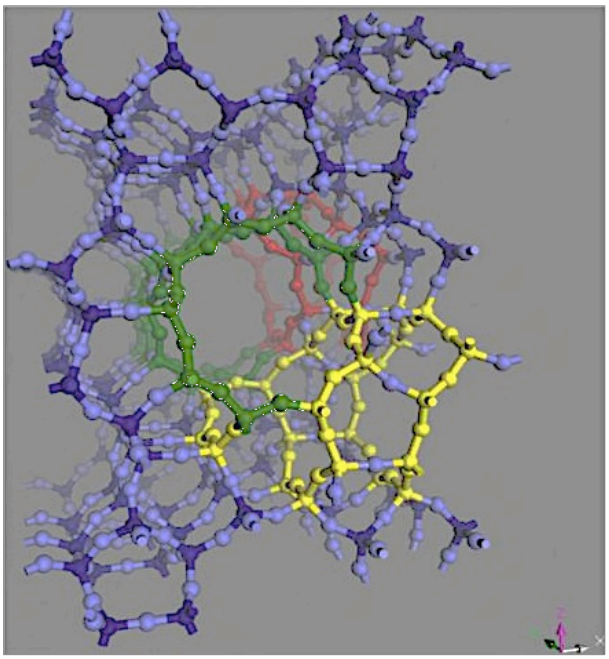

Figure 18: 3D Zeolite structure of ZSM-5 (MFI) from Y-axis (Niwa 2010, pp. 4)

For hydroprocessing of heavy wax feeds usually dewaxing catalysts are used. Dewaxing catalysts are carried out as bifunctional catalysts, which improve some fuel properties such as cold flow properties. (Scherzer et al.1996, pp. 223-224) Bifunctional catalysts, also called dual function catalysts, have a metal and acid side. The metal side has a hydrogenating function and the acid side an acid function. The typical reactions are hydrogenating on the metal side (Eq. 33) and isomerisation and cracking on the acid side (Eq.32). (Jones et al. 2006, pp. 295-296) The hydrogenating components can be non-noble metals like nickel but also aluminum or noble metals like platinum. (Ribeiro et al.1984, pp. 398)

2.5.1 Catalyst Deactivation

Catalysts can decrease their activity during the cracking process. The main types of deactivation mechanisms are poisoning, coke formation and sintering. Poisoning occurs at sulfur- or nitrogen containing feedstocks. Sintering describes the deactivation through structure alteration of the catalyst. The coke blocks the active sites on the surface of the catalyst and can also plug the pores of the catalyst. Deactivation by coke formation is the common mechanism at the conversion of hydrocarbons. The coke reactions are very complex, however the coke formation originates at the cracking mechanism and forms organic byproducts, which deposits as coke on the catalyst. Thermal treatment needs to be performed in order to regenerate the catalyst. This can be done in regular intervals. (Scherzer et al.1996, pp. 112-115)

2.6 The influence of cracking on the fuel properties

The molecule structure and chain length define the properties of a compound. Properties can be influenced by the used feedstock or process conditions like temperature, pressure and by a catalyst. The most important properties of kerosene were described in chapter 1.1. This section describes how kerosene properties can be influenced by the cracking process.

The most important property for an aviation fuel is the cold flow property freezing point (cloud point, pour point) of the fuel. It can be influenced by catalysts with isomerisation abilities, which isomerise and crack linear hydrocarbons to branched hydrocarbons. Branched hydrocarbons have a low freezing point due to their structure. The jet fuel specification for the freezing point is given in table 1. (Speight 2011, pp. 378) (Jones et al. 2006, pp. 311) (De Klerk 2012, pp. 276)

The flash point and viscosity depend in the broadest sense on the carbon number and chain length of hydrocarbons. Both can be influenced by the process condition like temperature, pressure and the catalyst. The carbon number decreases with increase of the branched hydrocarbons. During the cracking process the process condition and the catalyst can partly regulate the mechanism and shift the outcome distribution to the required end product. (McElroy 2009, pp. 126) (De Klerk 2012, pp. 275, 290)

The smoke point depends on the chemical structure of the fuel. Linear paraffines have a high smoke point so a catalyst without isomerisation abilities would be optimal to avoid branching of the hydrocarbons. This is a contradiction to the cold flow properties and therefore additives need to be added to meet the jet fuel specification. Also to increase the density of biokerosene aromatics need to be added to meet the jet fuel specification. (Wauquier 2001, pp.127) (De Klerk 2012, pp. 276,492)

3 EXPERIMENTAL PART

3.1 Wax Feedstock

For proper investigation two feedstocks of biowax were investigated. The Fischer-Tropsch biowax were produced at the Fischer Tropsch plant Güssing and were linear highly paraffinic biowax with melting points of 95°C and 132°C. The wax with a melting point of 95°C was used for the catalytic cracking process because the unit was not constructed for the handling with higher temperatures. The biowaxes with the melting point of 132°C were converted in the hydroprocessing plant.

The biowax had a total volume of 200l and it has been transported in seven bottles to the research centre in Thessaloniki. A boiling range distribution was done with a simulated distillation (SimDist) of every bottle. The simulated distillation is explained in detail in the literature (Osenbach 2010). The results are shown in Appendix A.

3.2 Catalysts

The catalysts were used for the cracking reactions during the upgrading process. Based on the characteristics of a catalyst one or more product-groups are produced. Linear, high paraffinic biowaxes are converted into biokerosene by cracking and isomerising. The isomerisation ability of the catalyst is of significance in order to obtain branched hydrocarbons.

3.2.1 Catalyst for Catalytic Cracking

H-ZSM-5 Catalyst

The used catalysts for the catalytic cracking process were conventional zeolite based aluminosilicate catalysts. These catalysts are porous material with a three-dimensional tetrahedral structure with aluminum and silicon atoms. (Argauer 1972) The H-ZSM-5-23 with ratio 23/77 of SiO_2/Al_2O_3 and H-ZSM-5-28 with ratio 80/20 of SiO_2/Al_2O_3 were the catalysts used. The H-ZSM-5-23 was a high acidic catalyst due to its high amount of Al_2O_3; the other was a less acidic. For the experiments, ZSM-5 catalysts were applied, because they are capable of cracking waxy feedstocks with a high conversion rate. (Triantafyllidis et al. 2007)

3.2.2 Catalysts for Hydroprocessing

Ni/Mo Catalyst

The nickel-molybdenum catalyst was used for the hydroprocessing experiments. It contained nickelmonoxide and molybdenumtrioxide. The catalyst has significant qualities, which are highly selectivity, good regeneration procedure and resistance to catalyst poison. (Gary et al. 2001, pp.165) The catalyst is convenient for the cracking process but not so much for the upgrading through isomerisation.

Dewaxing Catalyst

For dewaxing a zeolite based catalyst was used, in this case for the selective hydrocracking of linear, heavy paraffines. It is also suitable for the isomerisation of the Fischer-Tropsch biowaxes. The isomerisation ability of the dewaxing catalyst depends mainly on their pronounced molecular shape selectivity. (Bouchy et al. 2009)

3.3 Catalytic Cracking Experiments

The catalytic cracking experiments were performed at the research centre CERTH/CERPI in Thessaloniki. The experiments were performed to evaluate the ability of producing biokerosene via catalytic cracking in the boiling range of 150°C and 300°C. To find the optimum process conditions for catalytic cracking a parameter variation of the temperature was done. The experiment results are shown in Appendix B.

3.3.1 Experimental Unit

The tests were performed in a bench scale automated fixed bed unit (SCT-MAT) (Figure 19) at Certh. The unit consists of a reactor, an injection system with a heater, a product receiver and a special motor pump for the injection. The reactor of the unit was heated to the reaction temperature by a three-zone furnace. At the end of the reactor the liquid products were collected in a receiver, which were cooled with water. The gas product was trapped in a gas collection vessel for further analyses. (Lappas et al. 2004)

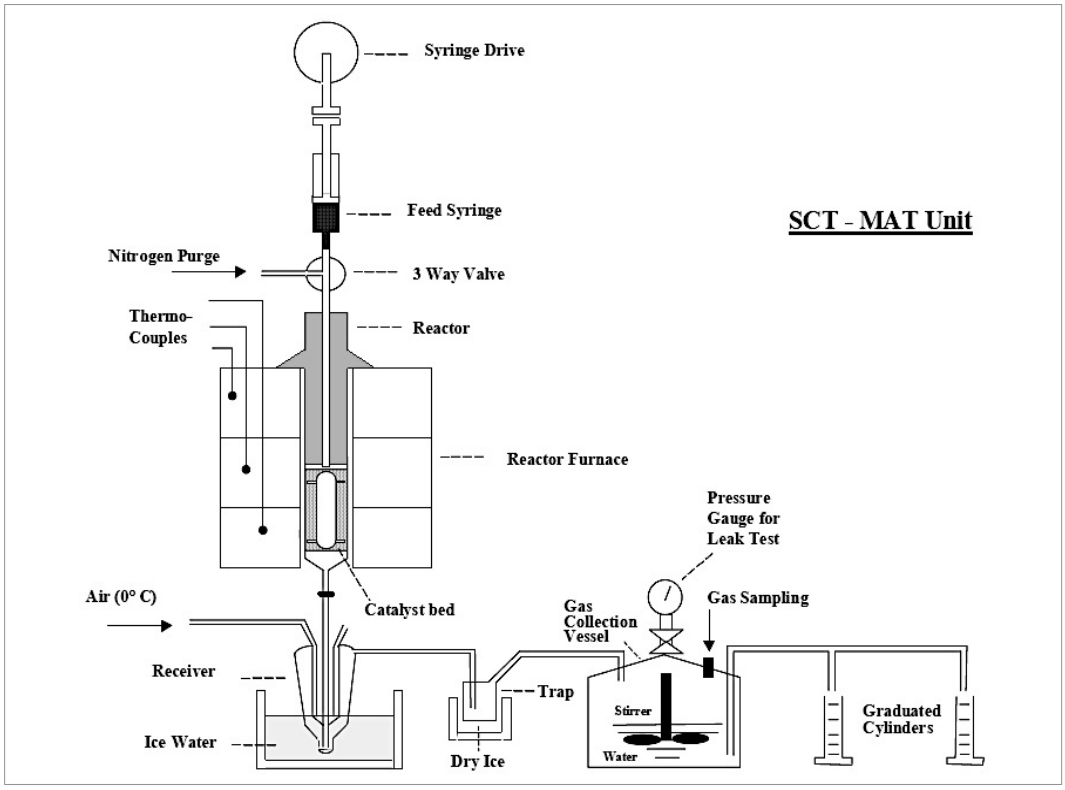

Figure 19: Schematic figure of short contact time micro activity test (SCT-MAT) unit for catalytic cracking of biowaxes (Lappas 2005)

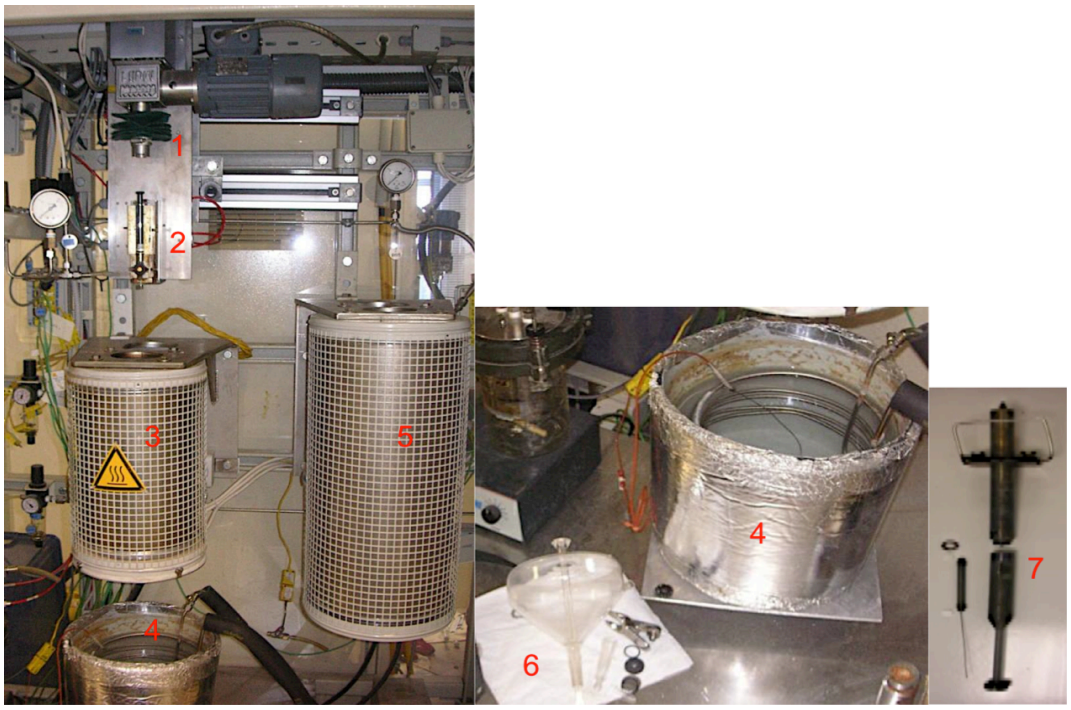

Figure 20: Picture of short contact time micro activity test (SCT-MAT) unit for catalytic cracking of biowaxes

1. Motor pump
2. Injection system with a heater
3. Three-zone reactor furnace
4. Water bath were the product got cooled
5. Second three-zone reactor furnace for preheating of the reactor
6. Receiver for the product
7. Reactor

The catalytic cracking experiments were carried out with two different catalysts and different temperatures to see the crack ability of the Fischer-Tropsch biowaxes. The Fischer-Tropsch biowaxes with the lower melting point of about 95°C were used for the experiments in the SCT-MAT unit. This was necessary because the unit was not constructed for a handling with higher temperatures. The samples were taken from each feedstock container (sample number 509-2 in Appendix A) with the lower melting point. The used catalysts were a ZSM-5 zeolite with SiO_2/Al_2O_3 with ratio 23/77 (high acidic) and another with ratio 80/20 (less acidic), see chapter 3.3.1 for more details. The preparation of the reactor started with the fixed bed, which consists of the catalyst and glass beads. The catalyst was mixed with glass beads to avoid a temperature gradient within the catalyst bed during the experiment. The total volume of the fixed bed was 10 ml. First, 0.9 g of the catalyst was filled in a bottle additional inert glass beads were added until the 10 ml mark. The mixture was blended until they were homogeneous usually for 10 min. Next the reactor was opened and a pad was put at the bottom of the reactor. These pads were used for the stability and to provide leak out of the bed. The reactor was filled with the mixture of catalyst and glass beads and after another pad was put at the top of the bed, the reactor got closed. Afterwards the reactor was preheated to the operating temperature by the three-zone furnace. The reactor got connected with the nitrogen to purge during the heating to prohibit a bed condensation. When the temperature of the reactor reached the required temperature the reactor was moved to the three-zone furnace and got connected to the nitrogen. In the mean time the syringe was filled with exactly 1.8g of molten biowax. The unused volume in the syringe was filled with N_2. The reactor was injected with the biowax from the syringe. The heater at the injection system was used in order to preheat the waxes for an easy injection. Before the experiment started a pressure test was done. When the unit passed the pressure test the injection started. The time window for the injection was 12 seconds within these seconds the wax had to be fully injected into the reactor. The reaction time was 420 seconds and afterwards a pressure test was done to check if the experiment has proceeded properly. At the end of the experiment the unit was depressurized and products were collected in a receiver, where they were separated into liquid and vapour products. The vapour products were analysed by a gas chromatograph and the liquid product by simulated distillation. The experiments were repeated at different temperatures (see table 5 and 6).

Parameter variation with catalyst ZSM-5 SiO_2/Al_2O_3 with ratio 23/77

	RUN1	RUN 2	RUN 3	RUN 4	RUN 5	RUN 6	RUN 7	RUN 8	RUN 9
Temperature [°C]	560	560	460	460	410	410	360	360	360
C/O*	1,10	0,45	0,50	0,50	0,50	0,49	0,51	0,59	0,49

Table 5: Parameter variation of catalytic cracking

*C/O……Catalyst to Oil ratio

Parameter variation with catalyst ZSM-5 SiO_2/Al_2O_3 with ratio 80/20

	RUN1	RUN 2	RUN 3	RUN 4	RUN 5	RUN 6
Temperature [°C]	460	460	410	410	360	360
C/O*	0.51	0.51	0.50	0.51	0.55	0.50

Table 6: Parameter variation of catalytic cracking

*C/O……Catalyst to Oil ratio

3.4 Hydroprocessing experiments

The hydroprocessing experiments were performed at the research centre CERTH/CERPI in Thessaloniki. The experiments were performed to evaluate the ability of producing biokerosene via catalytic cracking in the boiling range of 150°C and 300°C. To find the optimum process conditions for hydroprocessing a parameter variation of the temperature was done. The experiment results are shown in Appendix C.

3.4.1 Experimental Unit

The hydroprocessing experiments were done in a fully automated hydrodesulphurisation pilot plant unit. The main parts of the pilot plant unit for the hydroprocessing tests were a reactor for the fixed bed, a vessel with a heat system, a heated distributer pipe system, a specific pump for high temperatures and waxes, a pipe double cooler, a separator and a distillation column. (Lappas et al. 2004)

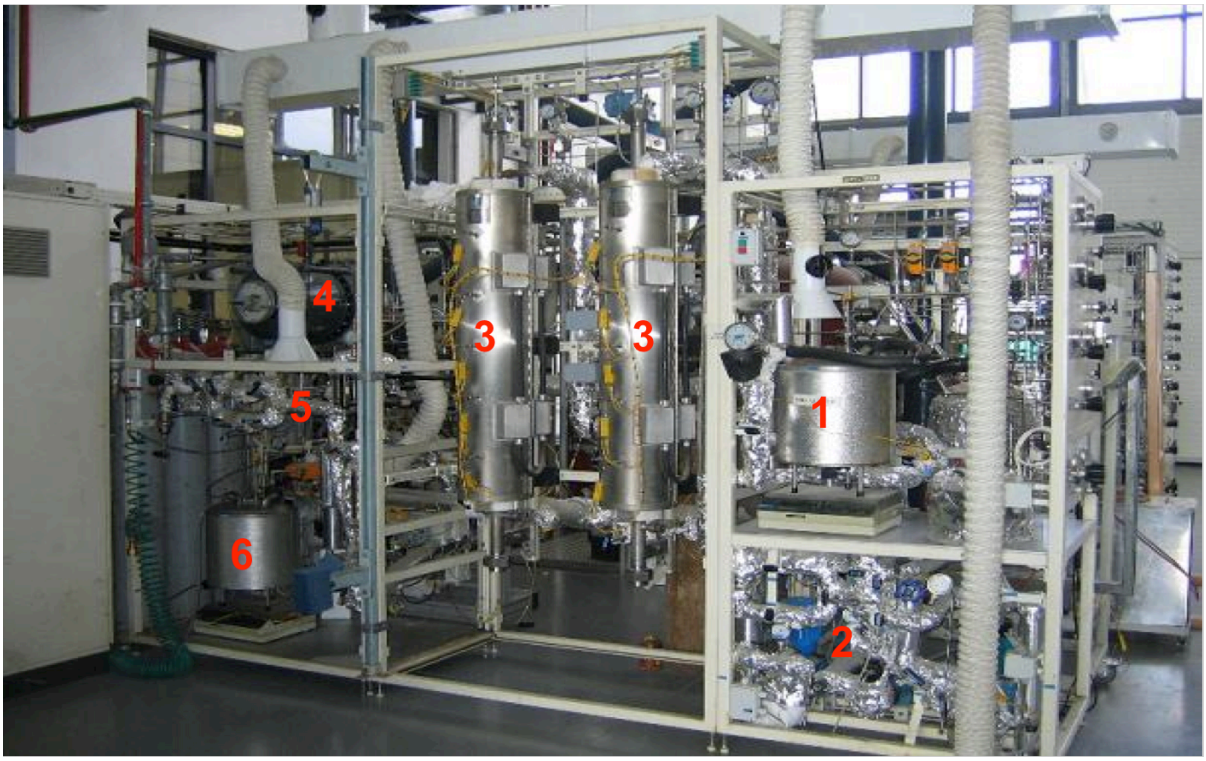

Figure 21: Hydrodesulfurisation pilot plant unit used for hydroprocessing of biowax

1. Vessel with heat system
2. Feed distribution system
3. Reactor
4. Gas volume counter
5. Double pipe cooler
6. Product vessel

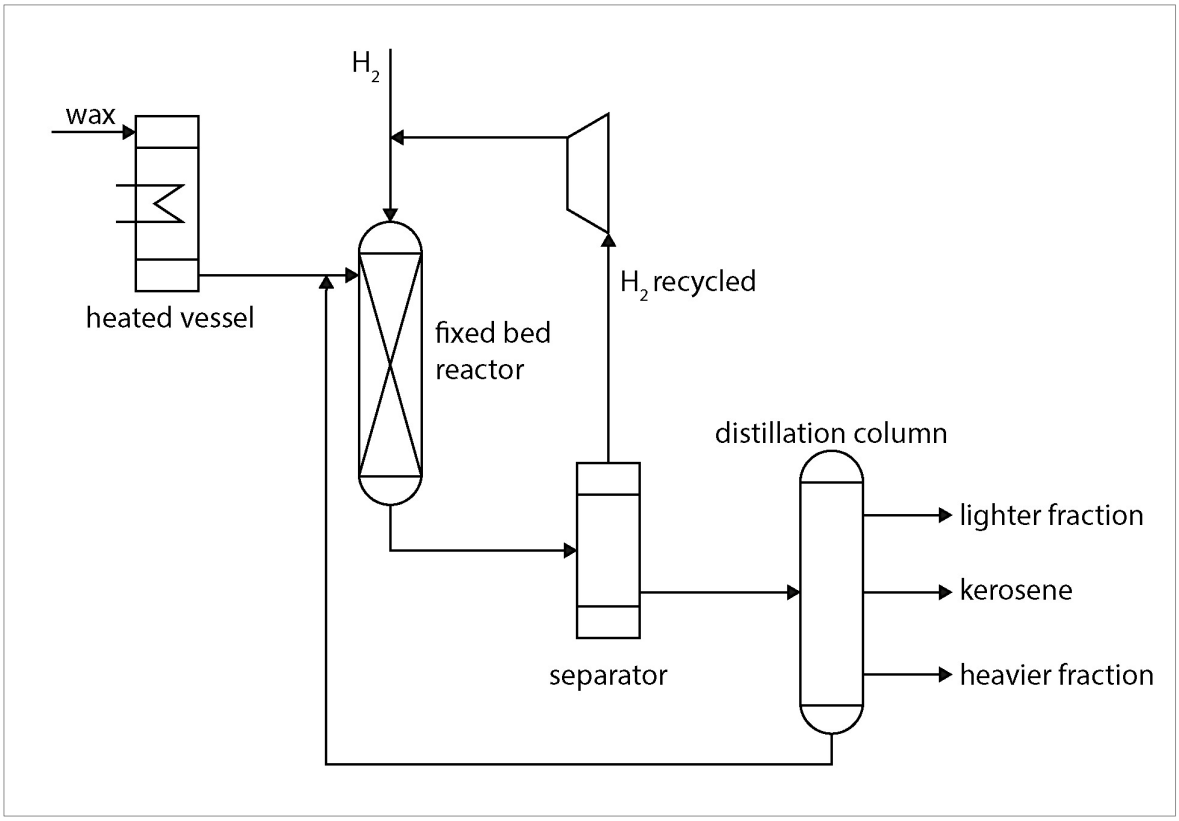

Figure 22: Simplified flow sheet of the hydroprocessing plant

The tests were done in a fixed bed reactor with two different catalysts at high temperature and high pressure conditions in a hydrogen atmosphere. The Fischer-Tropsch biowaxes with a melting point about 132°C were used for the experiments. The fixed bed consisted of a nickel - molybdenum (Ni/Mo) catalyst or a dewaxing catalyst mixed with silicone carbide (SiC). The nickel - molybdenum catalyst had the original size of 1mm and needed to be crashed into 250-500μm. The crushing ensued by hand because the particles were to hard for the crushing machine and were also sieved by hand as well. The dewaxing catalyst had the right size for an optimal homogeneous mixture with the silicone carbide (SiC). The whole amount of catalyst in the reactor was 200 g the rest was silicone carbide (SiC) that was added to a total volume of 555g. The reactor was separated in five zones (Figure 23). At the top and the bottom zone it was only filled with silicone carbide (SiC). The three other zones of the reactor were filled with the mixture of catalyst and silicone carbide (SiC). After the fixed bed of the reactor was set, the catalyst required a proper activation. The activation for both catalysts was the same, they were preheated with nitrogen and afterwards sulfurized with 0,1wt% dimethyl-disulphide (DMDS) relative to sulphur content. When hydrogen sulphide (H_2S) was detected in the gas flow the temperature was increased. First, the increase was up to 350°C and afterwards up to the required reaction temperature for the experiments.

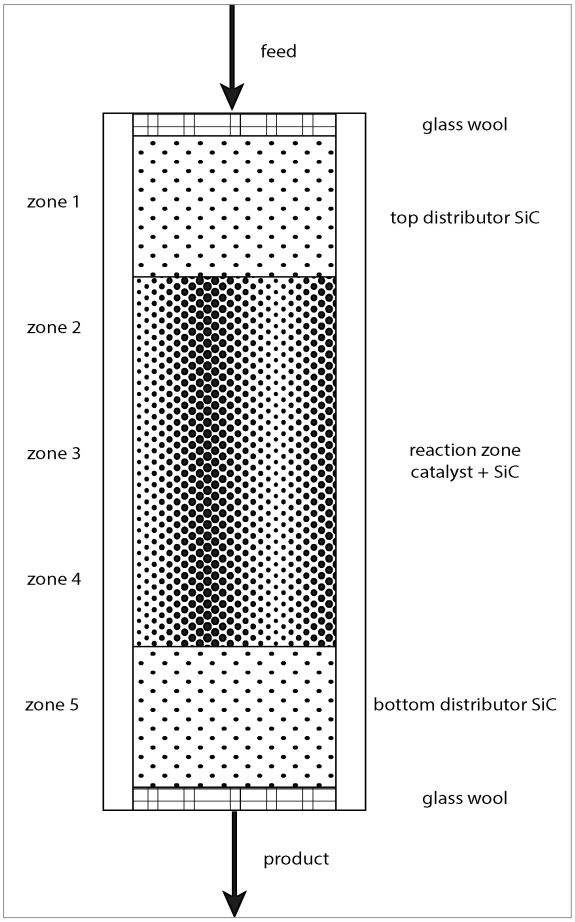

Figure 23: Hydroprocessing reactor

After the activation of the catalyst a pressure test was done with helium (He) at 100 barg to exclude a leak at the reaction side of the unit. For the hydrogen atmosphere the hydrogen gas was transported in the reactor by a feed system. Then the Fischer-Tropsch biowax was sliced and placed in a 65l heatable vessel. It was not possible to melt and homogenise the whole biowaxes because the amount of 200l was not able to fit in the heatable vessel. The 65l biowaxes were melted in the vessel and pumped through the heated pipe systems to the reactor inlet to the fixed bed where the cracking reaction took place. The product was transported to a separator for the separation of the hydrogen. Then the product was led through a double pipe cooler to a distillation column where gas and liquid products were separated. The liquid and gas products were analysed in analytical facilities at Certh.

During the experiments pressure and liquid hourly space velocity (LHSV) were kept constant. Meanwhile the temperatures were varied to find the optimal process conditions.

Experimental conditions hydroprocessing with Ni/Mo catalyst

	RUN 1	RUN 2	RUN 3
LHSV [h^{-1}]	1	1	1
Pressure [barg]	70	70	70
Temperature [°C]	350	380	450

Table 7: Experimental conditions of hydroprocessing

Experimental conditions hydroprocessing with Dewaxing catalyst

	RUN 1	RUN 2	RUN 3	RUN 4	RUN 5	RUN 6	RUN 7
LHSV [h^{-1}]	1	1	1	1	1	1	1
Pressure [barg]	70	70	70	70	70	70	70
Temperature [°C]	300	350	350	325	325	375	375

Table 8: Experimental conditions of hydroprocessing

4 RESULTS

4.1 Definitions

Kerosene

In this work the kerosene fraction is assumed to have a boiling range from 150°C to 300°C.

Conversion

Conversion represents the fraction of the reactant, which has reacted. (Towler et al. 2013, pp. 48) The conversion is defined as:

$$Conversion = \frac{amount\ of\ reactant\ consumed}{amount\ of\ reactant\ supplied}$$

Selectivity

Selectivity is given by the efficiency, converting the reactant to the required product. (Towler et al. 2013, pp. 49) The selectivity is defined in this work as 100% liquid with a content of kerosene, gasoline and diesel.

$$Selectivity = \frac{amount\ of\ product\ formed}{amount\ that\ could\ have\ been\ formed\ with\ all\ the\ used\ reactant}$$

Yield

The yield is described as the product of the conversion and selectivity. (Towler et al. 2013, pp. 49)

$$Yield = Conversion \cdot Selectivity$$

Fraction yield

Fraction yield is the yield calculated as described above for each fraction, e.g kerosene yield is the yield of the kerosene fraction.

4.2 Catalytic Cracking Results

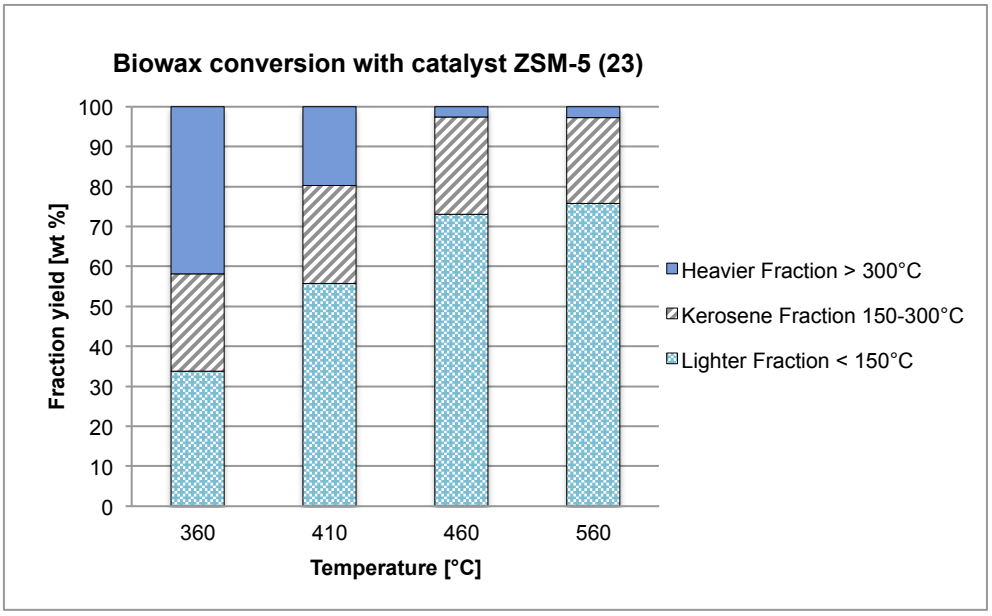

Figure 24: Conversion with the high acidic catalyst ZSM-5 (23) at different reaction temperatures (360°C, 410°C, 460°C, 560°C) at catalytic cracking

Figure 24 shows the composition after the catalytic cracking at different reaction temperatures done with ZSM-5 (23), which was the highly acidic catalyst. The mass content of the heavier fraction decreases with higher reaction temperature due to the fact that molecules crack more often. This results in a shift to lighter fraction since smaller molecules are formed. It can be assumed that middle chain length hydrocarbons get cracked to smaller ones and long chain hydrocarbons to middle chain hydrocarbons. This results in an almost constant kerosene yield at all temperatures through the experiments. At a temperature of 560°C, a high amount of coke was produced which blocked the reactor. Therefore, the experiments at 560°C were not repeated with the low acidic catalyst ZSM-5 (80).

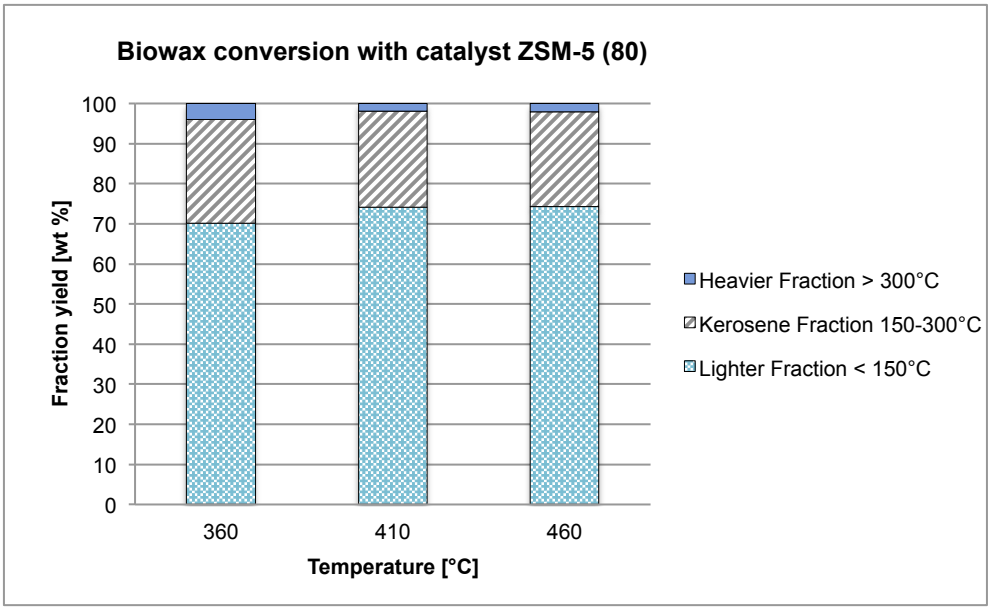

Figure 25: Conversion with the low acidic catalyst ZSM-5 (80) at different reaction temperatures (360°C, 410°C, 460°C) at catalytic cracking

Figure 25 shows the composition after the catalytic cracking at different reaction temperatures done with ZSM-5 (80), which was the low acidic catalyst. The fraction yield of all three fractions was near constant over the analysed reaction temperatures, thus, a temperature independency of the crack ability of the catalyst can be assumed.

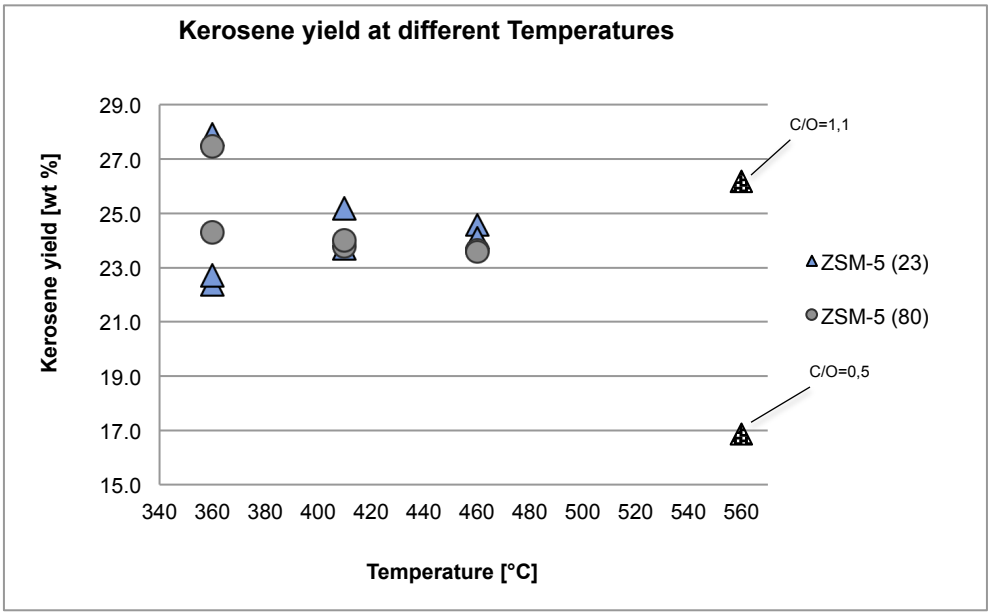

Figure 26: Kerosene yield at different reaction temperatures (360°C, 410°C, 460°C, 560°C) at catalytic cracking. Experiments done multiple times, C/O ratio=0,5 except 560°C.

Figure 26 shows the kerosene yield at different reaction temperatures converted by two different catalysts. The experiments shown in the figure are presented in detail in tables 5 and 6 in the experimental procedure section. The experiments at 560°C were performed with ZSM-5 (23) at a C/O=1,1 and C/O=0,5 (triangle with pattern). As the figure shows, both catalysts exhibited the highest kerosene yield at 360°C. The crack ability of both catalysts at temperatures of 360°C, 410°C and 460°C were very similar. A kerosene yield between 22%-28% was observed during all experiments at all temperatures, except at a temperature of 560°C.

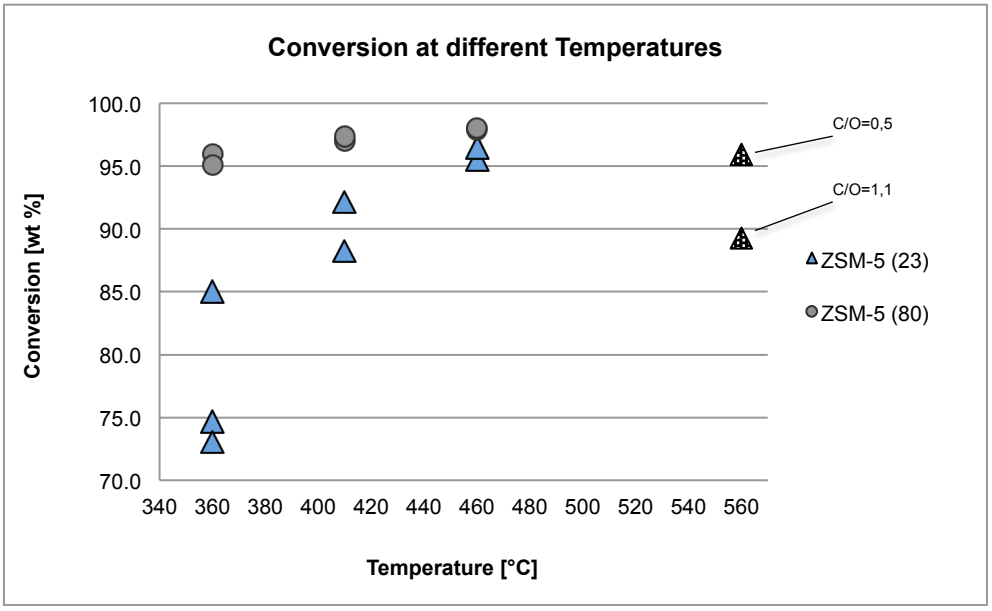

Figure 27: Conversion at different reaction temperatures (360°C, 410°C, 460°C, 560°C) at catalytic cracking. Experiments done multiple times, C/O ratio=0,5 except 560°C.

Figure 27 shows the conversion of the Fischer-Tropsch biowaxes at different reaction temperatures with the two catalysts. The conversion is very different especially at low temperatures. This is mainly due to the fact of the different selectivity of the catalysts. The catalyst ZSM-5 (80) shows an almost constant high conversion compared to the ZSM-5 (23) catalyst. The catalyst ZSM-5 (23) exhibits a low conversion at low temperatures, however, conversion increases as reaction temperature increases.

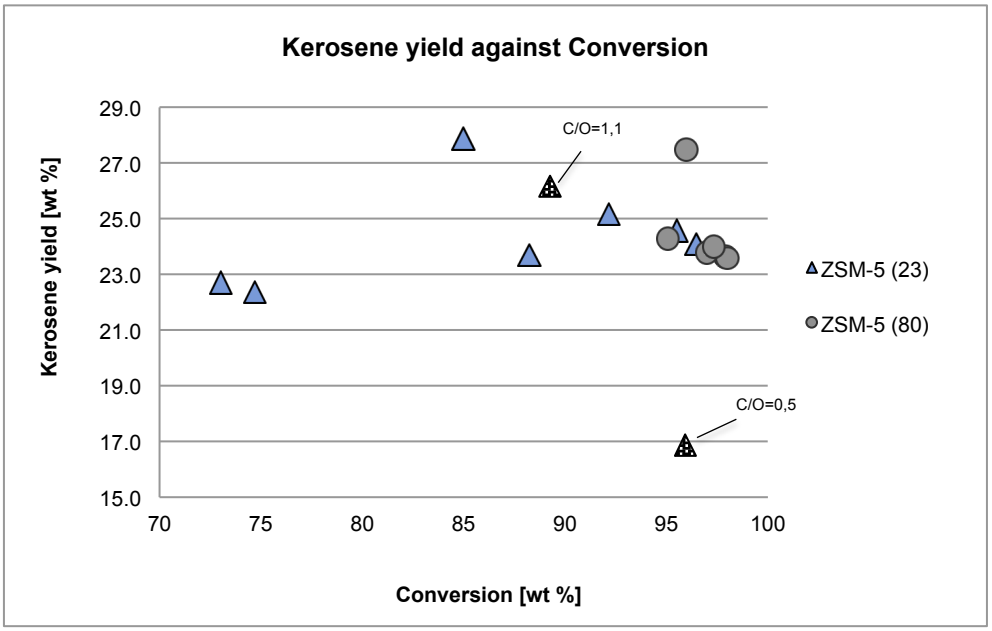

Figure 28: Kerosene yield versus conversion at catalytic cracking

The conversion of all experiments varied between 73% and 98%. The results for both catalysts ZSM-5 (23) and ZSM-5 (80) show that the highest conversion (~98%) was achieved at 460°C. Figure 28 displays the dependency of kerosene production versus wax conversion. The ZSM-5 (23) catalyst shows a wide range of conversion and no consistency throughout the experiments. The lower acidic catalyst ZSM-5 (80) exhibits constant conversions through the experiments and higher conversions compared to the ZSM-5 (23) catalyst.

4.3 Hydroprocessing Results

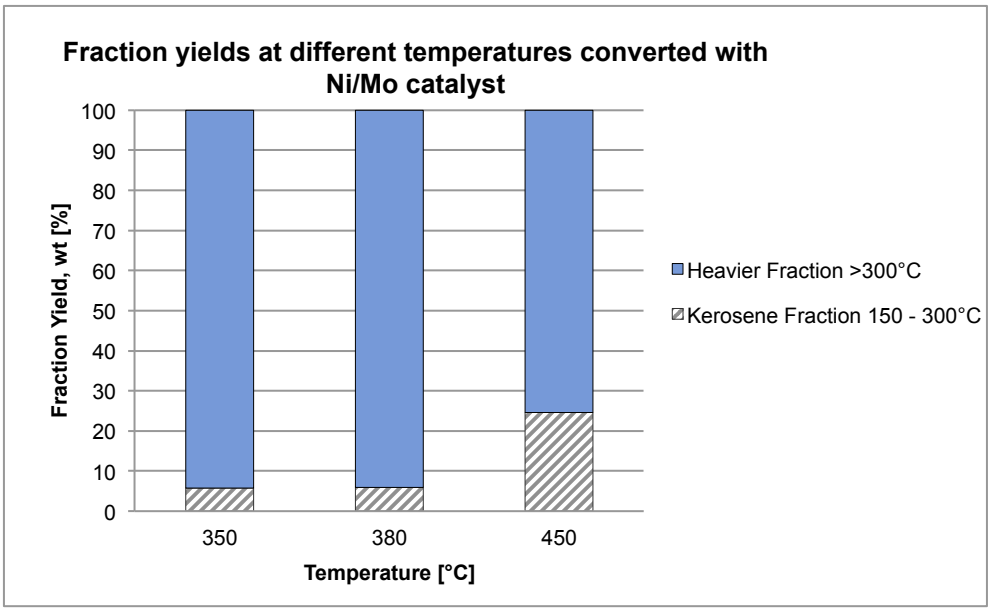

Figure 29: Kerosene yield at different reaction temperatures (350°C, 380°C, 450°C) at hydroprocessing

Figure 29 represents the kerosene fraction and the heavier fraction of the experiments performed with the nickel-molybdenum (Ni/Mo) catalyst. No lighter fractions (<150°C) were observed during these experiments, as the initial boiling point was over 150°C of the experiment. The kerosene yields at 350°C and 380°C were very low (about 5%) however, a higher yield (about 25%) was achieved at 450°C. It can be assumed that an increasing reaction temperature would increase the amount of kerosene fraction, since long chain hydrocarbons of the heavy fraction did get cracked poorly to middle and smaller hydrocarbons. In conclusion, the nickel-molybdenum (Ni/Mo) catalyst works better at higher temperatures.

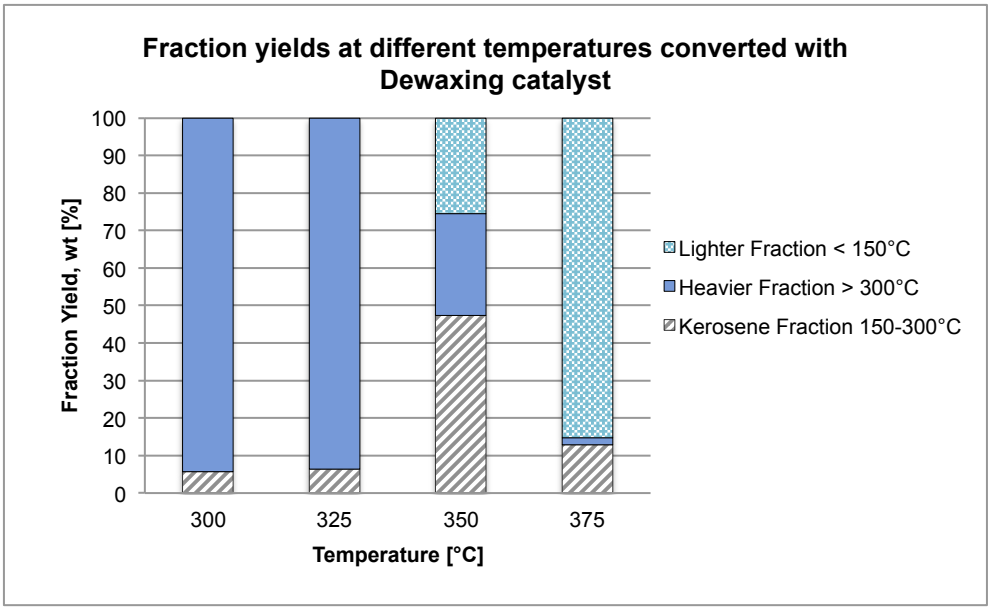

Figure 30: Kerosene yield at different reaction temperatures (300°C, 325°C, 350°C, 375°C) at hydroprocessing

Figure 30 shows the fraction yields produced from biowaxes with the dewaxing catalyst. In this case kerosene yield was comparable to the nickel-molybdenum catalyst at 300°C and 325°C. The heavy fraction at 300°C and 325°C is apparently high because of the poor crack ability at these temperatures, thus hindering the production of a lighter fraction. At 375°C the percentage of the light fraction is significantly increased as mainly gases were produced at these operating conditions due to the fact that the temperature was too high and the hydrocarbon got cracked to small molecules. At the temperature of 350°C the kerosene yield is between 40% and 50%. This seems to be the optimum operating temperature for future experiments to get an appropriate amount of kerosene.

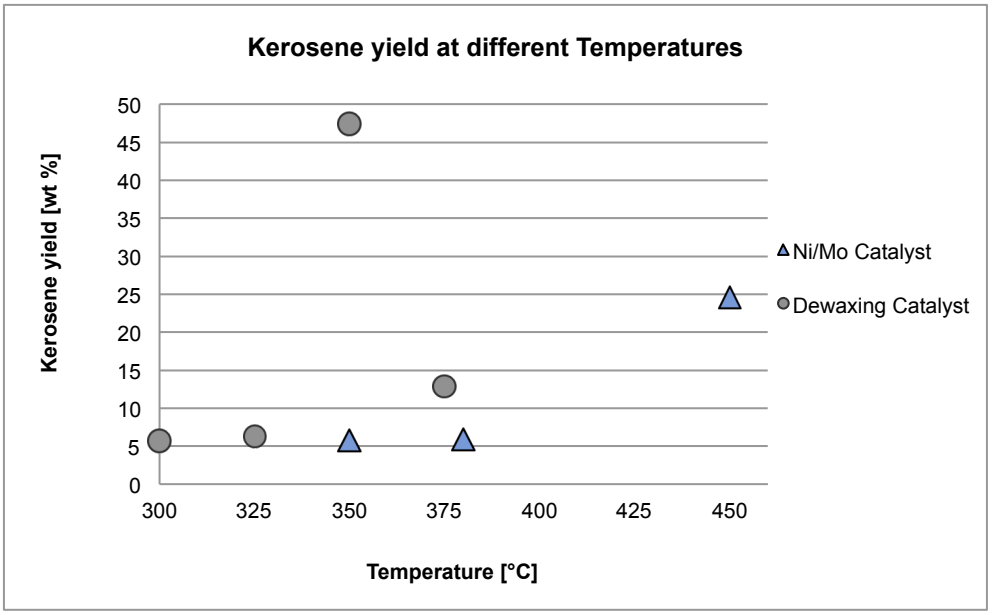

Figure 31: Kerosene yield at different reaction temperatures (300°C, 325°C, 350°C, 375°C, 380°C, 450°C) at hydroprocessing

Figure 31 shows the kerosene yield at different reaction temperatures converted by two different catalysts. The process conditions shown in the figure are presented in detail in tables 7 and 8 in the experimental procedure section. The nickel-molybdenum catalyst exhibited the highest kerosene yield of 25% at 450°C. It can be seen that the crack ability of the catalyst increases with the temperature. The dewaxing catalyst, which was carried out as a bifunctional catalyst, is more efficient at cracking and works better at lower temperatures. It shows the highest kerosene yield of 47% at 350°C.

4.4 Analysed Kerosene

The density and the freezing point of kerosene were analysed. The kerosene produced at the hydroprocessing with the dewaxing catalyst was used for the tests. The density test at 15°C was performed according to ASTM D4052 and the freezing point test according to ASTM D7153.

	Specification data for Jet A and Jet A1	Test results
Freezing Point max.	-40°C, -47°C	-32°C
Density at 15°C	775 – 840 kg/m3	780 kg/m3

Table 9: Comparison of the specification data of jet fuel with the test results of the cracked biokerosene at the hydroprocessing

The density test shows a typical value of 780 kg/m^3 at the lower edge of the specification of Jet A and Jet A1. This is common for Fischer-Tropsch derived fuels because of the low amount of aromatics in the used feedstock. Also it indicates a high value of branched hydrocarbons at the biokerosene. The freezing point has a value at -32°C which is too low in comparison with the specification. It can be assumed that the value of branched hydrocarbons is not high enough due to the fact that the freezing point increases with the degree of branched hydrocarbons. In order to meet the freezing point specification the isomerisation needs to be even higher. Because of the importance of the freezing point it would be advisable to lower the freezing temperature with more efficient isomerisation and add some aromatics and additives to meet the density specification.

5 CONCLUSION

The approaches in this work show that it is possible to convert biowaxes in kerosene. To what extend it can be used in a commercial scale only further experiments will tell. In this work first attempts were done to see the possibilities of an alternative jet fuel from wax conversion.

5.2 Catalytic Cracking

The catalytic cracking results demonstrate that the cracking of Fischer-Tropsch biowaxes with zeolite based ZSM-5 (23) and ZSM-5 (80) catalysts in a fixed bed reactor are suitable for producing kerosene. The conversion yield shows that the biowaxes are crackable at C/O =0,5 and achieved high conversions of about 73-98%. All experiments at all temperatures are presenting 22-28% amount of kerosene yield. Figure 24 and 25 shows that high amounts of lighter fraction and heavier fraction were produced during the experiments. To increase the kerosene yield the main fraction needs to be shifted to middle length hydrocarbons. This can be achieved through further variation of process conditions at lower temperatures to find the optimum operating temperature.

5.3 Hydroprocessing

The hydroprocessing experiments with the nickel-molybdenum catalyst achieved its highest kerosene yield at about 25% at 450°C. Figure 29 shows high amounts of heavier fraction were produced to increase the amount of kerosene yield. It would be more efficient to work at higher temperatures or to use a nickel-molybdenum catalyst carried out as zeolite. Due to the shape selective property, molecules get cracked depending on their molecule size and the pore size of the zeolite. Thus shifting the main fraction to kerosene.

The Dewaxing catalyst was carried out as a bifunctional catalyst, which was more efficient than the nickel-molybdenum catalyst and achieved an amount of 50% kerosene at 350°C. It seems that especially the temperature in combination with the catalyst is very important for the experiments and influences the product yield. The hydroprocessing experiments seem very promising of producing a commercial amount of kerosene. In order to achieve even higher kerosene yield it would be appropriate for further variation of process conditions to increase the output of kerosene fraction to 70-90%.

5.4 Comparison of Hydroprocessing and Catalytic Cracking

Both processes were performed with zeolite catalysts at a similar temperature range. The hydroprocessing experiments achieved an amount of 50% kerosene at 350°C in comparison to the catalytic cracking process, which achieved the highest amount of 28% kerosene at 360°C. Therefore hydroprocessing seems to be the better choice to complete further experiments and produce biokerosene in an commercial scale. In addition to the yield also the quality of the biokerosene needs to be considered. Further chemical analysis of the produced biokerosene will show if there are further differences of the two processing routes. Also it should be noted that the catalytic cracking experiments were performed in a bench scale unit, so it can be assumed that the potential has not reached its limit.

6 OUTLOOK

The produced kerosene needs to be further analysed according to ASTM D1655 to establish the composition and the properties of the produced kerosene. This is necessary for further usage of the kerosene as aviation fuel. In this project tests on a wankel engine were planned. They will be carried out at the Institute for Powertrains and Automotive Technology at the Vienna University of Technology. A total amount of 50 liters kerosene will be compared to fossil kerosene. These tests were realized under the project greenfly, which is funded by the Austrian Program TAKE OFF from the relevant call in 2012. Industrial partners include Austro Engine GmbH, which plans to use the technology later in their small aircrafts.

7 LITERATURE

1. Miller R. G., Sorrell S. R. (2014). The future of oil supply. *Philosophical Transactions of the Royal Society A: Mathematical, Physical and Engineering Sciences*, *372*(2006), 20130179.

2. Andruleit H., Babies H. G., Bahr A., Kus J., Meßner J., Schauer M. (2011): Rohstoffagentur, D. Bundesanstalt für Geowissenschaften und Rohstoffe, Deutschland–Rohstoffsituation 2010, DERA *Rohstoffinformationen (7), pp.9-32*

3. Hallock Jr. J. L., Tharakan P. J., Hall C. A., Jefferson M., Wu W. (2004). Forecasting the limits to the availability and diversity of global conventional oil supply. Energy, 29(11), 1673-1696.

4. *Dorian J. P., Franssen H. T., Simbeck D. R. (2006). Global challenges in energy. Energy policy, 34(15), 1984-1991.*

5. *Bentley R. W. (2002). Global oil & gas depletion: an overview. Energy policy, 30(3), 189-205.*

6. *Stocker D. Q. (2013). Climate change 2013: The physical science basis. Working Group I Contribution to the Fifth Assessment Report of the Intergovernmental Panel on Climate Change, Summary for Policymakers, IPCC.*

7. *Birol F. (2008). World energy outlook 2008. International Energy Agency, pp. 37, 407- 434*

8. *UNFCCC/CCNUCC. CDM – Executive Board. EB 20. Report. Annex 8 page 1. Annex 8. CLARIFICATIONS ON DEFINITION OF BIOMASS AND CONSIDERATION. 27.05.2014 15:30*

9. *Basu P. (2010): Biomass gasification and pyrolysis: Practical design and theory. Academic press, pp. 5-12, 27-29, 29-35, 65, 69-74, 77-81, 119, 167-192*

10. *Naik, S. N., Goud, V. V., Rout, P. K., Dalai, A. K. (2010). Production of first and second generation biofuels: a comprehensive review. Renewable and Sustainable Energy Reviews, 14(2), 578-597.*

11. *Damartzis T., Zabaniotou A. (2011). Thermochemical conversion of biomass to second generation biofuels through integrated process design—A review. Renewable and Sustainable Energy Reviews, 15(1), 366-378.*

12. *Antizar Ladislao, B., Turrion Gomez, J. L. (2008). Second generation biofuels and local bioenergy systems. Biofuels, Bioproducts and Biorefining, 2(5), 455-469.*

13. Havlík P., Schneider U. A., Schmid E., Böttcher H., Fritz S., Skalský R., Obersteiner M. (2011). Global land-use implications of first and second generation biofuel targets. *Energy Policy*, *39*(10), 5690-5702.

14. Agarwal A. K. (2007). Biofuels (alcohols and biodiesel) applications as fuels for internal combustion engines. Progress in energy and combustion science, 33(3), 233-271.

15. Beurskens L. W. M., Hekkenberg M., Vethman P. (2011). Renewable energy projections as published in the national renewable energy action plans of the European member states. European Research Centre of the Netherlands (ECN) and European Environmental Agency (EEA), Petten. pp 17-27

16. Schnepf R. D. (2006). European Union biofuels policy and agriculture: An overview. Congressional Research Service, Library of Congress.

17. Thompson, C., Nathanail, P. (Eds.). (2009). Chemical analysis of contaminated land. John Wiley & Sons. pp. 137, 172

18. Gaïl S., Dagaut P. (2007). Kinetic study of aviation fuels oxidation in a JSR: Jet-A1 and Bio-Kerosene. In *Third European Combustion Meeting ECM*.

19. De Klerk, A. (2012). Fischer-Tropsch Refining. John Wiley & Sons. pp. 73-76, 270, 275-276, 290, 492

20. Wauquier, J. P. (2001). Petroleum Refining. Editions OPHRYS. pp. 127-128, 227, 228

21. Speight, J. G. (Ed.). (2011). The biofuels handbook (No. 5). Royal Society of Chemistry. pp. 245, 378

22. Jones, D. S., & Pujadó, P. R. (Eds.). (2006). Handbook of petroleum processing. Springer. pp. 311

23. National Research Council (US). Committee on Aviation Fuels with Improved Fire Safety. (1997). Aviation fuels with improved fire safety: a proceedings. National Academies. pp.49

24. Kaltschmitt M., Hartmann H., Hofbauer H. (2001). Energie aus Biomasse: Grundlagen, Techniken und Verfahren, Eds. *Berlin, Heidelberg, New York*. pp. 2-6, 38, 75, 378-379, 385, 376-389, 390-391, 397, 601-619

25. Kumar P., Barrett D. M., Delwiche M. J., Stroeve P. (2009). Methods for pretreatment of lignocellulosic biomass for efficient hydrolysis and biofuel production. *Industrial & Engineering Chemistry Research*, *48*(8), 3713-3729.

26. Reddy N., Yang Y. (2005). Biofibers from agricultural byproducts for industrial applications. *TRENDS in Biotechnology*, *23*(1), 22-27.

27. Stöcker M. (2008). Biofuels and biomass-to-liquid fuels in the biorefinery: Catalytic conversion of lignocellulosic biomass using porous materials. *Angewandte Chemie International Edition*, *47*(48), 9200-9211.

28. Demirbas, A. (2007). Progress and recent trends in biofuels. *Progress in energy and combustion science*, *33*(1), 1-18.

29. Boichenko, S., Vovk, O., Iakovlieva, A. (2013). Overview of innovative technologies for aviation fuels production.

30. Llamas A., Al-Lal A. M., Hernandez M., Lapuerta, M., Canoira L. (2012). Biokerosene from babassu and camelina oils: production and properties of their blends with fossil kerosene. *Energy & Fuels*, *26*(9), 5968-5976.

31. Llamas A., García-Martínez M. J., Al-Lal A. M., Canoira L., Lapuerta M. (2012). Biokerosene from coconut and palm kernel oils: Production and properties of their blends with fossil kerosene. Fuel, 102, 483-490.

32. Chuck C. J., Donnelly J. (2014). The compatibility of potential bioderived fuels with Jet A-1 aviation kerosene. Applied Energy, 118, 83-91.

33. Jansen, R. A. (2013) Biokerosene. Second Generation Biofuels and Biomass: Essential Guide for Investors, Scientists and Decision Makers, 183-191.

34. Demirbas, A. (2008). Biofuels sources, biofuel policy, biofuel economy and global biofuel projections. Energy conversion and management, 49(8), 2106-2116.

35. Hamelinck C. N., Faaij A. P. (2006). Outlook for advanced biofuels. *Energy Policy*, *34*(17), 3268-3283.

36. Chiaramonti, D., Prussi, M., Buffi, M., Tacconi, D. (2014). Sustainable bio kerosene: Process routes and industrial demonstration activities in aviation biofuels. Applied Energy.

37. McElroy, M. B. (2009). Energy: perspectives, problems, and prospects. Oxford University Press. pp.126

38. Dukek, W. G., Strauss, K. H. (Eds.). (1979). Factors in Using Kerosine Jet Fuel of Reduced Flash Point: A Symposium (No. 688). ASTM International. pp. 22

39. Llamas A., García-Martínez M. J., Al-Lal A. M., Canoira L., Lapuerta M. (2012). Biokerosene from coconut and palm kernel oils: Production and properties of their blends with fossil kerosene. *Fuel*, *102*, 483-490.

40. You F., Wang B. (2011). Life cycle optimization of biomass-to-liquid supply chains with distributed–centralized processing networks. *Industrial & Engineering Chemistry Research*, *50*(17), 10102-10127.

41. Lappas A., Voutetakis S., Drakaki N., Papapetrou M., Vasalos I. (2004): Production of Transportation Biofuels through Mild-Hydrocracking of Waxes produced from Biomass to Liquid (BTL) Process. 14th Biomass European Conference, Paris

42. Baliban, R. C., Elia, J. A., & Floudas, C. A. (2013). Biomass to liquid transportation fuels (BTL) systems: process synthesis and global optimization framework. *Energy & Environmental Science*, *6*(1), 267-287.

43. Rauch R., Hofbauer H., Bosch K., Siefert I., Aichernig C., Voigtlaender K., Lehner R. (2004). Steam gasification of biomass at CHP plant Guessing-Status of the demonstration plant. na.

44. Prins M. J., Ptasinski K. J., Janssen F. J. (2007). From coal to biomass gasification: comparison of thermodynamic efficiency. Energy, 32(7), 1248-1259.

45. Rezaiyan J., Cheremisinoff N. P. (2005). Gasification technologies: a primer for engineers and scientists. CRC press. pp.1-2

46. Klass D. L. (1998). Biomass for renewable energy, fuels, and chemicals. Academic press. pp. 289-290

47. Küçük, M. M., & Demirbaş, A. (1997). Biomass conversion processes. *Energy Conversion and Management*, *38*(2), 151-165.

48. Pfeifer, C., Koppatz, S., Hofbauer, H. (2011). Steam gasification of various feedstocks at a dual fluidised bed gasifier: Impacts of operation conditions and bed materials. Biomass Conversion and Biorefinery, 1(1), 39-53.

49. Devi L., Ptasinski K. J., Janssen F. J. (2003). A review of the primary measures for tar elimination in biomass gasification processes. *Biomass and Bioenergy*, *24*(2), 125-140.

50. De Klerk, A. (2011): Fischer-Tropsch Refining, Wiley-VCH. pp.6

51. Quaak P., Knoef H., Stassen H. E. (1999). *Energy from biomass: a review of combustion and gasification technologies* (Vol. 23). World Bank Publications.

52. Bolhàr-Nordenkampf M., Rauch R., Bosch K., Aichernig C., Hofbauer H. (2003): Biomass CHP plant Güssing-Using gasification for power generation. K. Kirtikara: 2nd RCETCE, Phuket, Thailand, 567-572.

53. Rauch R., Hofbauer H., Bosch K., Siefert I., Aichernig C., Tremmel H., Koch R., Lehner R. (2004): Steam gasification of biomass at CHP plant Guessing-Status of the demonstration plant. In 2nd world conference and technology exhibition on biomass for energy, industry and climate protection, Rome, Italy.

54. Kirnbauer F., Hofbauer H. (2011). Investigations on bed material changes in a dual fluidized bed steam gasification plant in Gussing, Austria. *Energy & Fuels*, *25*(8), 3793-3798.

55. Bolhar-Nordenkampf M., Bosch K., Rauch R., Kaiser S., Tremmel H., Aichernig C., Hofbauer H. (2002/1). Scaleup of a 100 kWth pilot FICFB-gasifier to a 8 MWth FICFB-gasifier demonstration plant in Güssing (Austria). In *Proc. 1st International Ukrainian Conference on Biomass For Energy, Kyiv, Ukraine*.

56. Bolhàr-Nordenkampf M., Rauch R., Bosch K., Aichernig C., Hofbauer H. (2002/2): A Biomass CHP Plant Güssing – Using Gasification for Power Generation. Int. Conference on Biomass Utilisation, Thailand.

57. Sauciuc A., Abosteif Z., Weber G., Potetz A., Rauch R., Hofbauer, H., Dumitrescu L. (2012). Influence of operating conditions on the performance of biomass-based Fischer–Tropsch synthesis. Biomass Conversion and Biorefinery, 2(3), 253-263.

58. Bolhar-Nordenkampf M., Hofbauer H. (2004). *Gasification demonstration plants in Austria*. na.

59. Boerrigter H., and R. Rauch (2006): Review of applications of gases from biomass gasification. ECN Biomass, Coal and Environmental Research, Holanda.

60. Schulz H. (1999). Short history and present trends of Fischer–Tropsch synthesis. *Applied Catalysis A: General*, *186*(1), 3-12.

61. De Klerk A., Furimsky E. (2010): Catalysis in the refining of Fischer-Tropsch Syncrude (No. 4). Royal Society of Chemistry, pp.1, 7-10, 14-17, 115

62. Boerrigter H., den Uil H., Calis H. P. (2003). Green diesel from biomass via Fischer-Tropsch synthesis: new insights in gas cleaning and process design. *Pyrolysis and gasification of biomass and waste*, 371-383

63. Ciobîcă I. M., Kramer G. J., Ge Q., Neurock M., Van Santen R. A. (2002). Mechanisms for chain growth in Fischer–Tropsch synthesis over Ru (0001). *Journal of Catalysis*, *212*(2), 136-144.

64. Patzlaff J., Liu Y., Graffmann C., Gaube J. (1999). Studies on product distributions of iron and cobalt catalyzed Fischer–Tropsch synthesis. *Applied Catalysis A: General*, *186*(1), 109-119

65. Tavakoli A., Sohrabi M., Kargari A. (2008). Application of Anderson–Schulz–Flory (ASF) equation in the product distribution of slurry phase FT synthesis with nanosized iron catalysts. *Chemical Engineering Journal*, *136*(2), 358-363.

66. Maitlis P. M., de Klerk A. (Eds.). (2013). Greener Fischer-Tropsch Processes for Fuels and Feedstocks. John Wiley & Sons. pp. 61-70

67. Steynberg A., Dry M. (Eds.). (2004). Fischer-Tropsch Technology. Elsevier. pp. 64-77

68. Sauciuc A., Potetz A., Weber G., Rauch R., Hofbauer H., Dumitrescu L. (2011). Synthetic diesel from biomass by Fischer-Tropsch synthesis.

69. Hofbauer H., Rauch R., Fürnsinn S., Aichernig C. (2005): Energiezentrale Güssing. Energiesysteme der Zukunft "-Endbericht, pp. 57-69

70. Götz F. (2012) Integration vom Hydroprocessing in die Fischer-Tropsch Synthese. Diplomarbeit pp. 19-25

71. Dupain, X., Krul, R. A., Makkee, M., & Moulijn, J. A. (2005). Are Fischer–Tropsch waxes good feedstocks for fluid catalytic cracking units?. *Catalysis today*, *106*(1), 288-292.

72. Latscha, H. P., Kazmaier, U., & Klein, H. A. (2008). Chemie Basiswissen/Band 2 (Organische Chemie). pp. 483

73. Wollrab A. (2009). Organische Chemie. Eine Einführung für Lehramts-und Nebenfachstudenten, 3. pp. 281-285

74. Scherzer J., Gruia A. J. (1996). Hydrocracking science and technology. CRC Press. pp. 75, 112-115, 223-224

75. Weissermel K., Arpe H. J. (2008). Industrial organic chemistry. John Wiley & Sons. pp. 60

76. Marafi, M., Stanislaus, A., Furimsky, E. (2010). Handbook of spent hydroprocessing catalysts: regeneration, rejuvenation, reclamation, environment and safety. Elsevier. pp. 22

77. Jones, D. S., & Pujadó, P. R. (Eds.). (2006). Handbook of petroleum processing. Springer. pp. 295-296, 311

78. Niwa, M., Katada, N., & Okumura, K. (2010). Characterization and Design of Zeolite Catalysts: Solid Acidity, Shape Selectivity and Loading Properties (Vol. 141). Springer. pp. 1-7

79. Ribeiro, F. R. (Ed.). (1984). Zeolites: Science and Technology: Science and Technology (Vol. 80). Springer. pp. 398

80. Osenbach T., (2010). *Fast Simulated Distillation Analysis by modified ASTM D2887, D6352 and* D7169, Waltham, USA: PerkinElmer, Inc..

81. Argauer R. J. (1972): Crystalline zeolite zsm-s and method. U.S. Patent No. 3,702,886.

82. Triantafyllidis K. S., Komvokis V. G., Papapetrou M. C., Vasalos I. A., Lappas A. A. (2007): Microporous and mesoporous aluminosilicates as catalysts for the cracking of Fischer-Tropsch waxes towards the production of “clean” bio-fuels. Studies in Surface Science and Catalysis, 170, 1344-1350.

83. Gary J. H., Handwerk G. E. (2001): Petroleum refining. CRC press, pp.165

84. Bouchy C., Hastoy G., Guillon E., Martens J. A. (2009): Fischer-Tropsch waxes upgrading via hydrocracking and selective hydroisomerization. Oil & Gas Science and Technology-Revue de l'IFP, 64(1), 91-112.

85. Lappas, A. (2005) Fischer-Tropsch heavy products up-grading.

86. Towler, G. P., & Sinnott, R. K. (2013). Chemical engineering design: principles, practice, and economics of plant and process design. Elsevier. pp.48-50

8 APPENDIX

8.1 Appendix A

The wax feedstock was filled up in seven bottles. The following data shows the results of these analyses of these 7 bottles. The analyse was done by CERTH/CPERI. SimDist HighTemp (GC 265) Boiling Range Distribution of Petroleum Fraction by GC (ASTM D-6352) to 700°C

	SampleA	**SampleB**	**SampleC**	**SampleD**	**SampleE**	**SampleF**	**SampleG**
Sample Name	wax509-4	wax509-6	wax509-2	wax509-7	wax509-5	wax509-1	wax509-3
Lims Code	163904	163906	163902	163907	163905	163901	163903
Report Date	18/6/2013	18/6/2013	18/6/2013	18/6/2013	18/6/2013	18/6/2013	18/6/2013
Sample Date	18/6/2013	18/6/2013	18/6/2013	18/6/2013	18/6/2013	18/6/2013	18/6/2013
	°C	°C	°C	°C	°C	°C	°C
mass%							
IBP	269	269,4	270,2	253,4	253,4	270,2	270,8
1	271,2	271,4	274	270,2	270,2	285,8	286
2	287,2	287,4	287,4	285,2	284,2	300,2	288,6
3	288,6	291	301,6	287,6	288	302,8	302,4
4	302,4	302,6	302,8	300	296,8	315,8	303,4
5	303,6	303,6	307,6	302,8	303	317,2	316,2
6	308,6	309,6	316,4	303,6	304,2	318,2	317,6
7	316,8	317	317,4	312,4	309	330,6	318,4
8	318	318	318,2	316,8	317	331,8	330
9	319	319	329,2	317,8	318,4	332,8	331,6
10	326,2	326	331,2	318,6	319,2	341,6	332,4
11	331,4	329,6	332,2	327	323,4	345	333,2
12	332,6	331,8	332,8	331,2	331,4	346	344
13	333,4	332,8	339,8	332,2	332,6	346,6	345,4
14	334,2	333,4	344,6	332,8	333,6	354,4	346,2
15	344,4	337,6	345,6	334	334,4	357,6	347
16	345,8	344,4	346,2	344	343,8	358,6	355,2
17	346,8	345,6	346,8	345,4	345,8	359,4	357,6
18	347,4	346,4	356	346,2	346,8	363,6	358,6
19	351,4	347,2	357,6	346,8	347,6	369,6	359,4
20	357,6	353,8	358,6	351,8	349,6	370,6	361,6

21	358,8	357,6	359,2	357,2	357,4	371,4	369
22	359,6	358,6	360,8	358,4	358,8	373	370,4
23	360,4	359,4	368,8	359,2	359,8	381	371,2
24	366,8	362,8	370	359,8	360,6	382,2	371,8
25	370,2	369,4	370,8	368,2	366,2	383	379,2
26	371,2	370,6	371,6	370	370,4	383,8	381,6
27	372	371,6	375,2	370,8	371,6	392	382,4
28	372,8	372,2	380,8	371,6	372,4	393,2	383,2
29	380,6	380,2	382	376	373,8	394	386
30	382,2	382	382,8	381,2	381,4	395,6	392,2
31	383,2	382,8	383,4	382,2	382,8	402,6	393,4
32	384	383,6	391	383	383,8	403,8	394,2
33	387,6	386,4	392,6	385,8	384,6	404,6	395,4
34	392,8	392,4	393,6	392	392,2	409,2	402,4
35	394	393,6	394,2	393,2	393,8	413	403,6
36	394,8	394,4	398,2	394	394,8	414	404,4
37	396	395,2	402,6	398,4	395,8	414,8	405,8
38	402,8	402,4	403,6	402,6	403	421,8	412,4
39	404,2	403,8	404,4	403,8	404,4	423,2	413,6
40	405	404,6	406,6	404,6	405,4	424,2	414,6
41	405,8	405,4	412,4	411,8	410,4	429,6	417,8
42	412,6	412,2	413,6	413,2	413,6	432,2	422,6
43	414,2	413,6	414,4	414,2	414,8	433,2	423,6
44	415	414,6	417,2	420	416,2	435,4	424,4
45	416,4	415,6	422,2	422,6	422,8	441,2	431
46	422,6	422,2	423,4	423,6	424,2	442,4	432,6
47	424	423,6	424	428,4	425,2	444,2	433,4
48	425	424,4	430	431,8	432	450,2	438,8
49	429,6	428,2	432	433	433,6	451,4	441,6
50	432,6	432,2	433	439,2	435,2	454,6	442,6
51	433,8	433,4	434,6	441,4	441,6	459,2	446
52	435	434,4	440,6	442,4	443,2	460,4	450,4
53	441,2	440,8	442	449,4	448,6	466,2	451,6
54	442,8	442,4	442,8	450,8	451,4	468	456,2
55	443,8	443,4	449,2	455,8	452,6	469	459,2
56	449,8	449,4	450,8	459	459,2	474,8	460,4

57	451,6	451,2	451,8	460,4	460,8	476,2	466,2
58	452,6	452,2	457,8	467	466,8	481	468
59	458,6	458,2	459,4	468,2	468,6	483	469,2
60	460,4	459,8	460,4	474,2	473,4	484,8	474,8
61	461,6	461	466,6	475,6	476	489,8	476
62	467,4	467	468	481,4	479,6	491,2	481,2
63	468,8	468,4	469,4	483	483,4	496,4	483
64	471,2	470,2	474,6	488,8	487,2	497,8	486,2
65	475,6	475,2	475,8	490,4	490,6	502,8	490
66	477	476,6	481	496	495,4	504,4	491,8
67	482	481,6	482,8	497,6	497,8	509,2	496,6
68	483,8	483,4	484,8	503	502,6	510,8	498,4
69	487,8	486,8	489,4	506,8	504,8	515,8	503,2
70	490,6	490,2	490,8	509,8	509,8	517,6	505,4
71	492,8	492	496,2	514,8	512,2	522,2	509,8
72	497,2	497	497,6	516,8	516,8	526	513,8
73	499,2	498,6	502,6	521,8	521,4	528,6	516,4
74	503,8	503,4	504,2	526,4	523,8	533,2	521,2
75	506,2	505,4	509	528,8	528,6	535,8	523,4
76	510,4	510	510,8	533,4	533	539,8	528
77	514,4	513,8	515,6	538,2	535,8	544,2	532,6
78	517	516,6	519,6	542,4	540,2	548,2	535,2
79	521,8	521,4	522,4	545,4	545	551,4	539,6
80	524,2	523,6	527	550,2	549,4	555,8	544,4
81	528,6	528,2	530	555	553,6	560,2	549
82	533,2	532,8	533,8	559,6	557,4	564,6	553,6
83	537	536,2	538,6	564,4	561,8	569	558,2
84	540,6	540	543,4	569	566,6	573,6	562,8
85	545,4	545	547,6	573,8	571,4	578,4	567,8
86	550,2	549,8	551,2	579	576,8	583,4	573
87	555,2	554,8	556	585,4	582,6	588,4	578,4
88	560	559,6	560,8	590,8	588	594,2	584,4
89	564,8	564,4	566,2	597,2	593,8	599,8	590,8
90	570	569,6	572,2	603,6	600	606,6	598
91	575,8	575	577,8	611,2	607,2	613,8	605,8
92	582,6	582,2	584	619,8	615	621,4	614,8

93	589	588,2	590,8	628,4	623,4	630,2	625
94	596	595,4	598,2	638,4	632,6	639,8	637,4
95	604,8	604,2	606,6	649,8	643,2	651,2	653
96	614,6	614,2	616,8	663,2	656	665,4	674,4
97	627	626,6	628,6	679,4	671,4	683,8	707
98	642,8	642,4	644,2	698,8	691,6	707,2	750
99	668,6	668	669,2	721,6	715,6	743	-
FBP	691,6	691,4	692,2	734	730,4	750	-

Version 6,6,0,0

SimDis 2 ASTM High temperature 1

Sample name	: 163904		
Acquired on	: 17/6/2013 12:23:52 ìì	Vial	: 21
Processed on	: 18/6/2013 8:20:31 ðì	Injection	: 1
Sample type	: FCC HT	Sample (g)	: 0.0711
Method name	: ht750a	Solvent (g)	: 5.0000
Operator	: DP	ISTD (g)	: 0.0000
Sequence name	: H130617A.S		

Data File : H130617A\021F0201.D

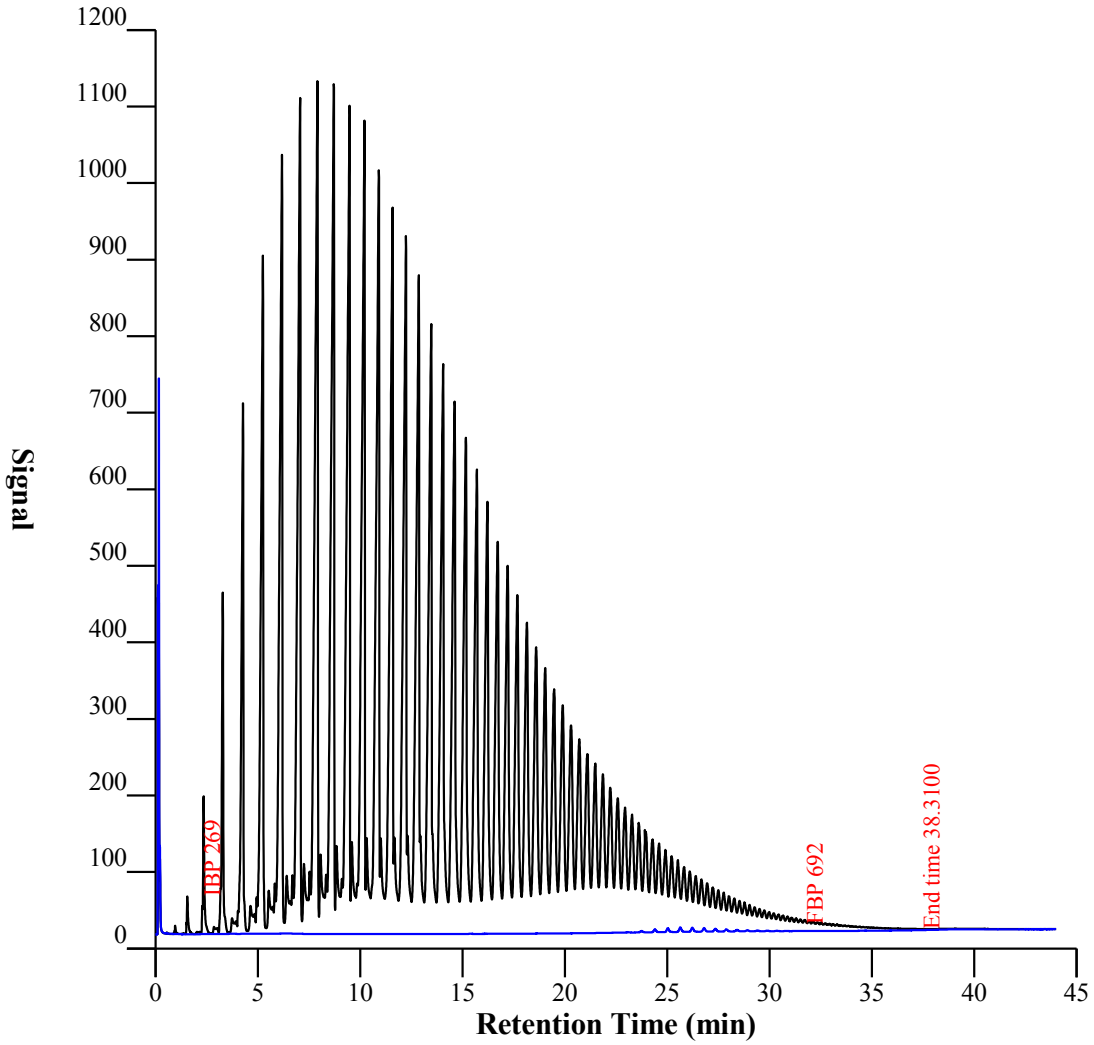

SimDis 2 ASTM High temperature 1

Sample name	: 163906		
Acquired on	: 17/6/2013 13:24:28 ìì	Vial	: 22
Processed on	: 18/6/2013 8:21:21 ðì	Injection	: 1
Sample type	: FCC HT	Sample (g)	: 0.0618
Method name	: ht750a	Solvent (g)	: 5.0000
Operator	: DP	ISTD (g)	: 0.0000
Sequence name	: H130617A.S		

Data File : H130617A\022F0301.D

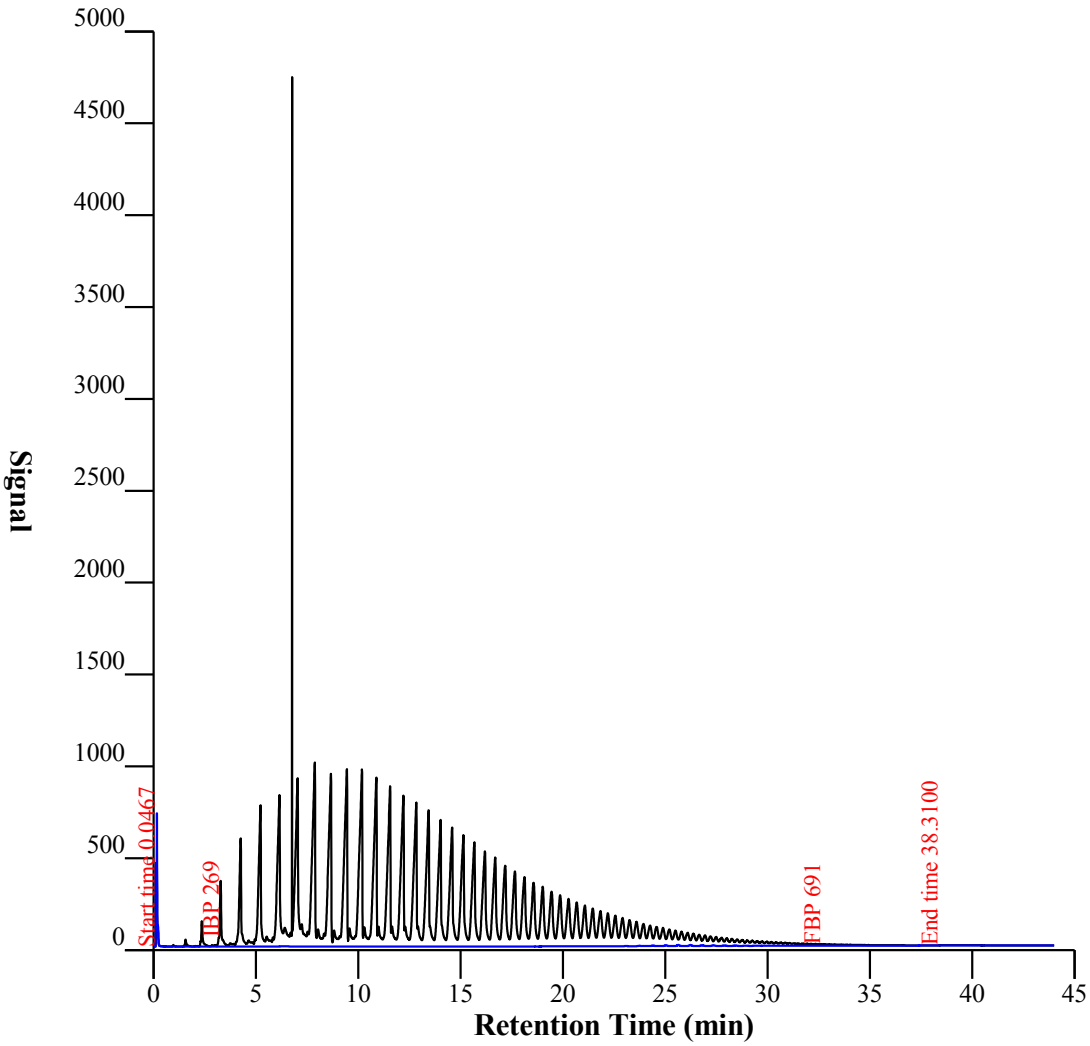

SimDis 2 ASTM High temperature 1

Sample name	: 163902		
Acquired on	: 17/6/2013 14:34:22 ìì	Vial	: 23
Processed on	: 18/6/2013 8:23:23 ðì	Injection	: 1
Sample type	: FCC HT	Sample (g)	: 0.0509
Method name	: ht750a	Solvent (g)	: 5.0000
Operator	: DP	ISTD (g)	: 0.0000
Sequence name	: H130617A.S		

Data File : H130617A\023F0401.D

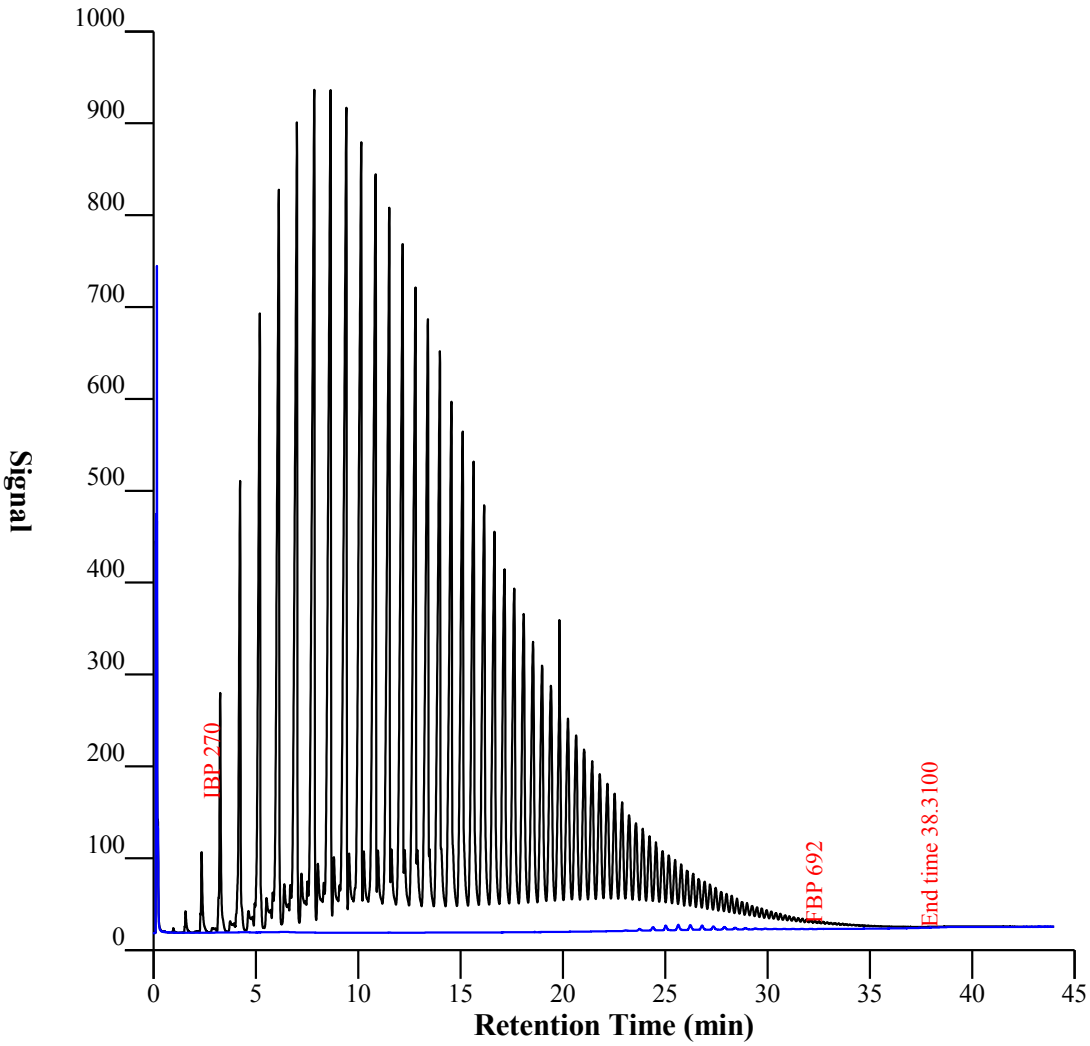

Version 6,6,0,0

SimDis 2 ASTM High temperature 1

Sample name	: 163907		
Acquired on	: 17/6/2013 15:35:54 ìì	Vial	: 24
Processed on	: 18/6/2013 9:20:16 ðì	Injection	: 1
Sample type	: Resids	Sample (g)	: 0.1062
Method name	: ht750a	Solvent (g)	: 10.0000
Operator	: DP	ISTD (g)	: 0.0000
Sequence name	: H130617A.S		

Data File : H130617A\024F0501.D

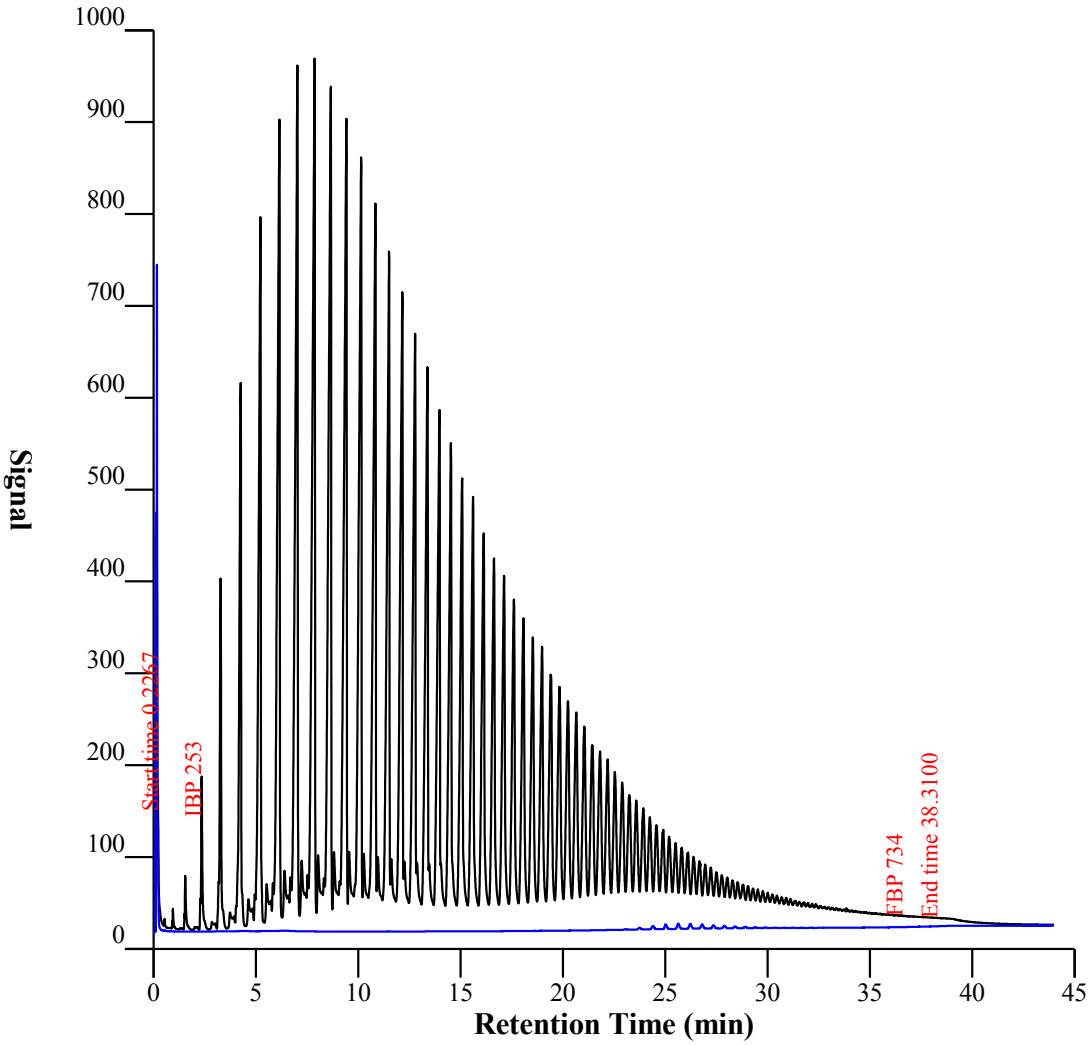

SimDis 2 ASTM High temperature 1

Sample name	: 163905		
Acquired on	: 17/6/2013 17:39:49 ìì	Vial	: 26
Processed on	: 18/6/2013 9:20:41 ðì	Injection	: 1
Sample type	: Resids	Sample (g)	: 0.0706
Method name	: ht750a	Solvent (g)	: 5.0000
Operator	: DP	ISTD (g)	: 0.0000
Sequence name	: H130617A.S		

Data File : H130617A\026F0701.D

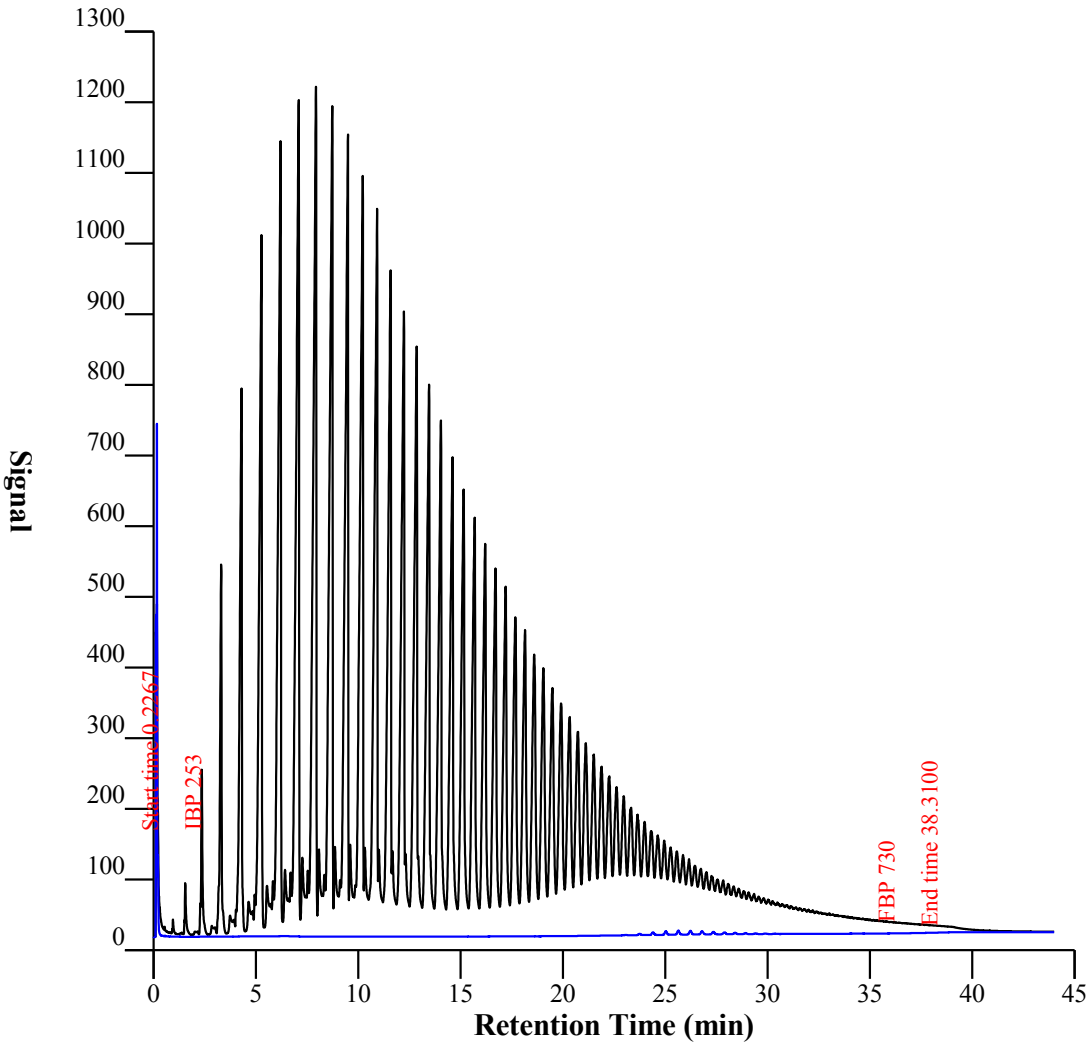

SimDis 2 ASTM High temperature 1

Sample name	: 163901		
Acquired on	: 17/6/2013 18:41:08 ìì	Vial	: 27
Processed on	: 18/6/2013 9:20:52 ðì	Injection	: 1
Sample type	: Resids	Sample (g)	: 0.0596
Method name	: ht750a	Solvent (g)	: 5.0000
Operator	: DP	ISTD (g)	: 0.0000
Sequence name	: H130617A.S		

Data File : H130617A\027F0801.D

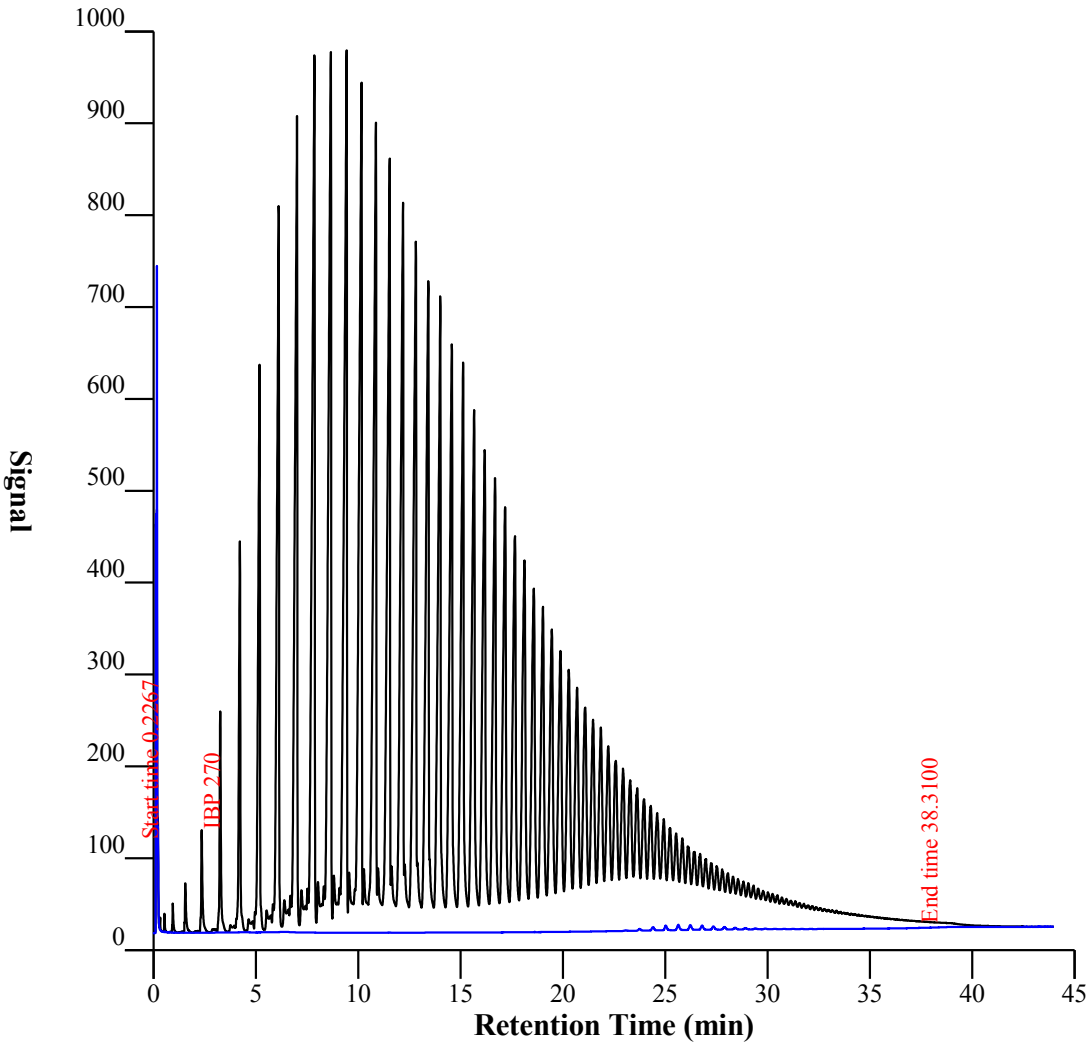

SimDis 2 ASTM High temperature 1

Sample name	: 163903		
Acquired on	: 17/6/2013 16:37:43 ìì	Vial	: 25
Processed on	: 18/6/2013 9:20:31 ðì	Injection	: 1
Sample type	: Resids	Sample (g)	: 0.0565
Method name	: ht750a	Solvent (g)	: 5.0000
Operator	: DP	ISTD (g)	: 0.0000
Sequence name	: H130617A.S		

Data File : H130617A\025F0601.D

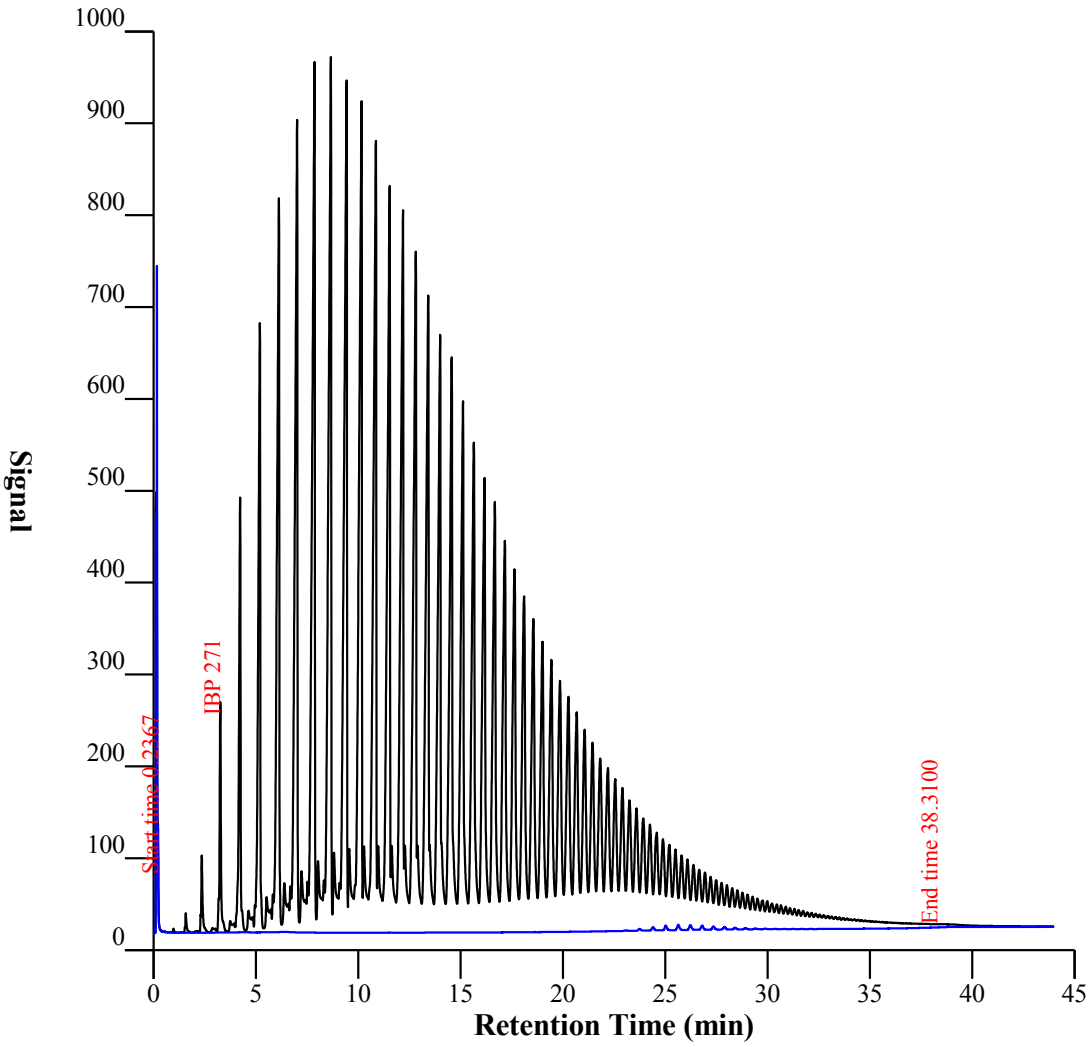

8.2 Appendix B

Appendix B-1 shows the experiment conditions of catalytic cracking with wax feedstock **SampleC** 509-2.

Experiment Number	Catalysator mass [g]		Mass before and afterwards [g]				Reaction	Feed T [°C]	Receiver		Pressure	
			Crucible	Filter	Syringe	Receiver	T [°C]		Vessel T [°C]	Bath T [°C]	1. Drop [mbar]	2. Drop T [mbar]
1	1,8225	before	1,8225	2,7052	66,7534	267,6264	560	108,2	23,2	17,5	1488 - 985,7	1287 - 984,2
		afterwards	0,0209	2,8	64,8848	268,2535						
2	0,9019	before	0,9019	2,6589	66,8628	267,6113	560	95,2	24,1	17,8	1405 - 982,7	1473,9 - 982,5
		afterwards	0,0081	2,6589	64,8717	268,4142						
3	0,9006	before	0,9006	2,6589	66,6844	267,6341	460	96,4	21,1	17,6	1341 - 983,6	1351 - 981,2
		afterwards	0,0008	2,6589	64,8923	268,636						
4	0,9013	before	0,9013	2,6589	66,6935	267,6245	460	96,2	23,7	18	1468 - 983,1	1423 -982
		afterwards	0,0025	2,6589	64,8747	268,6345						
5	0,9014	before	0,9014	2,6589	66,6837	267,6555	460	95,2	23,7	17,8	1203,4 - 981,4	1273,3 - 982
		afterwards	0,0015	2,6589	64,9005	268,6646						
6	0,9083	before	0,9083	2,6589	66,6815	267,6250	460	95,3	23,2	17,8	1212,7 - 984,2	1260,8 - 985,3
		afterwards	0,0016	2,6589	64,9193	268,621						
7	0,9029	before	0,9029	2,7126	66,709	267,6262	410	95,2	23	17,8	1162,7 - 983	1240,6 - 982,6
		afterwards	0,0007	2,7126	64,9123	268,7118						
8	0,9047	before	0,9047	2,7126	66,7108	267,6680	410	96,2	23,6	17,8	1181 - 983,1	1250 - 983,1
		afterwards	0,0001	2,7126	64,9224	268,7216						
9	0,9057	before	0,9057	2,7115	66,7070	267,5997	410	94,5	22,2	17,8	1402,7 - 984	1388,4 - 983,4
		afterwards	0,0017	2,7121	64,878	268,7466						
10	0,9033	before	0,9033	2,6980	66,7227	267,5853	410	95,5	22,7	17,6	1315 - 983,3	1361,7 - 983,4
		afterwards	0,0021	2,6980	64,8766	268,7344						
11	0,9049	before	0,9049	2,6980	66,6761	267,6015	360	95,5	23	17,5	1372,6 - 983,6	2137,4 - 982,3
		afterwards	0,0030	2,6980	64,8999	268,8451						
12	0,9024	before	0,9024	2,6991	66,7014	267,6274	360	95,8	22,5	18	1176,7 - 983,7	1185,5 - 983,7
		afterwards	0,0010	2,6991	65,0693	268,668						
13	0,9041	before	0,9041	2,7005	66,7555	267,6303	360	95,3	23,6	18	1168,5 - 983,9	1248,1 - 985
		afterwards	0,0017	2,7005	64,9370	268,7913						
14	0,9034	before	0,9034	2,7000	66,7203	267,6127	360	95,7	23,7	18	1211,9 - 983,4	1414 - 983,5
		afterwards	0,0020	2,7000	65,1996	268,4293						
15	0,9017	before	0,9017	2,6998	66,8773	267,6816	360	96,2	23,4	18	1338 - 984,5	1287 - 984,2
		afterwards	0,0007	2,7053	65,0329	268,9106						

Appendix B-2 shows the experiment results of catalytic cracking with wax feedstock **SampleC** 509-2 for temperature range of 180-225°C.

CATALYST: ZSM-5 (23)
Reaction
Time=12sec

T-Reaction (°C)	**560**	**560**	**460**	**460**	**410**	**410**	**360**	**360**	**360**
Run No	**1**	**2**	**3**	**4**	**5**	**6**	**7**	**9**	**10**
Date	*18.6.13*	*19.6.13*	*19.6.13*	*20.6.13*	*26.6.13*	*26.6.13*	*26.6.13*	*27.6.13*	*28.6.13*
Recovery (%)	98,941	78,609	98,214	96,982	100,501	100,432	99,267	84,920	97,582
C/O	1,060	0,449	0,502	0,494	0,494	0,488	0,508	0,593	0,490
Conversion	89,261	95,927	95,499	96,497	88,237	92,148	74,690	85,001	73,038
Gasoline	43,304	37,232	39,905	41,414	41,869	45,302	42,446	45,397	40,821
Coke	2,102	1,075	1,857	1,607	1,555	1,247	1,331	1,794	1,243
Dry gases	14,514	9,321	3,328	2,933	1,070	1,027	0,402	0,545	0,445
C_1+C_2	14,016	9,063	3,243	2,868	1,052	1,009	0,402	0,545	0,445
Total C_3	23,655	31,316	25,107	23,176	15,533	15,561	10,112	12,586	10,579
Total C_4	5,654	16,949	25,267	27,327	28,172	28,974	20,323	24,654	19,930
C_4 paraffins	4,737	12,279	18,491	20,306	14,570	15,639	8,281	10,603	9,250
C_4 olefins	0,917	4,670	6,776	7,021	13,602	13,334	12,043	14,051	10,680
LPG	29,309	48,265	50,374	50,502	43,704	44,535	30,436	37,241	30,510
Olefinicity C_2	0,166	0,628	0,725	0,776	0,850	0,847	0,899	0,914	0,884
Olefinicity C_3	0,081	0,250	0,249	0,260	0,413	0,376	0,501	0,501	0,446
Olefinicity C_4	0,162	0,276	0,268	0,257	0,483	0,460	0,593	0,570	0,536
I-butane/Sat.C_4	0,496	0,516	0,536	0,528	0,484	0,480	0,425	0,474	0,466
Kerosene	3,630	1,780	2,024	1,710	1,697	1,879	2,066	1,791	2,311
Heavier	7,109	2,293	2,477	1,793	10,066	5,973	23,243	13,208	24,651
GC RON	105,780	106,170	100,840	100,790	94,030	93,800	88,950	88,580	90,820
GC MON	91,300	91,030	87,160	87,260	80,890	80,750	76,350	76,220	77,880
Hydrogen	0,498	0,258	0,085	0,066	0,018	0,018	0,000	0,000	0,000
Methane	5,127	1,619	0,382	0,270	0,045	0,044	0,004	0,000	0,000
Ethane	7,414	2,771	0,786	0,581	0,151	0,148	0,040	0,047	0,052
Ethylene	1,475	4,673	2,075	2,017	0,855	0,818	0,358	0,498	0,393
Propane	21,731	23,497	18,866	17,159	9,111	9,715	5,048	6,284	5,863
Propylene	1,924	7,819	6,241	6,017	6,422	5,847	5,064	6,302	4,717
I-butane	2,348	6,338	9,920	10,728	7,054	7,502	3,517	5,026	4,312
N-butane	2,389	5,940	8,572	9,578	7,516	8,137	4,763	5,578	4,939
1-butene	0,174	0,890	1,067	1,085	1,853	1,781	1,488	1,720	1,321
I-butene	0,366	1,825	2,942	3,011	5,907	5,958	5,159	6,185	4,664
Trans-butene-2	0,214	1,126	1,597	1,681	3,402	3,254	3,180	3,633	2,777
Cis-butene-2	0,163	0,830	1,169	1,244	2,440	2,341	2,216	2,513	1,917
Kinetic conversion	8,312	23,551	21,218	27,546	7,502	11,735	2,951	5,667	2,709

SimDist									
IBP (0.5)	42,8								
5	80,8	79,4	67,6	55,2	41,2		48	69,6	40,2
10	81,8	81,4	80,4	80,2	69,8	63,8	70,8	94,4	70,2
20	112,6	112,4	111,8	111,6	100,4	88,6	110,6	112,6	110,8
30	114,2	114	113,4	113,8	114,4	111,6	140,2	139,4	139,6
40	115,2	115	120,4	115,4	139,8	125	171,8	159,6	175,2
50	138,4	139,4	140,4	140,4	150,2	140,2	271	200,8	270,6
60	141,4	141,8	142	142	182,6	146	324	286,4	322,8
70	146,2	142,8	145,4	143	276	169	356,6	329,8	356,6
80	193	147	163	162,6	344,4	229,2	382	356,8	381,2
90	230,4	199,4	207,4	197,4	391,4	331,6	413,6	386,8	420,2
95	250,6	229,4	243,4	229,4	424	374,8	435,4	411,4	447,2
99,5	362,6	359,6	359,8	348,4	498,4	457,4	490,2	464,8	507,6
FBP (99.5)									

CATALYST: ZSM-5 (80)

Reaction Time=12sec

T-Reaction (°C)	**460**	**460**	**410**	**410**	**360**	**360**
Run No	**1**	**2**	**3**	**4**	**5**	**6**
Date	*20.6.13*	*25.6.13*	*25.6.13*	*25.6.13*	*27.6.13*	*27.6.13*
Recovery (%)	99,930	99,565	98,302	98,915	101,630	98,105
C/O	0,505	0,512	0,502	0,505	0,552	0,496
Conversion	97,917	98,011	96,979	97,338	95,981	95,081
Gasoline	44,790	43,905	52,054	49,248	54,152	54,751
Coke	1,248	1,026	1,018	1,623	1,465	1,225
Dry gases	2,193	2,399	1,278	1,320	0,516	0,459
C_1+C_2	2,173	2,377	1,265	1,303	0,516	0,459
Total C_3	17,055	18,127	13,259	14,371	10,438	10,099
Total C_4	32,606	32,523	29,339	30,739	29,302	28,518
C_4 paraffins	14,307	13,657	13,189	14,511	12,228	10,774
C_4 olefins	18,299	18,867	16,150	16,228	17,075	17,744
LPG	49,661	50,650	42,598	45,110	39,740	38,617
Olefinicity C_2	0,940	0,945	0,953	0,926	0,957	0,965
Olefinicity C_3	0,632	0,647	0,607	0,564	0,606	0,628
Olefinicity C_4	0,561	0,580	0,550	0,528	0,583	0,622
I-butane/Sat.C_4	0,511	0,509	0,524	0,538	0,517	0,487
Kerosene	1,250	1,190	1,898	1,606	2,227	2,310
Heavier	0,833	0,800	1,123	1,056	1,792	2,610
GC RON	92,620	91,890	89,140	90,380	86,400	84,530

GC MON	80,380	79,680	77,420	78,380	74,860	73,460
Hydrogen	0,020	0,022	0,012	0,017	0,000	0,000
Methane	0,052	0,044	0,015	0,022	0,000	0,000
Ethane	0,126	0,128	0,058	0,095	0,022	0,016
Ethylene	1,995	2,205	1,192	1,186	0,494	0,443
Propane	6,273	6,392	5,214	6,263	4,112	3,762
Propylene	10,783	11,736	8,045	8,108	6,326	6,337
I-butane	7,304	6,950	6,910	7,803	6,317	5,250
N-butane	7,003	6,707	6,279	6,708	5,911	5,524
1-butene	2,792	2,902	2,147	2,169	1,955	2,037
I-butene	7,692	7,963	7,251	7,258	8,179	8,523
Trans-butene-2	4,473	4,585	3,922	3,948	4,086	4,240
Cis-butene-2	3,342	3,416	2,829	2,853	2,855	2,944
Kinetic conversion	46,998	49,269	32,099	36,564	23,882	19,329
SimDist						
5		6	18,6	25	38,8	
10		36,6	36,6	38,8	63,6	41
20	69	68,4	66,2	70,8	84,4	69,6
30	96,4	92,8	86,8	96,8	98,8	87,4
40	111,2	110,8	104,2	111,2	112	99,8
50	119,8	116,2	115	121,4	127	116,8
60	138,6	137,6	133,2	137,6	139,4	133
70	141,4	141,4	141,4	141,6	151,2	147,2
80	161,6	161,2	161,6	162	168,4	168,4
90	181,8	181,2	183	184,4	202,4	212
95	215	214	215,4	220,6	248,4	284,8
99,5	346,4	346,6	340,8	335	407,2	396,2
FBP (99.5)						

8.3 Appendix C

Appendix C-1 shows the experiment pathway of the catalyst presulfiding on Ni/Mo and Dewaxing catalyst.

Condition	H_2 Pressure (barg)	T (°C)	LHSV	H_2/oil (scf/b)	Catalyst volume (ml)	Liquid flow rate (ml/h)	Gas flow rate (l/h)	Time (hours)	Rate (°C/hr)
N_2 flash	1	20	0	0	200	0	100	0,5	0
N_2	1	120	0	0	200	0	100	1	100
N_2 hold	1	120	0	0	200	0	100	10	0
Liquid intro	70	120	3	1500	200	600	151,7	1	0
1 Step	70	250	3	1500	200	600	151,7	2,2	60
Hold	70	250	3	1500	200	600	151,7	2	0
2 Step	70	350	3	1500	200	600	151,7	1,7	60
Hold	70	350	3	1500	200	600	151,7	2	0
Ready for experiment	70	275	1	3000	200	200	101,1	4	0

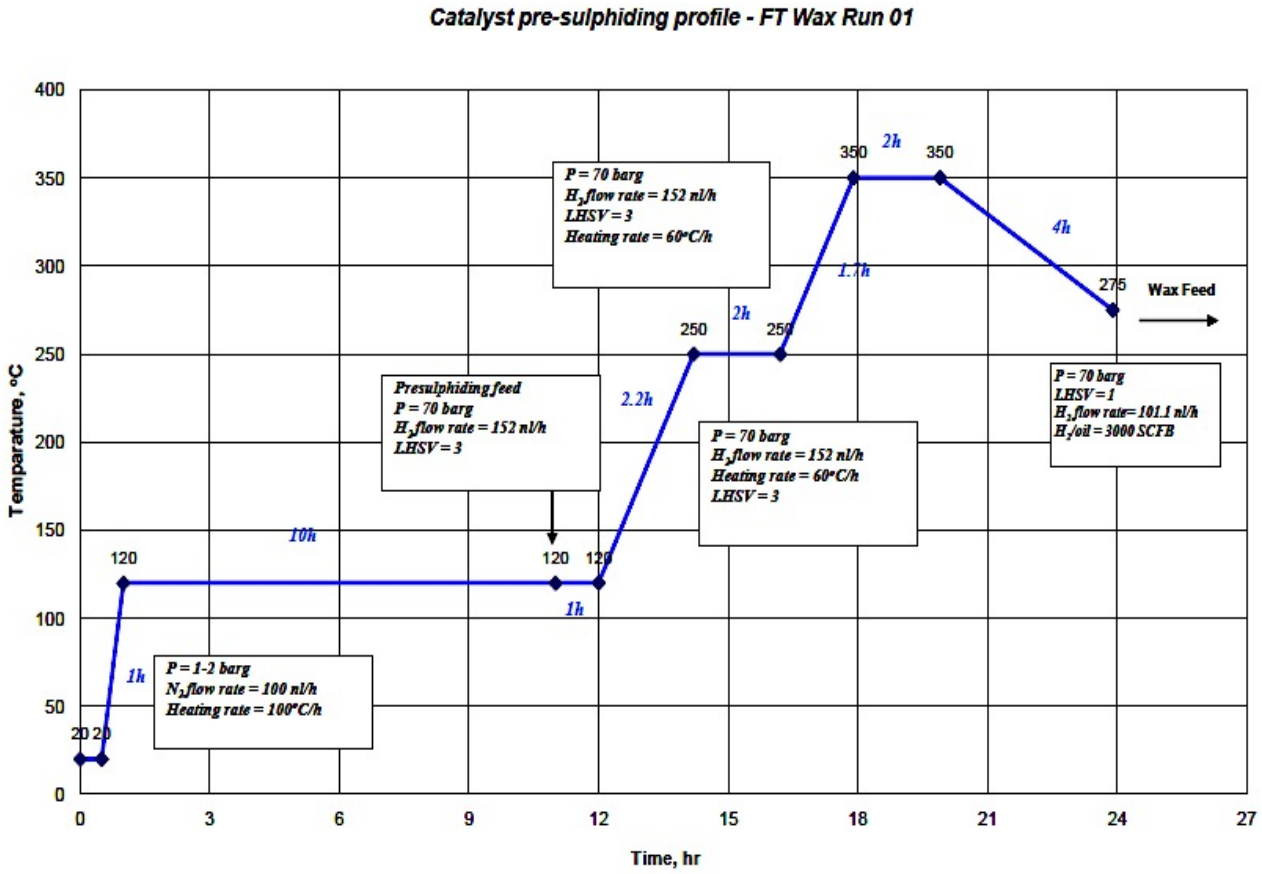

Appendix C-2 shows the experiment results of the Ni/Mo and Dewaxing catalyst for temperature range of 180-225°C.

Experiments with the Ni/Mo catalyst

LHSV	hr-1		0,98	1,02	0,98
Pressure	barg		69,99	70,00	70,00
Temp R-101	oC		350,20	379,99	450,02
H2 flow	nl/h		101,14	101,17	169,59
Sim Dist					
GASOLINE			0,1	0,2	2,1
Gasoline cut point 180°C					
Kersosene			0,4	0,3	5,5
Diesel cut point 225°C			99,6	99,7	94,5
RESIDUE			99,5	99,5	92,4
mass%_IBP		0	226,6	226,4	171,4
mass%_1		1	250	252,2	173,2
mass%_2		2	270,8	270	175,2
mass%_3		3	279	279,8	195,6
mass%_4		4	288	286,6	196,6
mass%_5		5	289	289	207,8
mass%_6		6	302,6	301,4	216,2
mass%_7		7	303,8	302,2	217
mass%_8		8	304,6	302,8	229,2
mass%_9		9	316,6	315,4	235,6
mass%_10		10	318	316,2	236,2
mass%_11		11	318,8	316,8	246,6
mass%_12		12	319,6	317,6	254,4
mass%_13		13	331	329,6	255,2
mass%_14		14	332,4	330,4	255,8
mass%_15		15	333,2	331	270,4
mass%_16		16	334	331,4	271,8
mass%_17		17	341	340	272,6
mass%_18		18	345,6	343,8	273,2
mass%_19		19	346,6	344,4	282
mass%_20		20	347,4	345	287,6
mass%_21		21	348	345,6	288,4
mass%_22		22	357,2	355,8	289,2
mass%_23		23	358,6	356,6	289,6
mass%_24		24	359,6	357,2	296,8
mass%_25		25	360,2	357,8	302,6
mass%_26		26	364,8	363,6	303,6
mass%_27		27	370,2	368,4	304,2
mass%_28		28	371,2	369	304,6
mass%_29		29	372,2	369,6	305,2
mass%_30		30	373,2	372	311,6
mass%_31		31	381,2	379,6	316,8
mass%_32		32	382,6	380,4	317,8
mass%_33		33	383,6	381	318,6
mass%_34		34	384,4	381,8	319,2
mass%_35		35	392,2	390,6	319,6
mass%_36		36	393,6	391,6	323
mass%_37		37	394,6	392	329,6
mass%_38		38	396,2	395	331,6
mass%_39		39	403	401,2	332,4

mass%_40	40	404,4	402	333,2
mass%_41	41	405,2	402,6	333,6
mass%_42	42	411,8	410,4	334,2
mass%_43	43	413,8	411,8	337,4
mass%_44	44	414,8	412,4	343,8
mass%_45	45	418	417,8	345,4
mass%_46	46	423,2	421,2	346,2
mass%_47	47	424,4	422	346,8
mass%_48	48	427,2	427,4	347,4
mass%_49	49	432,6	430,6	347,8
mass%_50	50	433,8	431,4	351,2
mass%_51	51	439,6	438,8	356,8
mass%_52	52	442,2	440	358,2
mass%_53	53	443,4	441	359
mass%_54	54	450,2	448,6	359,6
mass%_55	55	451,8	449,6	360,2
mass%_56	56	456,8	456,4	361,4
mass%_57	57	460	458	365,4
mass%_58	58	461,6	462	369,6
mass%_59	59	468	466,2	370,6
mass%_60	60	469,2	468,4	371,4
mass%_61	61	475,4	473,6	372
mass%_62	62	476,8	475,6	372,6
mass%_63	63	482,8	481,2	376,8
mass%_64	64	484,4	483,8	381,2
mass%_65	65	490,2	488,4	382,4
mass%_66	66	492	493,8	383
mass%_67	67	497,4	495,8	383,6
mass%_68	68	501,4	501,2	385,8
mass%_69	69	504,4	502,8	391,2
mass%_70	70	509,4	508,2	392,8
mass%_71	71	511,6	512,8	393,8
mass%_72	72	516,6	515,2	394,4
mass%_73	73	521,2	520,6	396,4
mass%_74	74	523,8	524,8	401,4
mass%_75	75	528,6	527,2	403,2
mass%_76	76	533,2	532,4	404,2
mass%_77	77	536	537,4	404,8
mass%_78	78	540,6	541,8	408,4
mass%_79	79	545,6	544,6	412,6
mass%_80	80	550,4	549,4	413,8
mass%_81	81	555	554,6	414,6
mass%_82	82	559,4	559,4	418,2
mass%_83	83	564	564,2	422,4
mass%_84	84	569,2	569,2	423,6
mass%_85	85	574,6	574,2	425,6
mass%_86	86	579,8	581,2	431
mass%_87	87	585,8	586,4	432,6
mass%_88	88	592,2	592	434,8
mass%_89	89	599,2	598,8	440,4
mass%_90	90	606,6	606,2	442
mass%_91	91	614,8	613,8	446,2
mass%_92	92	623,4	621,8	450,2
mass%_93	93	633	631,2	454
mass%_94	94	644	641,4	459
mass%_95	95	656,2	653	465,4
mass%_96	96	670,4	666,4	469,2
mass%_97	97	688	682,8	475,8

mass%_98	98	706,6	701,6	484,2		
mass%_99	99	728,4	722,6	497		
mass%_FBP	100	742,2	743,8	509		

Experiments with the Dewaxing Catalyst

LHSV	hr-1		1,0	1,0	1,0	1,0	1,0	1,0	1,0
Pressure	barg		70,0	70,0	70,0	70,0	70,0	70,0	70,0
Temp R-101	oC		300,0	350,0	350,0	325,0	325,0	375,0	375,0
Temp R-201	oC								
Condition		**Feed**	**1**	**2**	**2**	**3**	**3**	**4**	**4**
Date			11/11/13	12/11/13	13/11/13	14/11/13	15/11/13	18/11/13	18/11/13
Nitrogen	ppmwt								
Sulfur	ppmwt								
H_2	% wt	15,31		15,14	15,57	15,37	15,13	15,94	
C	% wt	84,09		84,31	84,01	84,29	84,63	83,90	
		99,40		99,45	99,58	99,66	99,76	99,84	
Sim Dist									
GASOLINE		0,00	0,00	19,60	27,00	0,00	0,50	85,00	85,8
Gasoline cut point									
KEROSENE		0,00	0,80	27,20	20,8	1,50	0,60	8,50	8,20
Kerosene cut point	180°C								
DIESEL		9,00	10,3	31,5	22,4	10,8	10,7	5,1	4,5
Diesel cut point	225°C								
RESIDUE		91,00	88,90	21,70	29,80	87,70	88,20	1,40	1,50
mass%_IBP				36		165	150,2		
mass%_1	1		211	41,6		180,8	196,6		
mass%_2	2		256	69	36	223	255		
mass%_3	3		272,6	98,6	45,4	258,2	271,8		
mass%_4	4		287,2	104,6	53,2	273	286,8		
mass%_5	5		294,6	104,6	61,2	286,6	288,6		
mass%_6	6		302,2	110,8	76,4	294	301,8		
mass%_7	7		303,2	110,8	98,6	301,8	303		
mass%_8	8		312,6	116,8	104,6	302,6	305,2		
mass%_9	9		316,6	116,8	110,8	310,6	316		
mass%_10	10		317,4	122,8	110,8	316	317,2		
mass%_11	11		318,2	122,8	110,8	316,8	318		
mass%_12	12		330	127,2	116,8	317,6	323,6		
mass%_13	13		331,2	129,8	116,8	329,2	330,6		
mass%_14	14		332	132,4	116,8	330,6	331,8		
mass%_15	15		332,8	134,8	116,8	331,6	332,6		
mass%_16	16		343,8	140	116,8	332,2	333,4		
mass%_17	17		345	145,2	122,8	341,4	343,8		
mass%_18	18		345,8	145,2	122,8	344,2	345,2		
mass%_19	19		346,4	150,2	127,2	345,2	346		
mass%_20	20		355,8	151,6	127,2	345,8	346,8		
mass%_21	21		357,4	153,6	127,2	350	352		

mass%_22	22	358,2	155,6	127,2	356,4	357,2		
mass%_23	23	359	157,4	127,2	357,6	358,2		
mass%_24	24	365,8	159,4	129,8	358,2	359,2		
mass%_25	25	369,2	161,2	132,4	359	359,8		
mass%_26	26	370,2	163,2	132,4	368	368,4		
mass%_27	27	371	165	134,8	369,4	370		
mass%_28	28	377	167	137,4	370,2	370,8		
mass%_29	29	380,8	168	140	370,8	371,6		
mass%_30	30	381,8	169,8	145,2	379,2	377,2		
mass%_31	31	382,6	171,8	147,6	380,8	381,2		
mass%_32	32	390,2	173,8	150,2	381,6	382,2		
mass%_33	33	392,2	175	150,2	382,4	383		
mass%_34	34	393,2	176,4	152,6	390,4	387,2		
mass%_35	35	394	177,6	154,6	392	392,2	36	
mass%_36	36	401,8	179,2	155,6	392,8	393,2	41,6	
mass%_37	37	403	180,8	158,4	394,4	394,2	41,6	
mass%_38	38	403,8	182,8	160,2	401,4	399,4	41,6	
mass%_39	39	411	184,8	163,2	402,6	402,8	45,4	41,6
mass%_40	40	412,8	187	165	403,4	403,8	45,4	41,6
mass%_41	41	413,6	188,6	167	410,2	404,6	45,4	41,6
mass%_42	42	420	190,2	169	412,2	411,8	49,4	41,6
mass%_43	43	422,2	192,2	171,8	413,2	413,2	49,4	45,4
mass%_44	44	423,2	195	174,6	417,6	414,2	49,4	45,4
mass%_45	45	430	197	176	421,8	420,4	53,2	49,4
mass%_46	46	431,8	198,6	178	422,8	422,6	53,2	49,4
mass%_47	47	432,8	200,6	180,4	427,8	423,6	57,2	49,4
mass%_48	48	440	202,4	183,2	431	429	57,2	53,2
mass%_49	49	441,4	204,8	186	432,2	431,8	61,2	57,2
mass%_50	50	446,4	207,2	188,2	439	433	61,2	57,2
mass%_51	51	449,8	209,2	191	440,8	439,2	65	61,2
mass%_52	52	451	211,8	195,4	442,4	441,4	65	61,2
mass%_53	53	458	215,4	197,8	449	442,6	69	65
mass%_54	54	459,4	217,8	200,6	450,2	449,2	76,4	69
mass%_55	55	466	220,2	204	456,8	450,8	83,8	69
mass%_56	56	467,6	223	207,2	458,6	455,6	83,8	76,4
mass%_57	57	473,6	226,2	210,6	464	458,8	91,4	83,8
mass%_58	58	475	229	216,2	466,8	460,4	98,6	83,8
mass%_59	59	481	233	219,6	470,2	466,8	98,6	91,4
mass%_60	60	482,6	236,4	224	474,2	468,2	104,6	91,4
mass%_61	61	488,4	240	228,4	477,4	474	104,6	91,4
mass%_62	62	490,2	244,4	235	481,6	475,6	104,6	91,4
mass%_63	63	495,8	248,4	240	486	481,2	104,6	98,6
mass%_64	64	499,8	253,8	246,2	489	482,8	110,8	98,6
mass%_65	65	502,8	256,8	253,8	494,2	488,4	110,8	98,6
mass%_66	66	508	262	259,4	496,2	490,2	110,8	98,6
mass%_67	67	510,2	266,6	267	501,6	495,6	110,8	104,6
mass%_68	68	515,2	271,4	272	503,6	497,6	110,8	104,6
mass%_69	69	520	275	280,2	508,6	502,6	110,8	104,6
mass%_70	70	522,4	280,8	287,2	513,4	506	110,8	110,8
mass%_71	71	527,2	286,8	291,4	515,6	509,6	116,8	110,8
mass%_72	72	532,2	288,8	301	520,6	514,4	116,8	110,8
mass%_73	73	536,8	295	302,8	525,2	516,6	116,8	116,8
mass%_74	74	539,8	301,8	309,6	527,8	521,4	122,8	116,8
mass%_75	75	544,4	303,2	316,2	532,6	525,8	122,8	116,8
mass%_76	76	549,4	309,4	317,8	537,4	528,6	127,2	116,8
mass%_77	77	554,4	316	328,6	542	533,2	127,2	122,8
mass%_78	78	559,2	317,6	331,2	545,8	537,8	127,2	122,8
mass%_79	79	564,2	325,6	337,6	550	541,8	129,8	127,2

mass%_80	80	569,2	330,8	344,4	555	545,4	134,8	129,8
mass%_81	81	575,4	336,2	348,8	559,8	550,2	140	134,8
mass%_82	82	581,4	344	356,6	565	555	142,6	137,4
mass%_83	83	587,2	348,2	361,2	570,8	559,8	145,2	140
mass%_84	84	594	356,2	368,6	576,6	564,6	147,6	142,6
mass%_85	85	601,4	361,6	376	582,2	569,6	150,2	147,6
mass%_86	86	609,4	368,8	381	589	575,2	155,6	151,6
mass%_87	87	618,8	378,2	391,2	596	581,4	161,2	155,6
mass%_88	88	629	385,2	400,8	603,6	587	164,2	161,2
mass%_89	89	640,2	394	410,6	612	593,8	168	164,2
mass%_90	90	654	403,8	420,6	621,4	600,8	172,8	169
mass%_91	91	671	415,6	432	631,8	608,4	179,6	176
mass%_92	92	692,6	429,2	447,6	643,4	616,6	184,8	181,2
mass%_93	93	718	442,8	464,2	657,2	626	196,4	188,6
mass%_94	94	750	459,8	480,2	673,8	636,2	204,2	200,2
mass%_95	95		479,8	500,6	693,8	647,6	218	212,2
mass%_96	96		503,2	524,2	715,4	661,2	233,2	229
mass%_97	97		534,4	551,8	740,6	677,6	255,8	254,8
mass%_98	98		575	586,4	750	696,8	289,8	294,4
mass%_99	99		637,6	634,8		718,6	347	357,6
mass%_FBP	100		692	676		730,8	396,6	411,4